(96)

Department of Water and Power the City of Los Angeles

(69)

ANTONIO R. VILLARAIGOSA
Mayor

RONALD F. DEATON, *General Manager*

January 30, 2006

Ms. Selica Potter, Acting Clerk to the Board
State Water Resources Control Board
Executive Office
1001 'I' Street, 24th Floor
Sacramento, CA 95814

Dear Ms. Potter:

Subject: Comments on Proposed Revision to the 2006 Section 303(d) List of Water Quality Limited Segments for California

The Los Angeles Department of Water and Power (LADWP) has reviewed the proposed revisions to the 2006 Section 303(d) List and appreciates the opportunity to provide the following comments on some of the aspects of the proposed revisions to the 303(d) list.

The draft 2006 Section 303(d) List proposes to delist Crowley Lake for nitrogen and phosphorus and at the same time to add it to the list for dissolved oxygen (DO) and Ammonia water quality impairments. With regard to the delisting rationale, the Lahontan Regional Board and the State Board state that the eutrophication of the lake by nitrogen and phosphorus is natural and that "controllable, man-induced nutrient inputs are not significantly affecting the trophic state of the lake and are not impairing beneficial uses". It is further stated that seasonal occurrences of algal blooms (presumably due to seasonal nitrogen, phosphorous and temperature fluctuations) will persist.

Keeping in mind the above discussion regarding the nitrogen and phosphorous analyses, natural lake ecology and the fundamental science associated with lake eutrophication drives the discussion about the presence of ammonia and the depressed DO for which the State is proposing to add Lake Crowley to the impaired water body list. There is a direct correlation between the naturally occurring nitrogen, the naturally occurring seasonal cycles, and the naturally occurring lake ecology that drives the elevated 4-day average ammonium levels that occur during the summer. The elevated ammonium, like the elevated nitrogen and phosphorous, is not man-induced and therefore no TMDL can conceivably be developed to control natural processes. Likewise, the DO drop below the hypolimnion patterns natural lake ecology and can be exacerbated by the naturally high nitrogen and phosphorous levels. It makes no sense to delist Crowley Lake for naturally occurring nitrogen and phosphorous and then turn around and list the water body for the same causative factors plus natural ecological processes.

Based on the 2003 SWRCB # 9-175-256-0 Report, Crowley Lake is a eutrophic lake (over enriched) and is characterized by an ample supply of nutrients from many sources, including runoffs, and significant summer algal blooms. Algal blooms are largely responsible for DO depletion and Ammonia (Ammonium) production.

1. DO Depletion:

In Crowley Lake, the DO concentrations showed marked seasonal variation which is typical of eutrophic lakes. Crowley Lake field sampling data indicated that the DO concentrations increased in spring, depleted in August (beneath 12 m), and was nearly uniformed in autumn. This pattern is generally consistent with normal lake ecology, particularly for a eutrophic lake.

Algal blooms occur when the lake's condition is optimum (nutrient, temperature, etc.). They cause DO depletion through algal decomposition. As the dead algae are metabolized by decomposing bacteria, the oxygen in the water column is consumed. The mass fraction of the naturally dying algal population is large and therefore, its decomposition can consume significant amounts of oxygen (DO depletion) in the water.

2. Ammonia (Ammonium) Production:

The Crowley lake-wide survey for ammonia concentration showed seasonal variations similar to the DO concentration. The ammonia concentration reached its pick in the hypolimnion (near bottom) in mid-August.

Algal blooms (which the delisting fact sheets already state as being caused naturally) cause DO depletion and in the absence of DO, the anaerobic bacteria metabolize the decaying material. Ammonia is the initial product of the decay of the nitrogenous compounds at the bottom of the lake. Additionally, in a report prepared by the United States Army Corps of Engineers in 1999 (Miscellaneous Paper EL-99-1) (Enclosure), it was indicated that the buildup of hypolimnetic ammonium is due to the release of ammonium from the sediments during anoxic conditions. The ammonia concentration in Crowley Lake is largely based on the amount of decaying material (dead algae) which exist at the bottom of the lake and, in part, also relates to the loading of dissolved inorganic fractions of nitrogen (NO3 and NH4) from other natural sources, such as the Owens River.

For the reasons discussed above, it is illogical for the State to list Crowley Lake for depressed DO and elevated ammonia which are due to causative factors that have already been identified as natural. The low oxygen content and high ammonia concentrations in the Crowley Lake are as a result of eutrophication in this lake; they are not caused by the treatment or disposal of wastes and are a nuisance condition as defined in the Basin Plan. The cause of eutrophication (over enrichment) is nutrient

enriched water, mainly nitrogen and phosphorous. For the same reasons that these two pollutants in Crowley Lake were delisted, the LADWP requests the removal of DO and Ammonia from the 2006 Federal Clean Water Act, Section 303(d) List of Water Quality Limited Segments for California.

If you require additional information or have any questions regarding these comments, please contact Ms. Fazi Mofidi at (213) 367-0280.

Sincerely,

Susan M. Damron, F.M.

Susan M. Damron
Manager of Wastewater Quality Compliance

FM: bdc
c: Ms. Fazi Mofidi

ENCLOSURE

Miscellaneous Paper EL-99-1
January 1999

US Army Corps of Engineers
Waterways Experiment Station

Water Quality Modeling of Lake Monroe Using CE-QUAL-W2

by Thomas M. Cole, Dorothy H. Tillman

WES

Prepared for U.S. Army Engineer District, Louisville

Miscellaneous Paper EL-99-1
January 1999

Water Quality Modeling of Lake Monroe Using CE-QUAL-W2

by Thomas M. Cole, Dorothy H. Tillman

U.S. Army Corps of Engineers
Waterways Experiment Station
3909 Halls Ferry Road
Vicksburg, MS 39180-6199

Final report

Prepared for U.S. Army Engineer District, Louisville
Louisville, KY 40201-0059

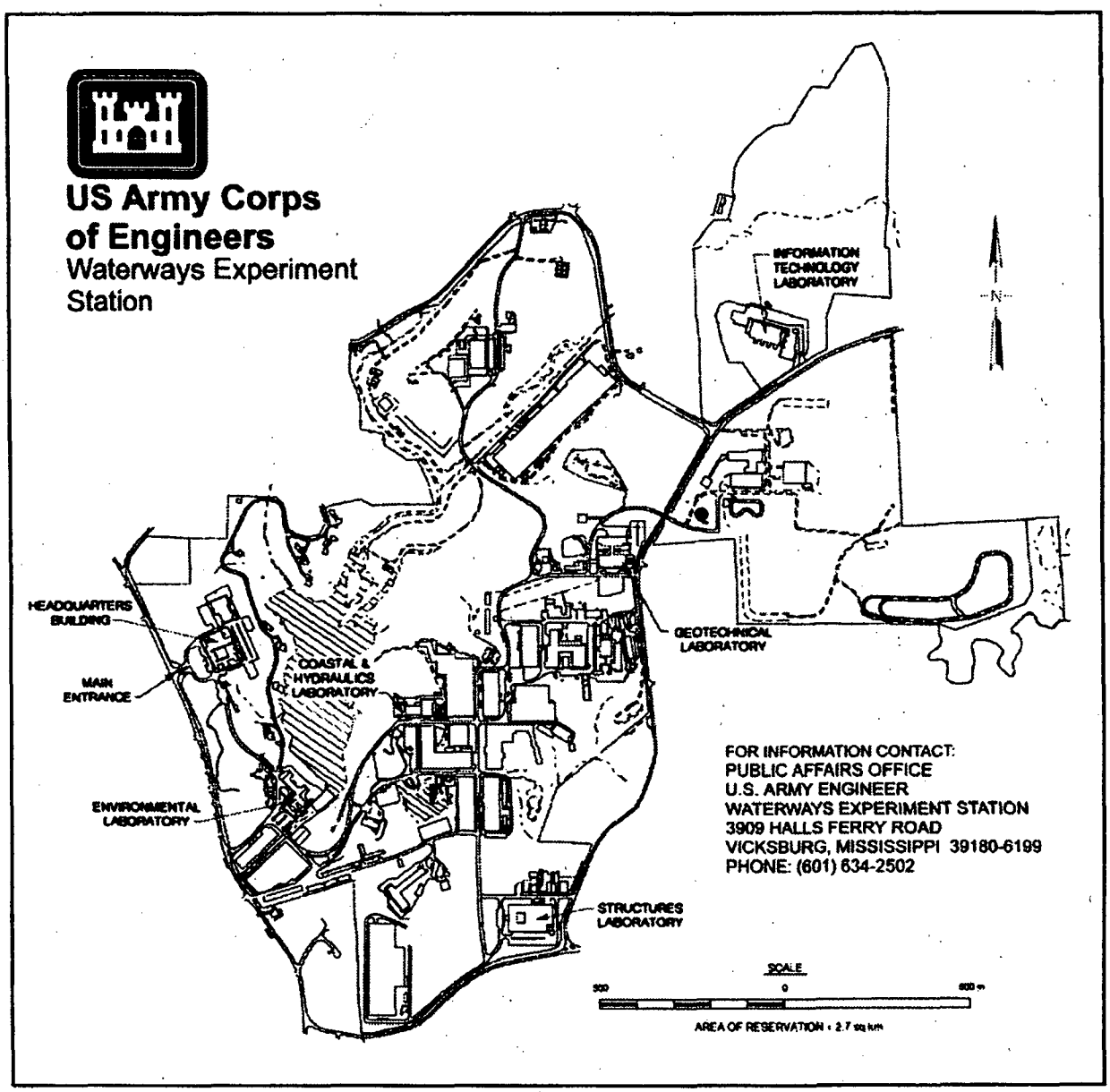

Waterways Experiment Station Cataloging-in-Publication Data

Cole, Thomas M.

Water quality modeling of Lake Monroe using CE-QUAL-W2 / by Thomas M. Cole, Dorothy H. Tillman ; prepared for U.S. Army Engineer District, Louisville.

94 p. : ill. ; 28 cm. — (Miscellaneous paper ; EL-99-1)

Includes bibliographic references.

1. Water quality — Indiana — Mathematical models. 2. Monroe, Lake (Ind.) 3. CE-QUAL-W2 (Computer program) 4. Environmental quality — Mathematical models. I. Tillman, Dorothy H. II. United States. Army. Corps of Engineers. Louisville District. III. U.S. Army Engineer Waterways Experiment Station. IV. Environmental Laboratory (U.S. Army Engineer Waterways Experiment Station) V. Series: Miscellaneous paper (U.S. Army Engineer Waterways Experiment Station) ; EL-99-1.

TA7 W34m no.EL-99-1

Table of Contents

Preface

This report documents the CE-QUAL-W2 temperature and water quality modeling results for Lake Monroe, IN. This report was prepared in the Environmental Laboratory (EL), US Army Engineer Waterways Experiment Stations (WES), Vicksburg, MS. The study was sponsored by the US Army Engineer District, Louisville (CEORL), and was funded under the Military Interdepartmental Purchase Request No. RMB96-289 dated 20 Mar 1966.

The Principal Investigators of this study were Mr. Thomas M. Cole and Ms. Dorothy H. Tillman of the Water Quality and Contaminant Modeling Branch (WQCMB), Environmental Processes and Effects Division, EL. This report prepared by Mr. Cole and Ms. Tillman under the direct supervision of Dr. Mark Dortch, Chief, WQCMB, and under the general supervision of Dr. Richard Price, Chief, EPED, and Dr. John Harrison, Director, EL. Technical reviews by Dr. Barry W. Bunch and Ms. Lillian T. Schneider are gratefully acknowledged. Mr. Fred Herrmann and Mr. Jace Pugh are gratefully acknowledged for generation of all figures in this report.

At the time of publication of this report, Director of WES was Dr. Robert Whalin. Commander of WES was Colonel Cababa.

This report should be cited as follows:

> Cole, Thomas M. and Dorothy H. Tillman (1997). "Water Quality Modeling of Lake Monroe Using CE-QUAL-W2," Miscellaneous Paper EL-99-1, US Army Engineer Waterways Experiment Station, Vicksburg, MS.

List of Figures

List of Tables

1 Introduction

Background

The Louisville District desires the capability to evaluate changes in water quality at their projects due to changes in environmental conditions or project operations. Water quality conditions in the lakes affect allowable waste loads thus impacting activities such as future development and changes in land use practices. If there are changes is environmental conditions or project operations, there is a concern for existing water quality conditions including dissolved oxygen and algal/ nutrient dynamics of these reservoirs. The ability to predict water quality under different conditions will allow the Louisville District to determine if water quality of the projects will be affected.

The Louisville District requested the assistance of the Water Quality and Contaminant Modeling Branch in developing a model of Lake Monroe capable of determining the effects of changes in project operations/loadings on water quality.

Objective

The objective of this study is to provide a calibrated 2D water quality model for Lake Monroe capable of predicting future water quality conditions resulting from potential changes in reservoir operations and/or environmental conditions.

Approach

The 2D hydrodynamic and water quality model, CE-QUAL-W2, was used for this study. CE-QUAL-W2 is a recognized state-of-the-art 2D (longitudinal and vertical) hydrodynamic/water quality model. The model has been successfully applied by the Corps of Engineers, federal and state agencies, universities, and consulting firms on over 100 systems during the last two decades. The model consists of a hydrodynamic module that predicts water surface elevations and horizontal/vertical velocities and a water quality module that contains mathematical descriptions for the kinetic interactions of the water quality state variables.

Site Description

Lake Monroe is located in south central Indiana approximately 20 miles southeast of Bloomington (Figure 1). The dam site is 25.9 miles upstream of the confluence of Salt Creek and East Fork of White River. The drainage area above the dam is 441 square miles. The

construction of Lake Monroe was authorized by the Flood Control Act of July 3, 1958 and was begun in November, 1960 and completed in February, 1965. The Louisville District operates the project that provides for flood control, augmentation of natural low-flow conditions on the White River, and fish and wildlife recreation.

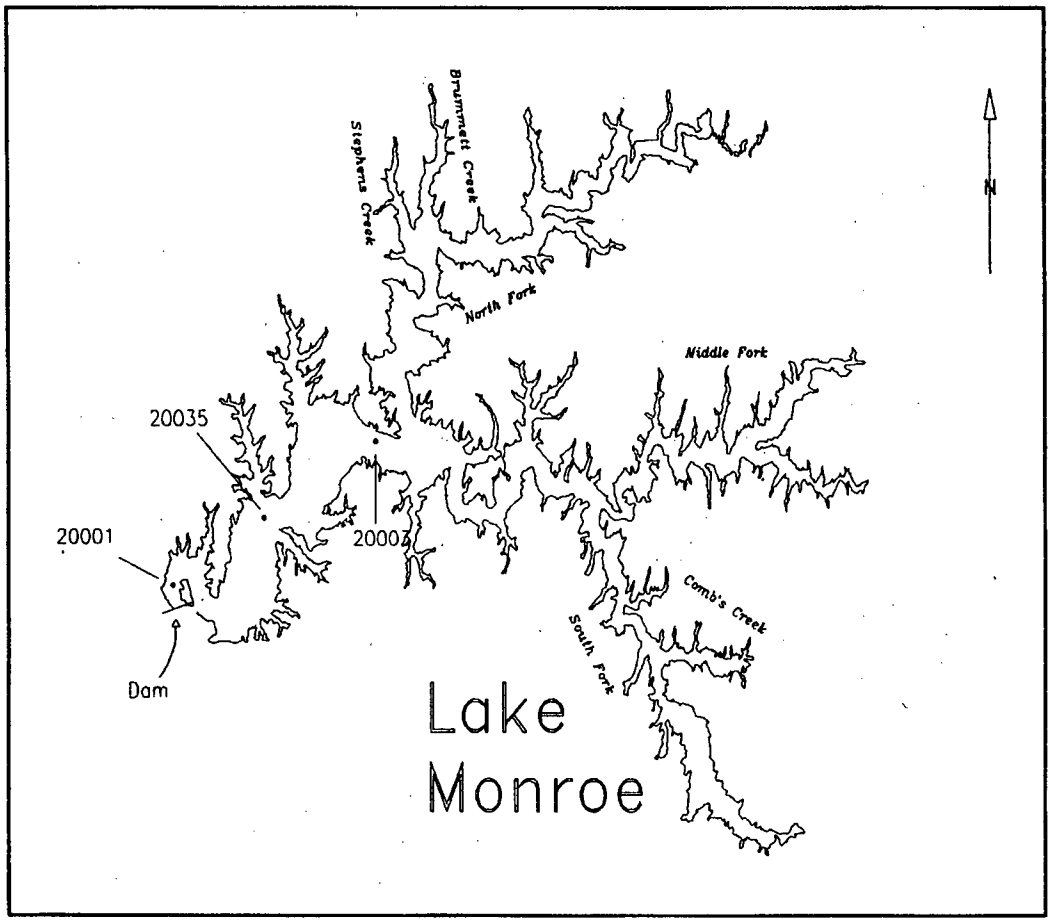

Figure 1. Lake Monroe site map

The dam is an impervious core with rock shell 411.5 m long and with a maximum height of 28 m. The spillway type is an uncontrolled open cut through the left abutment 183 m wide with a design capacity of 2133 m^3 sec^{-1}. The outlet works consist of a control tower at the upstream end, with three slide gates 0.9 m wide by 3.7 m high, a lower water bypass, a 3.75 m diameter semi-elliptical concrete conduit, and a conventional type stilling basin.

Table 1 lists the important morphological characteristics of the reservoir at normal pool elevation for the calibration years. The values are estimates based on the provided bathymetry and preprocessor outputs. Based on Wetzel's (1975) classification of trophic status of lakes, the reservoir is mesoeutrophic with a maximum chlorophyll *a* concentration of 30.4 $\mu g\ l^{-1}$ at station 35 during 1994.

Table 1
Morphological characteristics of Monroe Reservoir for calibration years

Year	Elevation, m	Volume, 10^6 m^3	Surface area, 10^6 m^2	Average width, m	Maximum depth, m	Average depth, m	Residence time, days
1992	164.56	366	57	635	16	6.4	408
1994	164.06	292	53	587	15.5	5.5	265
1995	165.64	428	61	676	17	7.0	185
1996	166.36	428	61	676	18	7.0	231

2 Model Description

CE-QUAL-W2 is a two-dimensional model that predicts vertical and longitudinal variations in hydrodynamics, temperature, and constituents in a water body through time (Cole and Buchak, 1995). The model is based upon the Generalized Longitudinal-Vertical Hydrodynamics and Transport model developed by Buchak and Edinger (1984). The inclusion of water quality algorithms resulted in CE-QUAL-W2 Version 1. Subsequent modifications to improve the model's computational efficiency, numerical accuracy, and prototype physical description resulted in Version 2.

The version used for this study is a prerelease of Version 3. Version 3 is being developed to include a more accurate description of the water quality portion of the code. Specifically, the model can now simulate algal succession from diatoms to greens to cyanobacteria. The ability to model diatoms required including the silica cycle. Eventually, Version 3 will include any number of carbon species, algal groups, and zooplankton groups specified by the user. The new version will also include a sediment diagenesis model that will make long-term water quality simulations more predictive as the effects of sediment phosphorus burial will be explicitly accounted for. Changes will also be made to the hydrodynamics that will allow modeling entire riverbasins including reservoirs and the riverine reaches between them.

CE-QUAL-W2 is based upon a finite-difference solution of the laterally averaged equations of fluid motion including:

1. free water surface
2. hydrostatic pressure
3. longitudinal momentum
4. continuity
5. equation of state relating density with temperature and also dissolved and suspended solids

The basic features of CE-QUAL-W2 are:

1. two-dimensional (laterally averaged) simulations of temperatures, constituents, and flow fields
2. hydrodynamic computations influenced by variable water density caused by temperature and dissolved/suspended solids
3. simulation of the interactions of numerous biological/chemical factors influencing water quality

4. multiple inflow loadings and withdrawals from tributaries, point and nonpoint sources, precipitation, branch inflows, and outflows from a dam.
5. multiple branches
6. ice cover computations
7. variable time steps computed by the model
8. flow or head boundary conditions, making it applicable for reservoir or estuarine modeling
9. simulation of circulation patterns
10. restart capability
11. inclusion of evaporation in water balance
12. heat transfer computations
13. variety of output options
14. selective withdrawal

CE-QUAL-W2 conceptualizes the reservoir as a grid consisting of a series of vertical columns (segments) and horizontal rows (layers), with the number of cells equal to the number of segments times the number of rows. The basic parameters used to define the grid are the longitudinal and vertical spacing and cell width that may vary spatially.

The beta version of CE-QUAL-W2 V3 used in this study currently contains 23 water quality state-variables in addition to temperatures and velocities (Table 2). Many of the constituents are simulated to include their effects upon other constituents of interest. The constituents are separated into four levels of complexity permitting flexibility in model application. The first level includes materials that are conservative or do not affect other materials in the first level. The second level allows the user to simulate algal/nutrient/DO dynamics. The third level allows simulation of pH and carbonate species, and the fourth level allows simulation of total iron which is important during anoxic conditions. Although not recommended, CBOD is included to accommodate organic loadings that are measured as such.

Table 2
Water Quality Constituent Levels

Level 1	Level 2
Conservative tracer	Labile DOM
Inorganic suspended solids	Refractory DOM
Coliform bacteria	Labile POM
TDS or salinity	Refractory POM
Residence time	Diatoms
	Greens
	Cyanobacteria
	Orthophosphate
	Ammonium
	Nitrate/nitrite

Table 2 Water Quality Constituent Levels	
Level 1	**Level 2**
	Dissolved silica Particulate biogenic silica Dissolved oxygen Organic sediments
Level 3	**Level 4**
Dissolved inorganic carbon Alkalinity	Total iron CBOD

3 Input Data

CE-QUAL-W2 requires reservoir bathymetry, initial conditions, inflow quantity and quality, outflow quantity, and outlet description. The model also requires time series of inflow rates and water quality, meteorological data, and water surface elevations. Calibration is dependent on the availability of observed in-pool water quality constituent concentrations at several locations within the reservoir and accurate descriptions of the loadings. Observed release water quality data are also used to evaluate predicted release conditions. Various kinetic rate coefficients are also required input.

Of the water quality constituents listed in Table 2, the constituents of primary interest in this study were:

1. dissolved oxygen
2. phytoplankton
3. orthosphate
4. ammonium
5. nitrate-nitrite

Of the ones listed, DO, phytoplankton, and phosphorus are the most important since phytoplankton are phosphorus limited in Lake Monroe. The subsequent growth and decay of phytoplankton are important mechanisms affecting DO depletion in the reservoir due to autochthonous carbon decay.

Bathymetry

CE-QUAL-W2 requires the reservoir be discretized into longitudinal segments and vertical layers that may vary in length and height. An average width must also be defined for each active cell where an active cell is defined as potentially containing water. Additionally, every branch has inactive cells at the upstream and downstream segments, top layer, and below the bottom active cell in each segment. Segment layer heights for Lake Monroe were constant while segment lengths varied.

Once the segment lengths and layer heights were finalized for each branch, average widths were determined for each cell from digitized data provided by the Louisville District. The grid consisted of three branches. The main branch, representing South Fork Salt Creek, contains 15 longitudinal segments and 24 vertical layers. Branch 2, representing Middle Fork Salt Creek, contains 4 longitudinal segments. The third branch, representing North Fork Salt Creek, contains 7 longitudinal segments. Figure 2 shows the discretized grid.

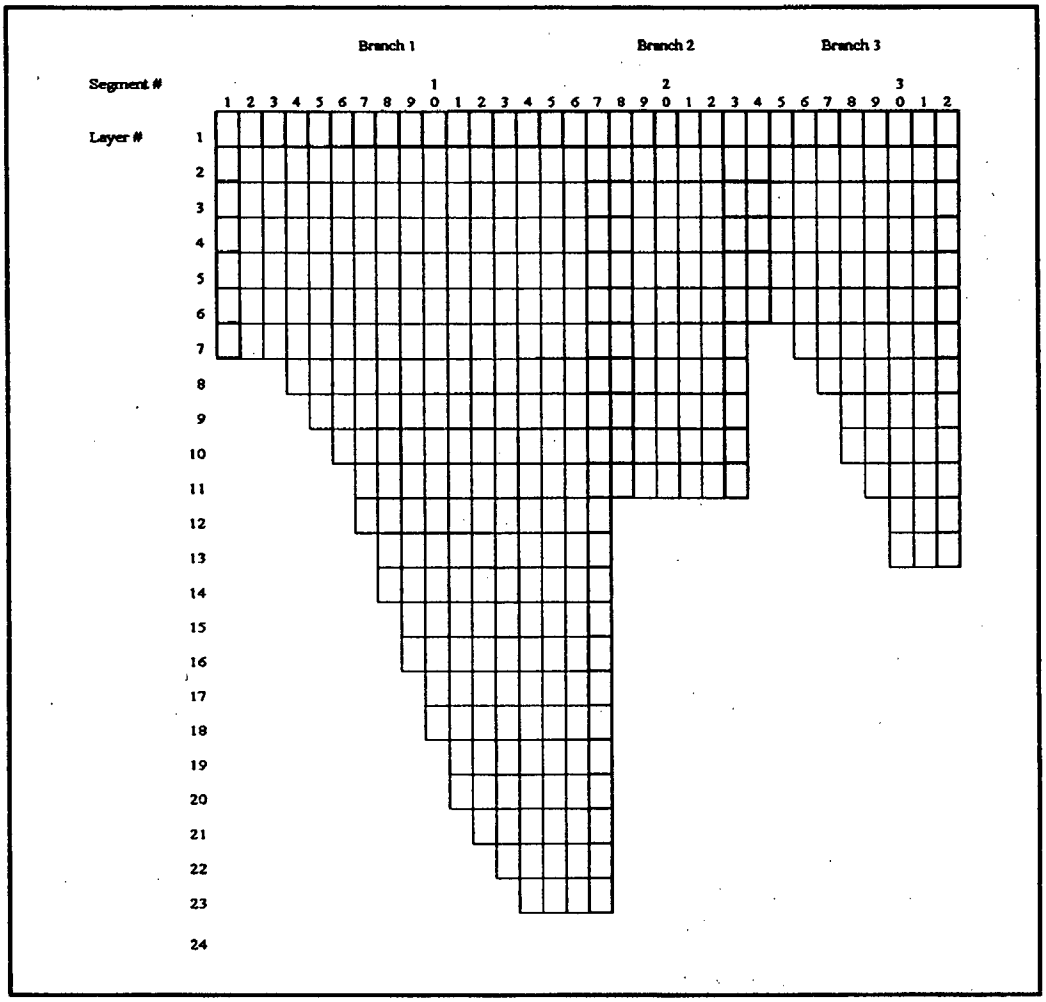

Figure 2. Lake Monroe computational grid

A comparison of the computed volume-elevation curve and USACE data is shown in Figure 3. The volume of the reservoir computed from the bathymetry used in the study does not match the data sent by the Louisville District although the bathymetry developed by the Louisville District was apparently developed from the same data.

Reservoir volume and thus residence time is highly dependent on the bottom elevation set for the grid. Initially, a bottom elevation of 149.35 m (490 ft) was used as this was the bottommost elevation in the volume-elevation data sent by the Louisville District. A bottom elevation of 147.39 m was used subsequently for several reasons. First, using an elevation of 149.35 m resulted in underprediction of depths at all stations. Second, there is a volume associated with an elevation of 149.35 m in the data supplied by the Louisville District indicating that the reservoir is deeper than 149 m. Third, using the higher bottom elevation resulted in unrealistically large negative inflows necessary to calibrate the water surface elevation. Fourth, and most importantly, temperature and water quality calibration was not possible using the higher elevation. Thus, all evidence indicated that the bottom elevation

of the reservoir is less than the bottom elevation in the volume-elevation data furnished by the Louisville District. Subsequent conversations with Louisville District staff indicated that the bottommost elevation is closer to the elevation used for calibration.

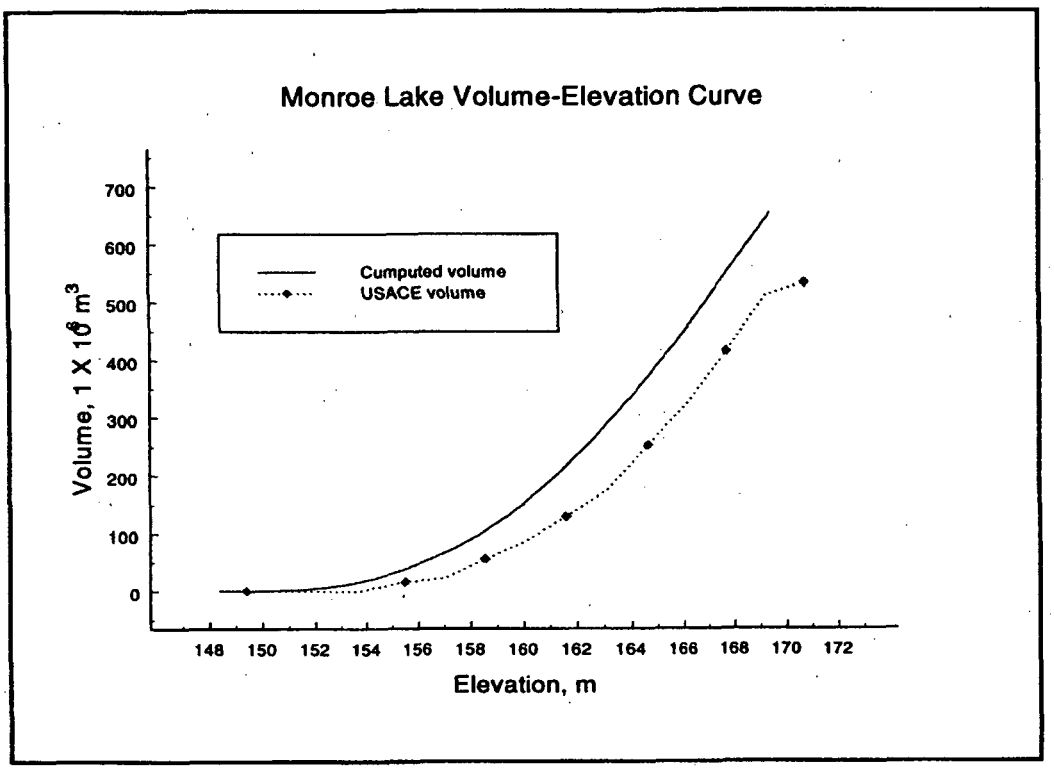

Figure 3. 1994 Lake Monroe volume-elevation curve

In-Pool Data

The model was calibrated using observed in-pool profile data collected and provided by the Louisville District. Observed data for Lake Monroe were collected monthly in 1994 and quarterly for the other years modeled. Table 3 lists the location, station number, time of collection, and observed water quality constituents used for comparisons with computed data for the in-pool stations at Lake Monroe.

Table 3
Observed water quality data collected at Lake Monroe

Year	Station #	Dates Collected	PO_4	NH_3	NO_2NO_3	Chlorophyll a	DO	Temp	DOC	TOC
1992	01	May 5				X	X	X		X
		June 17				X	X	X		X
		July 27				X				
		July 28					X	X		X
		September 9				X	X	X		X
	35	June 17				X	X	X		
		July 28				X	X	X		
	03	June 17				X	X	X		
		July 28				X	X	X		
1994	01	March 21					X	X		
		March 22	X	X	X	X				
		April 11	X	X	X		X	X		
		April 12				X				
		May 2	X	X	X		X	X		
		May 3				X				
		May 23	X	X	X		X	X		
		May 24				X				
		June 6	X	X	X					
		June 7				X				
		June 29	X	X	X		X	X		
		June 30				X				
		July 18		X	X		X	X		
		July 19				X				
		August 1	X	X	X					
		August 2				X				
		August 15	X	X	X		X	X		
		August 16				X				
		September 5	X	X	X		X	X		
		September 6				X				
	35	March 21					X	X		
		March 22	X	X	X	X				
		April 13	X	X	X		X	X		
		April 14				X				

Table 3 (continued)

Year	Station #	Dates Collected	PO_4	NH_3	NO_2NO_3	Chlorophyll a	DO	Temp	DOC	TOC
1994	35	May 2	X	X	X		X	X		
		May 3				X				
		May 23	X	X	X		X	X		
		May 24				X				
		June 8	X	X	X					
		June 9				X				
		June 29	X	X	X		X	X		
		July 18	X	X	X		X	X		
		July 19				X				
		August 2	X	X	X					
		August 3				X				
		August 15	X	X	X		X	X		
		August 16				X				
		September 5	X	X	X		X	X		
		September 6				X				
	03	March 22	X	X	X		X	X		
		March 23				X				
		April 12	X	X	X	X	X	X		
		April 13				X				
		May 3	X	X	X		X	X		
		May 4				X				
		May 23	X	X	X	X	X	X		
		June 6				X				
		June 8	X	X	X	X				
		June 28	X	X	X	X	X	X		
		July 18	X	X	X	X	X	X		
		August 1				X				
		August 2	X	X	X					
		August 15	X	X	X		X	X		
		September 6	X	X	X	X	X	X		
1995	01	May 10		X	X	X	X	X		
		June 19				X				
		June 20					X	X		

Table 3 (concluded)

Year	Station #	Dates Collected	PO_4	NH_3	NO_2NO_3	Chlorophyll a	DO	Temp	DOC	TOC
1994	01	August 2		X	X	X	X	X		
		August 29		X	X	X	X	X		
	35	May 10				X	X	X		
		June 20				X	X	X		
		August 2				X	X	X		
		August 29				X	X	X		
	03	May 10				X	X	X		
		June 19				X				
		June 20					X	X		
		August 2				X	X	X		
		August 29				X	X	X		
1996	01	June 12		X	X	X			X	X
		July 16				X	X	X		
		August 14				X	X	X		
		September 18		X	X	X	X	X	X	X
	35	June 12		X	X	X			X	X
		July 16				X	X	X		
		August 14				X	X	X		
		September 18		X	X	X	X	X	X	X
	03	June 12		X	X	X			X	X
		July 16				X	X	X		
		August 14				X	X	X		
		September 18		X	X	X	X	X	X	X

Sheet 3 of 3

Boundary Conditions

Meteorology. Hourly data for 1994 were furnished by the Louisville District from Bloomington, IN. Hourly meteorological data for 1992, 1995, and 1996 were obtained from the U.S. Air Force Environmental Technical Applications Center in Asheville, NC, for Bloomington and Indianapolis, IN. Data required by CE-QUAL-W2 for computation of surface heat exchange are air temperature, dew point temperature, wind speed and direction, and cloud cover. Plots of meteorological data for all modeled years are shown in figures A1-A16 in Appendix A.

Inflows. The Louisville District provided computed inflows based on outflows and change in water surface elevation every six hours for the years 1984-1996. During the water budget calibration, adjustments were made to the inflows to more accurately reproduce the observed water surface elevations. Plots of inflows are shown in figures A17-A20 in Appendix A.

Outflows. The Louisville District provided outflows every six hours for the years 1984-1996. The City of Bloomington Utilities provided daily withdrawal amounts for the Monroe Water Treatment Plant for all years modeled. Figures A17-A20 in Appendix A shows values for outflows and withdrawals used in the study.

Inflow Temperatures. Inflow temperature data were limited for the main branch of Lake Monroe. Therefore, these data were supplemented using a program called the response temperature calculator (RTC) developed by J. E. Edinger Associates, Inc. The RTC uses meteorological data and stream depth to calculate water temperatures based on equilibrium temperature computations as discussed in the User Manual (Cole and Buchak, 1995). These were then adjusted to match the values at the most upstream lake station. Plots of inflow temperatures are shown in Figure A21 in Appendix A.

Inflow Constituent Concentrations. Water quality inflow concentrations for other constituents of the main branch for Lake Monroe were also limited. Inflow concentrations were available for 1994 but not for the other years modeled. Thus, observed concentrations at the most upstream station of the reservoir were used as inflow boundary conditions to fill in where data were needed. These were then adjusted to match the values at the most upstream lake station. When in-lake or inflow concentrations were not available, 1994 inflow concentrations were used. For example in 1992 and 1995, phosphorus, ammonium, and nitrate-nitrite were not measured in the lake or on the tributaries, so their inflow concentrations were set to 1994 values. Similarly, in 1996 there was only one date where ammonium and nitrate-nitrite were collected in the lake. For the rest of the simulation, 1994 inflow concentrations were used.

Although inflow concentrations of LDOM, RDOM, LPOM and RPOM were not monitored, their boundary concentrations were estimated from total organic carbon (TOC). The portioning of the TOC into LDOM, RDOM, LPOM, and RPOM are presented in the equations below. The majority of the TOC was assumed to be refractory. To alleviate the uncertainty of these assumptions, data would have to be collected for the different forms. Listed below are the equations used in estimating these constituents from TOC.

$$LDOM = ((TOC - algae) * 0.75) * 0.30 \quad (1)$$

$$RDOM = ((TOC - algae) * 0.75) * 0.70 \quad (2)$$

$$LPOM = ((TOC - algae) * 0.25) * 0.30 \quad (3)$$

$$RPOM = ((TOC - algae) * 0.25) * 0.70 \quad (4)$$

Inflow algal concentrations were estimated from chlorophyll *a* data. CE-QUAL-W2 requires algal concentrations in units of g OM m^{-3}. Measured chlorophyll *a* concentrations were in units of micrograms of chlorophyll *a* per liter (μg chl-a l^{-1}) and were converted to gm OM m^{-3} using the conversion factor 65 as recommended by the QUAL2E (Brown and Barnwell,

1987) and CE-QUAL-W2 user manuals (Cole and Buchak, 1995). The conversion equation is given as:

$$\frac{ug\ chl\ a}{l} * \frac{mg}{10^3 ug} * \frac{gm}{10^3 mg} * \frac{10^3 l}{m^3} * 65 \frac{gm\ OM}{gm\ chl\ a} = \frac{0.065\ gm\ OM}{m^3} \qquad (5)$$

The chlorophyll *a* measurements were assumed to be corrected for pheophytin according to procedures in Standard Methods (1985). Plots of inflow constituent concentrations are given in figures A22-A29 in Appendix A.

Initial Conditions

The options for setting initial conditions in CE-QUAL-W2 are:

1. same concentration for temperature and constituents throughout reservoir
2. use vertical varying profile of temperature and constituents at the dam to initialize all segments in grid
3. use vertical profiles of temperature and constituents varying longitudinally for each segment in the grid.

For all years calibrated, simulation start date and initial conditions for each year were set to the first date observed date when data were collected (see Table 3). In 1994, initial conditions for DO, ammonium, phosphorus, nitrate-nitrite, algae, LDOM, RDOM, LPOM, and RPOM were set using option 1 since there was little variation in concentrations throughout the reservoir. In all other years, initial conditions for all the constituents discussed above except DO were also set using option 1. Initial conditions for temperature and DO for all years (except DO in 1994) were set using option 2 to capture the vertical variation.

4 Calibration

The concept of calibration/verification of a model has changed in recent years. Previously, calibration was performed on one year with coefficients adjusted to give the best results. Verification was then performed on another year with the same coefficients used during calibration, but with new boundary conditions and seeing how well the model performed. Now, all simulated years are termed calibration years and the process is performed simultaneously resulting in the same coefficients for all years modeled that give the best results.

Successful model application requires calibrating the model to observed in-pool water quality. If at all possible, two or more complete years should be modeled with widely varying flows and water surface elevations if corresponding water quality data are available. Preferably, a wet, dry, and average water year should be selected for calibration years. Output was evaluated both graphically and statistically in order to determine when the model was calibrated. Four years were chosen for calibration. The first calibration year, 1994, was chosen because it had the most water quality data. This year was a slightly below average water year. Additional years chosen were 1992, 1995, and 1996. These years represented slightly above average, low, and high flow years, respectively. Choosing different flow years ensures that the model is reproducing water quality variations due to differing hydrodynamics, meteorology, and loadings. All calibrations were begun on the first date observed data were collected and ended after the last data collection date.

Graphical comparisons of computed versus observed data were made to evaluate model performance. To distinguish between observed and computed data in profile plots, the dashed line represents computed values, and the x's represent observed values. For all profiles, computed data were compared to observed by plotting the day before, the day of, and the day after the sampled date. Comparisons were conducted this way because on some dates computed values compared favorably with observations at an earlier or later date. This is commonly due to inaccuracies in the meteorological boundary conditions.

A root mean square error (RMS) was calculated to statistically evaluate model performance and is indicated on each graph. The RMS was calculated as:

$$RMS = \sqrt{\frac{\sum (predicted - observed)^2}{number\ of\ observations}} \qquad (6)$$

The RMS is a measure of variability between predicted and observed concentrations. An RMS of 0.50 means predicted data are within ± 0.5 of the observed value 67 percent of the time.

Also indicated on each plot is the absolute mean error (AME). The AME represents the absolute average error as compared with observed data and is calculated as:

$$AME = \frac{\sum |predicted - observed|}{number\ of\ observations} \quad (7)$$

The absolute mean error gives an indication of how close on either side of the observed values the predicted values are. For example, an AME of 0.5 means that the computed values are, on the average, within ± 0.5 of the observed value. For temperature, this value would approach the accuracy of many temperature probes.

Table 4 shows final values of all coefficients that affect temperature. All parameters were set to default values except for wind sheltering. Temperature predictions were most sensitive to changes in the wind sheltering coefficient. All other coefficients affecting thermal predictions were set to default values. Table 5 shows final values of all coefficients that could potentially be adjusted during water quality calibration. An * indicates coefficients that were adjusted from their default value.

Table 4
Temperature Calibration Values

Coefficient	Variable	Value
Horizontal eddy viscosity	AX	1 $m^2 s^{-1}$
Horizontal eddy diffusivity	DX	1 $m^2 s^{-1}$
Bottom frictional resistance	CHEZY	70 $m^{1/2} s^{-1}$
Solar radiation fraction absorbed at the water surface	BETA	0.45
Solar radiation extinction - water	EXH2O	0.25 m^{-1}
Solar radiation extinction - detritus	EXOM	0.2 m^{-1}
Solar radiation extinction - algae	EXA	0.2 m^{-1}
Wind-sheltering coefficient	WSC	0.6

Table 5
Water Quality Coefficient Calibration Values

State Variable	Coefficient description	Variable	Value
Diatoms	growth rate	AG	1.5 day^{-1}
	mortality rate	AM	0.08 day^{-1}
	excretion rate	AE	0.04 day^{-1}
	dark respiration rate	AR	0.04 day^{-1}
	settling rate	AS	0.1 day^{-1}
	phosphorus half-saturation for algal growth	AHSP	0.003
	nitrogen half-saturation for algal growth	AHSN	0.014
	silica half-saturation for algal growth	AHSSI	0.003
	light saturation	ASAT	100 W m^{-2}
	lower temperature for minimum algal rates	AT1	5 °C
	lower temperature for maximum algal rates	AT2	18 °C
	upper temperature for maximum algal rates	AT3	20 °C
	upper temperature for minimum algal rates	AT4	24 °C
	lower temperature rate multiplier for minimum algal rates	AK1	0.1
	lower temperature rate multiplier for maximum algal rates	AK2	0.99
	upper temperature rate multiplier for maximum algal rates	AK3	0.99
	upper temperature rate multiplier for minimum algal rates	AK4	0.01
	phosphorus to biomass ratio	ALGP	0.005
	nitrogen to biomass ratio	ALGN	0.08
	carbon to biomass ration	ALGC	0.45
	silicon to biomass ratio	ALGSI	0.18
	algae to chlorophyll *a* ratio	ACHLA	65
Greens	growth rate	AG	1.5 day^{-1}
	mortality rate	AM	0.1 day^{-1}
	excretion rate	AE	0.04 day^{-1}
	dark respiration rate	AR	0.04 day^{-1}
	phosphorus half-saturation for algal growth	AHSP	0.003 g m^{-3}
	nitrogen half-saturation for algal growth	AHSN	0.014 g m^{-3}
	silica half-saturation for algal growth	AHSSI	0.0 g m^{-3}
	settling rate	AS	0.05 day^{-1}

sheet 1 of 4

Table 5 (continued)
Water Quality Coefficient Calibration Values

State Variable	Coefficient description	Variable	Value
Greens	light saturation	ASAT	100 W m^{-2}
	lower temperature for minimum algal rates	AT1	5 °C
	lower temperature for maximum algal rates	AT2	30 °C
	upper temperature for maximum algal rates	AT3	35 °C
	upper temperature for minimum algal rates	AT4	40 °C
	lower temperature rate multiplier for minimum algal rates	AK1	0.1
	lower temperature rate multiplier for maximum algal rates	AK2	0.99
	upper temperature rate multiplier for maximum algal rates	AK3	0.99
	upper temperature rate multiplier for minimum algal rates	AK4	0.01
	phosphorus to biomass ratio	ALGP	0.005
	nitrogen to biomass ratio	ALGN	0.08
	carbon to biomass ration	ALGC	0.45
	silicon to biomass ratio	ALGSI	0.18
	algae to chlorophyll *a* ratio	ACHLA	65
Cyanobacteria	growth rate	AG	1.5 day^{-1}
	mortality rate	AM	0.08 day^{-1}
	excretion rate	AE	0.04 day^{-1}
	dark respiration rate	AR	0.04 day^{-1}
	phosphorus half-saturation for algal growth	AHSP	0.003 g m^{-3}
	nitrogen half-saturation for algal growth	AHSN	0.0 g m^{-3}
	silica half-saturation for algal growth	AHSSI	0.0 g m^{-3}
	settling rate	AS	0.1 day^{-1}
	light saturation	ASAT	100 W m^{-2}
	lower temperature for minimum algal rates	AT1	5 °C
	lower temperature for maximum algal rates	AT2	18 °C
	upper temperature for maximum algal rates	AT3	20 °C
	upper temperature for minimum algal rates	AT4	24 °C
	lower temperature rate multiplier for minimum algal rates	AK1	0.1
	lower temperature rate multiplier for maximum algal rates	AK2	0.99

sheet 2 of 4

Table 5 (continued)
Water Quality Coefficient Calibration Values

State Variable	Coefficient description	Variable	Value
Cyanobacteria	upper temperature rate multiplier for maximum algal rates	AK3	0.99
	upper temperature rate multiplier for minimum algal rates	AK4	0.01
	phosphorus to biomass ratio	ALGP	0.005
	nitrogen to biomass ratio	ALGN	0.08
	carbon to biomass ration	ALGC	0.45
	silicon to biomass ratio	ALGSI	0.18
	algae to chlorophyll *a* ratio	ACHLA	65
Phosphorus	sediment release rate of phosphorous	PO4R	0.001
	fraction of phosphorus in organic matter	ORGP	0.005
Ammonium	ammonium decay rate, day^{-1}	NH4DK	0.04
	sediment release rate of ammonium (fraction of SOD)	NH4R	0.02
	lower temperature for ammonium decay,	NH4T1	5.0 °C
	upper temperature for ammonia decay	NH4T2	30.0 °C
	lower temperature rate multiplier for ammonium decay	NH4K1	0.1
	upper temperature rate multiplier for ammonium decay	NH4K2	0.99
Nitrate	nitrate decay rate, day^{-1}	NO3DK	0.01
	lower temperature for nitrate decay	NO3T1	5.0 °C
	upper temperature for nitrate decay	NO3T2	30 °C
	lower temperature rate multiplier for nitrate decay	NO3K1	0.1
	upper temperature rate multiplier for nitrate decay	NO3K2	0.99
Silica	sediment release rate	DSIR	0.1
	particulate biogenic silica settling rate	PSIS	0.04 m day^{-1}
	particulate biogenic silica decay rate	PSIDK	0.3 day^{-1}
Carbon	labile DOM decay rate	LDOMDK	0.12 day^{-1}
	refractory DOM decay rate	RDOMDK	0.001 day^{-1}
	labile to refractory DOM decay rate	LRDDK	0.001 day^{-1}
	labile POM decay rate	LPOMDK	0.08 day^{-1}
	refractory POM decay rate	RPOMDK	0.001 day^{-1}
	labile to refractory POM decay rate	LRPDK	0.001 day^{-1}

Sheet 3 of 4

Table 5 (Concluded)
Water Quality Coefficient Calibration Values

State Variable	Coefficient description	Variable	Value
Carbon	POM settling rate	POMS	0.5 m day^{-1}
	fraction of algae to POM	APOM	0.8
	fraction of carbon in organic matter	ORGC	0.45
	lower temperature for carbon decay,	OMT1	5.0 °C
	upper temperature for carbon decay	OMT2	30.0 °C
	lower temperature rate multiplier for carbon decay	OMK1	0.1
	upper temperature rate multiplier for carbon decay	OMK2	0.99
Sediment	sediment decay rate	SDK	0.1 day^{-1}
	zero-order sediment oxygen demand	SOD	1 g m^{-2} day^{-1}
	lower temperature for sediment decay	SODT1	5.0 °C
	upper temperature for sediment decay	SODT2	30.0 °C
	lower temperature rate multiplier for sediment decay	SODK1	0.1
	upper temperature rate multiplier for sediment decay	SODK2	0.99
Oxygen	oxygen limit for anaerobic processes	O2LIM	0.05 g m^{-3}
	stoichiometric ratio for nitrification	O2NH4	4.57
	stoichiometric ratio for organic matter decay	O2OM	1.4
	stoichiometric ratio for algal respiration	O2AR	1.1
	stoichiometric ratio for algal growth	O2AG	1.4

Sheet 4 of 4

1994

Water Surface Elevations. The water surface elevations were characterized by an increase of approximately two meters during spring, a rapid decrease in mid-may, and only a slight decrease throughout the summer. Predicted elevations were almost an overlay of the observed values (Figure 4).

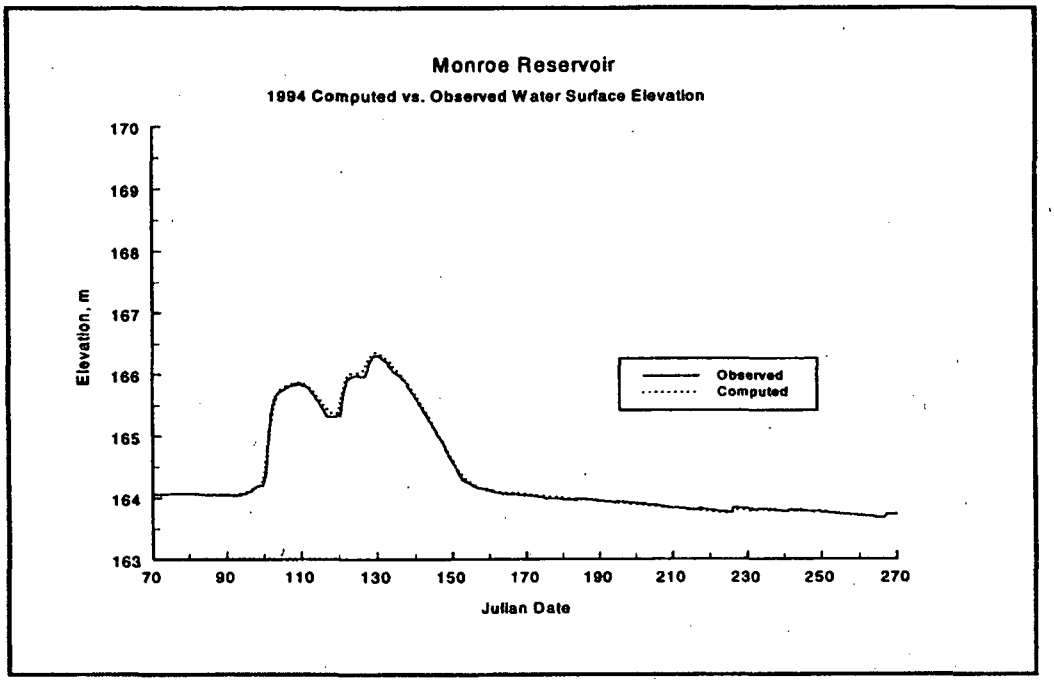

Figure 4. 1994 computed versus observed water surface elevations

Temperature. When interpreting predictions from CE-QUAL-W2, three points should be considered. First, temperature predictions are averaged over the length, height, and width of a cell. Observed data represent observations at a specific point within the reservoirs. Secondly, meteorological data were applied over the entire reservoir from one station located approximately 48 km from the project. Finally, computed temperatures are subject to large daily variations depending upon how rapidly inflows, outflows, and meteorological inputs are changing. The RMS can change more than one degree Celsius over a 24 hour period.

Observed and computed temperature profiles for the three stations are shown in Figures 5-7. Computed temperatures were in good agreement with observed for all dates at station 1. Notice the difference in the statistics from May 2 to May 3. The computed profile on May 2 exhibits the same observed behavior but is cooler. One day later on May 3, the model predictions have improved as evidenced by the lower RMS. Clearly, interpretation of model output must be tempered with the realization that temperature and other water quality predictions can exhibit a fairly large change from one day to the next.

Observed and computed temperature profiles for station 35 are shown in Figure 6. Similar to results at station 1, computed and observed data were in close agreement for all dates except May 23. The computed profile on this date is not as stratified as the observed profile. As with station 1, the statistics can change considerably from one day to the next as evidenced on April 12 and 13 where the AME and RMS have decreased by nearly 1 °C. The greatest differences between observed and computed temperature profiles occur at station 3. This is most likely due to inaccuracies in the inflow temperatures since this station

is located closest to the upstream boundary. Most of the discrepancies are due to underprediction of temperatures in the lower layers.

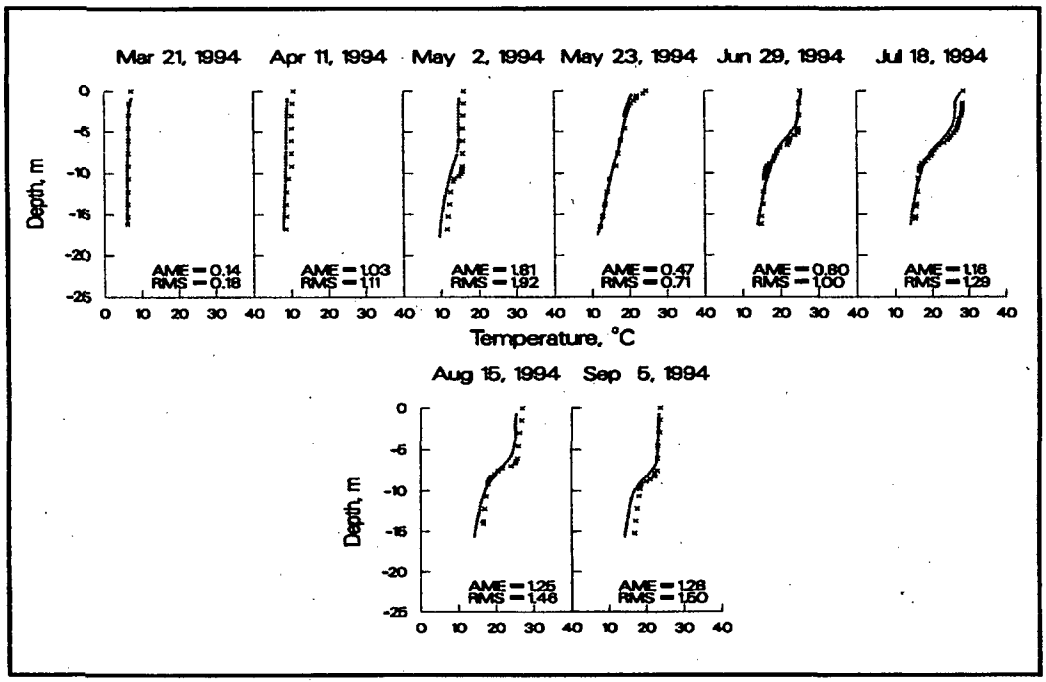

Figure 5. 1994 computed versus observed temperatures at station 1

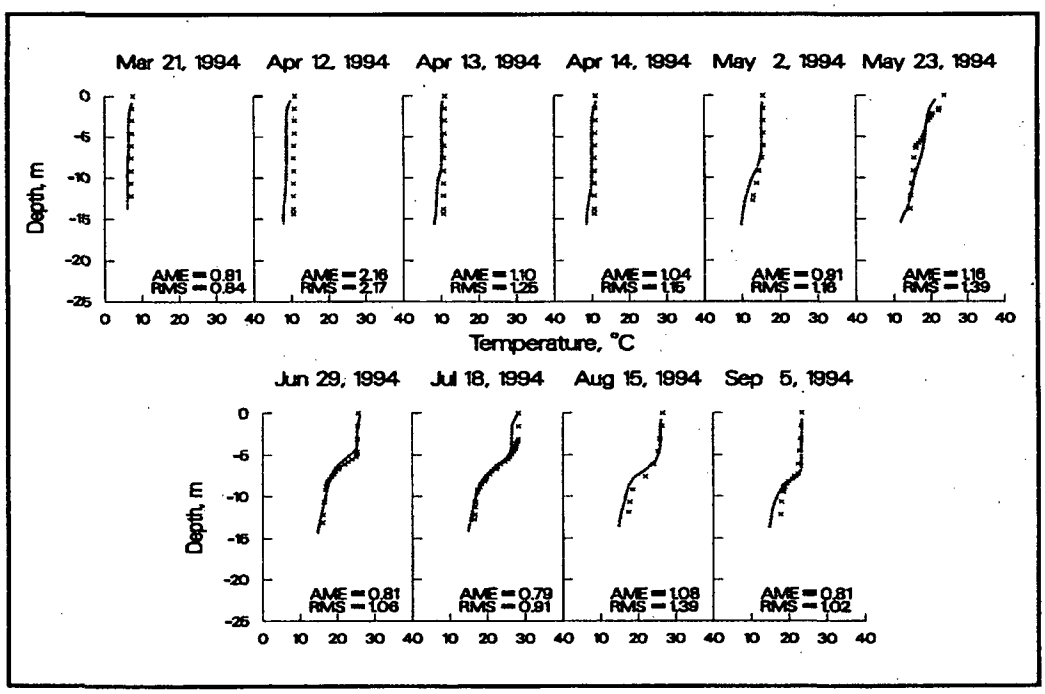

Figure 6. 1994 computed versus observed temperatures at station 35

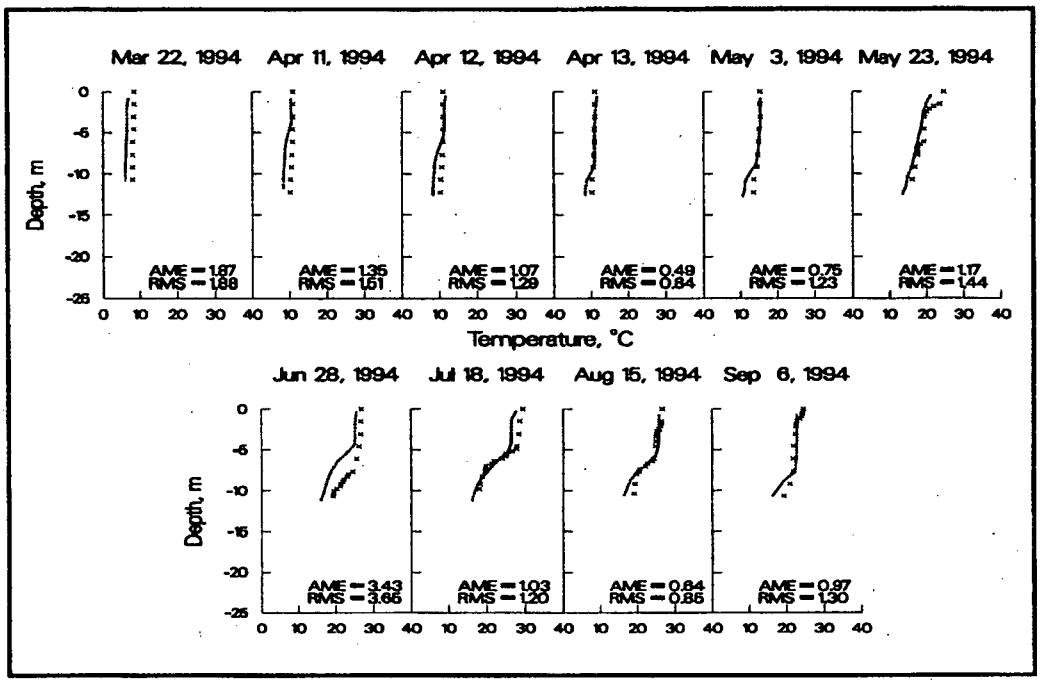

Figure 7. 1994 computed versus observed temperatures at station 3

Dissolved Oxygen. Observed and computed DO profiles for the three stations are shown in Figures 8-10. For station 1, the model captures the onset of hypoxia from April to May and the subsequent development of the anoxic hypolimnion from June to September.

The greatest discrepancies occur in the metalimnion at station 1 during mid-summer where the model tends to overpredict the chemocline depth. Sensitivity analyses showed that the depth of the chemocline with respect to DO is affected by the placement of inflows which are in turn dependent on inflow temperatures. If the inflow temperatures are a few degrees colder than actual inflow temperatures, then the inflows will be placed deeper than the actual inflows and more oxygen from the upstream boundary will be delivered to a greater depth. It is believed that more accurate inflow temperatures will result in more accurate thermal and DO predictions.

The effect of when computed and observed data are compared is illustrated during the two day period from June 28-30. The AME has decreased nearly 0.5 °C while the RMS has decreased about 0.8 °C.

At station 35, the model is capturing the temporal and spatial trends in DO. As mentioned for station 1, the date at which observed data are compared affects the perception of results. From June 28 to June 29, the AME has decreased from 0.75 to 0.46 and the RMS has decreased from 1.25 to 0.8.

For most dates at station 3, computed and observed profiles are in close agreement and show similar stratification trends. Note the change in statistics over the three day period from May 22-24.

Overall, DO predictions are in good agreement with observed DO. The model is accurately reproducing the spatial and temporal trends of DO within Lake Monroe for 1994.

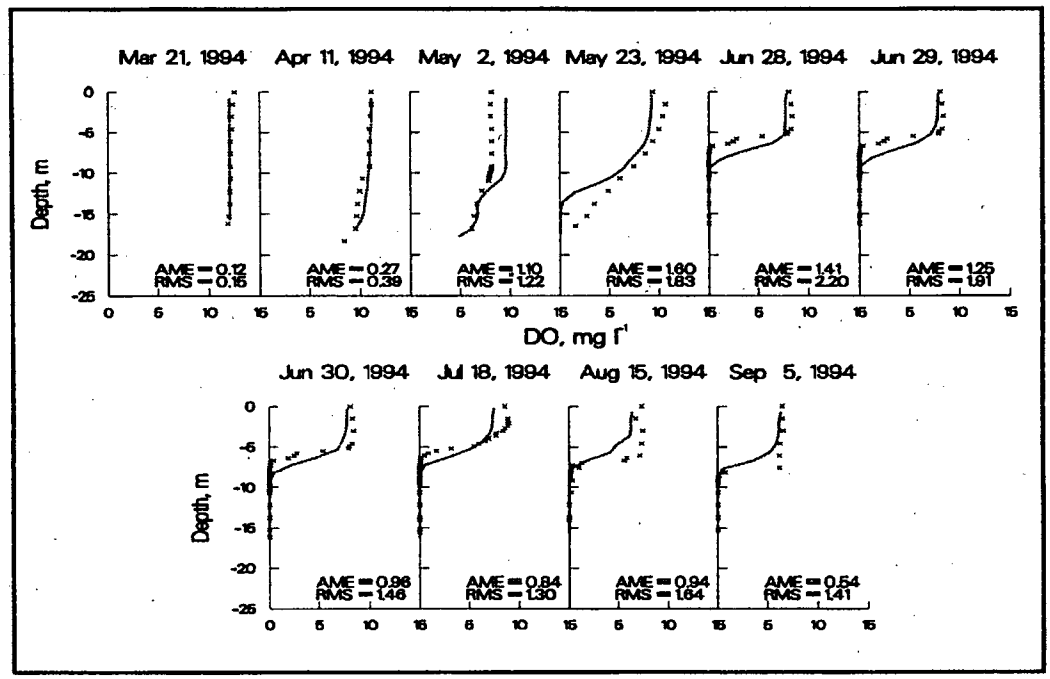

Figure 8. 1994 computed versus observed DO at station 1

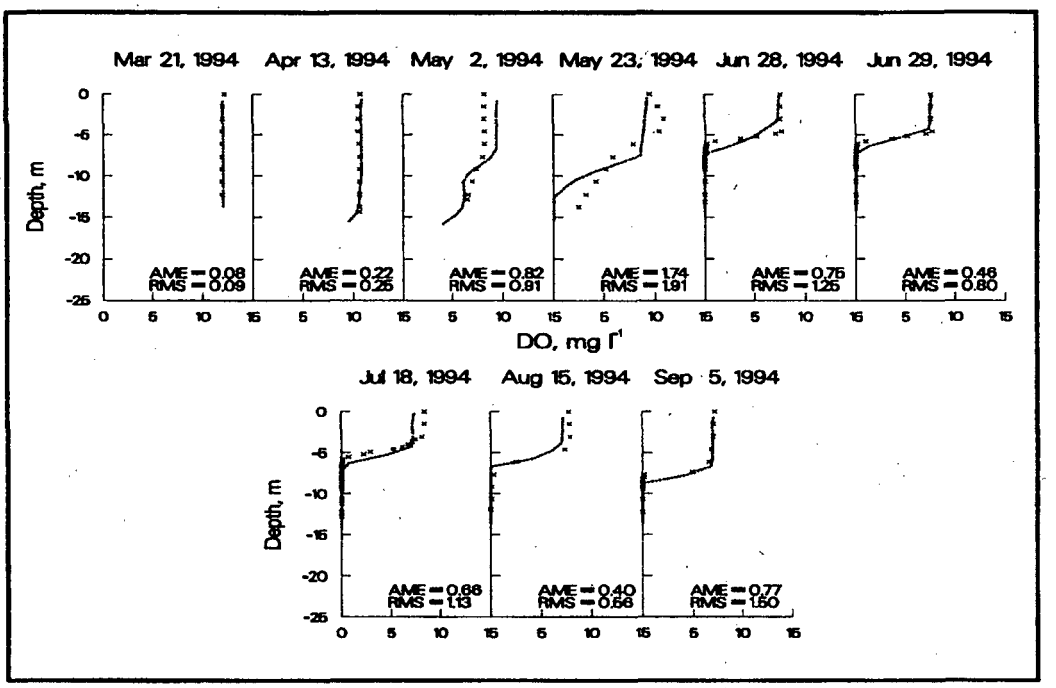

Figure 9. 1994 computed versus observed DO at station 35

Phosphorus. Figures 11-13 show the results for phosphorus. Soluble reactive phosphorus (SRP) measurements were used to represent orthophosphate available for algal uptake in the

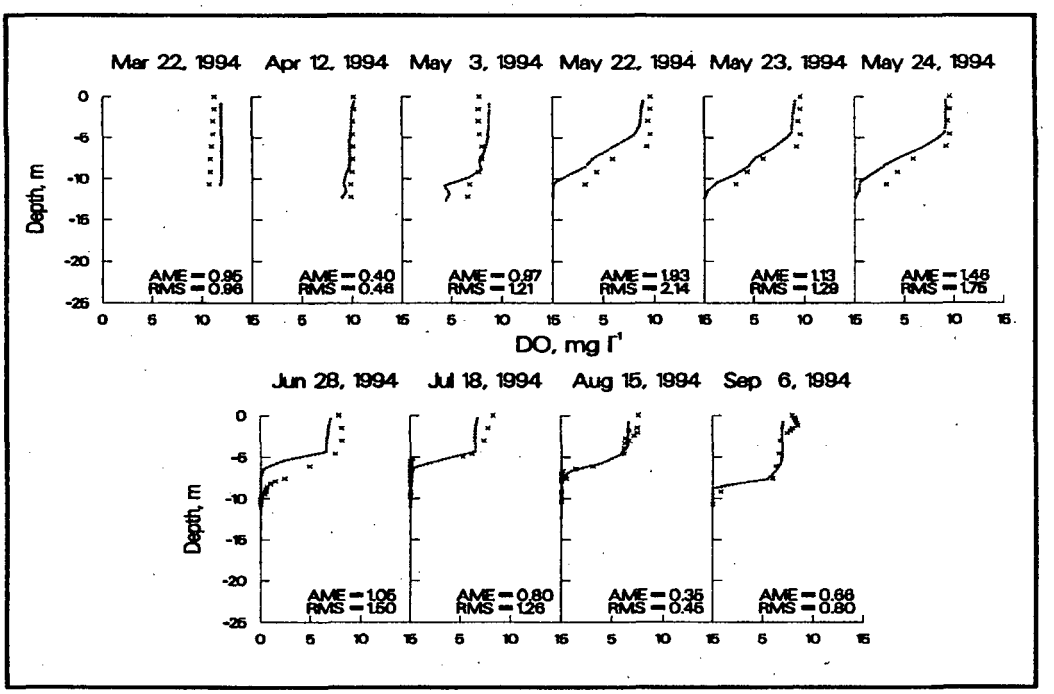

Figure 10. 1994 computed versus observed DO at station 3

study. For all profiles at all stations and inflowing concentrations, observed orthophosphate was at the detection limit (0.005 gm m^{-3}). Discussions with Louisville District personnel indicated that there may have been problems with the analytical procedures to determine orthophosphate concentrations determined by the soluble reactive phosphorus given in Standard Methods. However, algal dynamics were reasonably captured using the detection limit values. This is an indication that the observed orthophosphate concentrations may have been at or below the detection limit. This is not an uncommon situation in the photic zone where algae are rapidly growing.

Table 7 lists the observed phosphorus data available at the three stations located on the North, Middle, and South Forks of Salt Creek (stations 13001, 14001, and 15001, respectively). As can be seen, the observed phosphorus data for determining phosphorus loadings was extremely limited. Orthophosphorus and dissolved inorganic phosphorus were available for only one date in 1994 and dissolved inorganic phosphorus was available for only one date in 1995. Data were insufficient for developing any sort of relationship for phosphorus available for algal uptake and any other phosphorus form(s).

Although good reproduction of algal biomass was obtained using the detection limit data for SRP for 1994, there is some reason to question the data. The most important reason is the lack of increase in hypolimnetic SRP during anoxic conditions when phosphate should be released from the sediments. Due to lack of data, there is little additional evidence to support this contention except for data on a single date collected on July 19 for dissolved inorganic phosphorus where the concentration increased from 3 g m^{-3} in the surface waters to 119 g m^{-3} at the bottom.

In the model during anoxic conditions, phosphorus is being released from the sediments. This is consistent with most reservoirs that have an anoxic hypolimnion. The increase in hypolimnetic phosphorus in the model is a result of allowing zero-order phosphorus release during anoxic conditions. The model could be made to more closely reproduce the observed data by setting the phosphorus release rate to zero. However, without additional evidence that phosphorus is not being released from the sediments during anoxic conditions, phosphorus should be released from the sediments. More sampling needs to be done on Lake Monroe to determine what is occurring with phosphorus sediment recycling during anoxic conditions.

Table 7
Upstream boundary phosphorus samples

Station	Phosphorus species	Number of Samples			
		1992	1994	1995	1996
13001	Unfiltered water	4	1	1	2
	dissolved	4	1	2	2
	ortho	0	1	0	0
	dissolved inorganic	0	1	1	0
	total inorganic	0	1	1	0
14001	Unfiltered water	3	1	1	2
	dissolved	4	1	2	2
	ortho	0	1	0	0
	dissolved inorganic	0	1	1	0
	total inorganic	0	1	1	0
15001	Unfiltered water	3	1	1	2
	dissolved	4	1	2	2
	ortho	0	1	0	0
	dissolved inorganic	0	1	1	0
	total inorganic	0	1	1	0

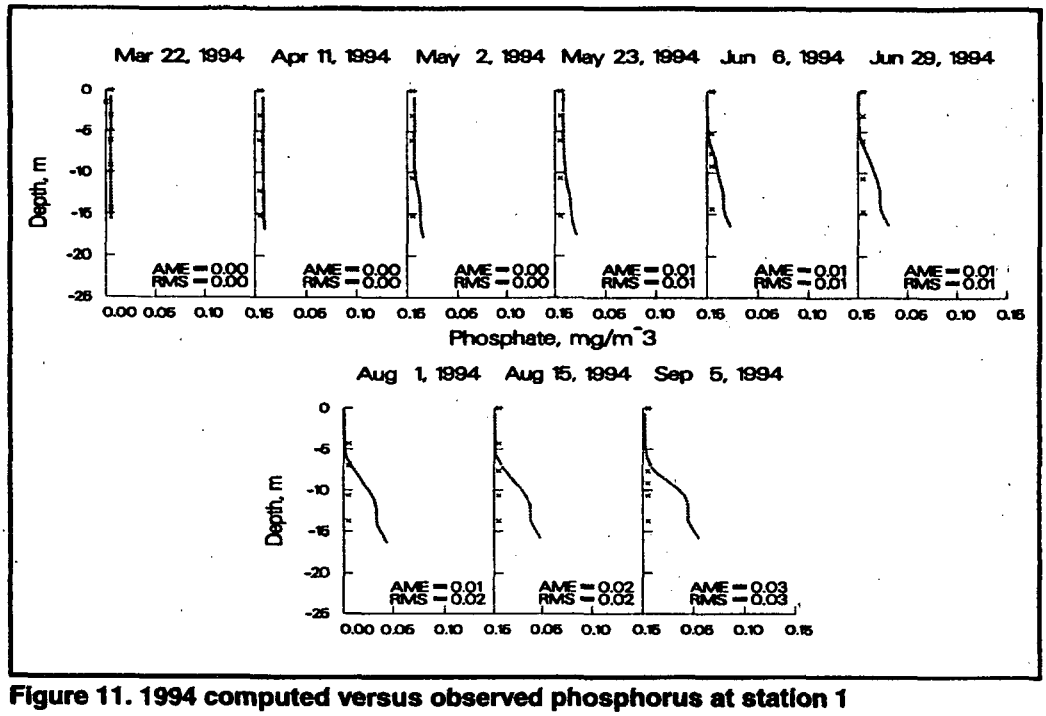

Figure 11. 1994 computed versus observed phosphorus at station 1

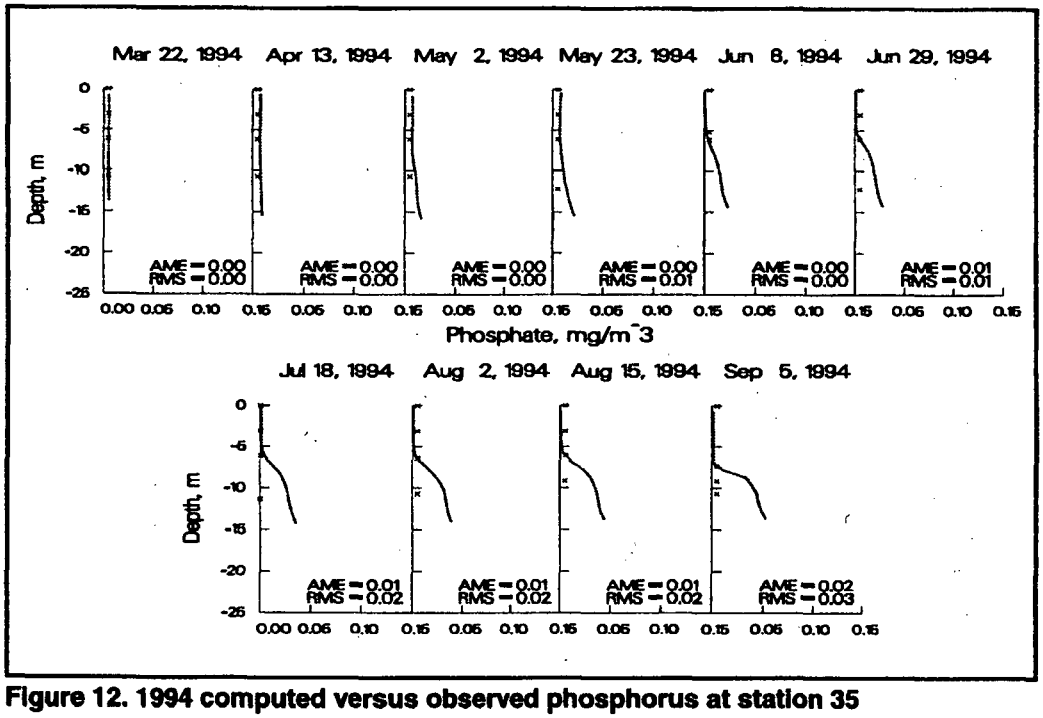

Figure 12. 1994 computed versus observed phosphorus at station 35

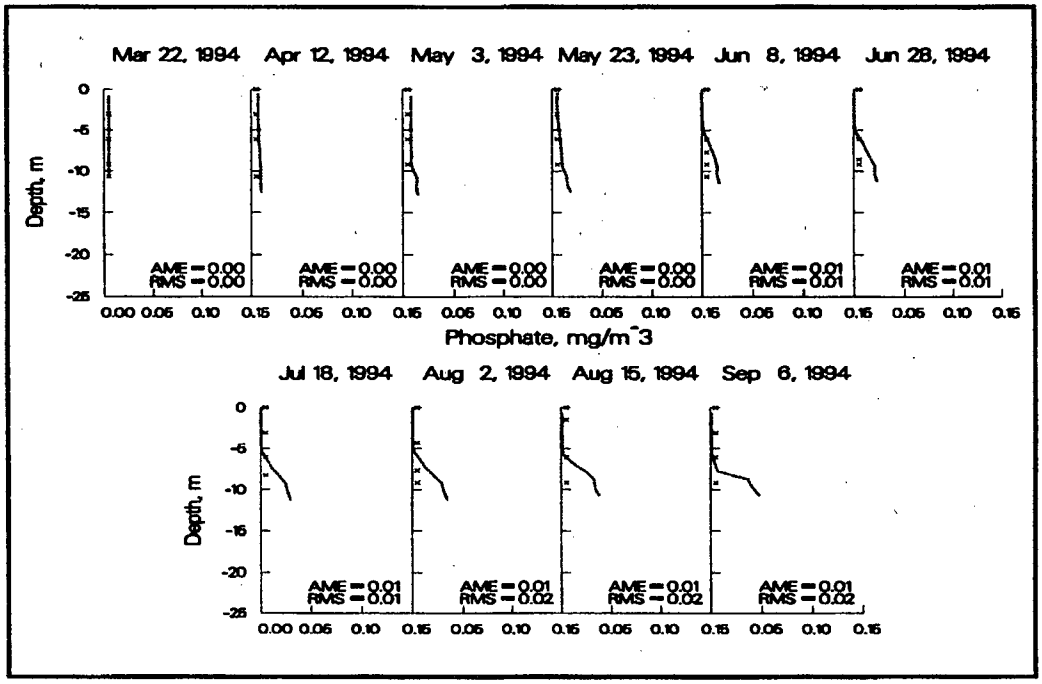

Figure 13. 1994 computed versus observed phosphorus at station 3

Ammonium. Results for ammonium are given in figures 14-16 for the three stations. The buildup of hypolimnetic ammonium as it is being released from the sediments during anoxic conditions is accurately represented by the model.

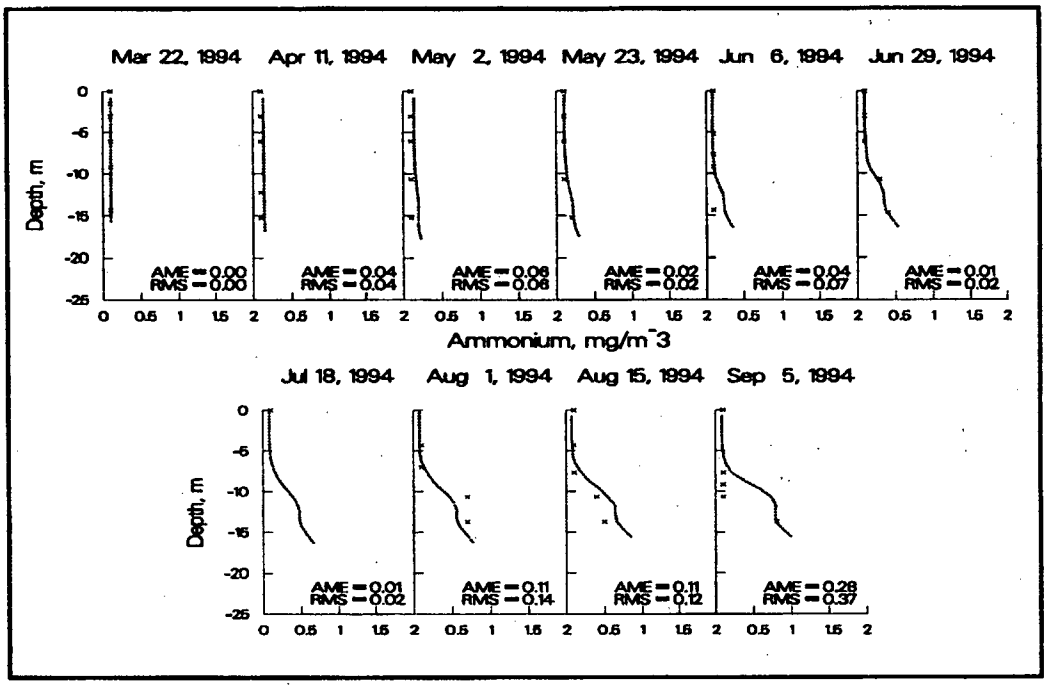

Figure 14. 1994 computed versus observed ammonium at station 1

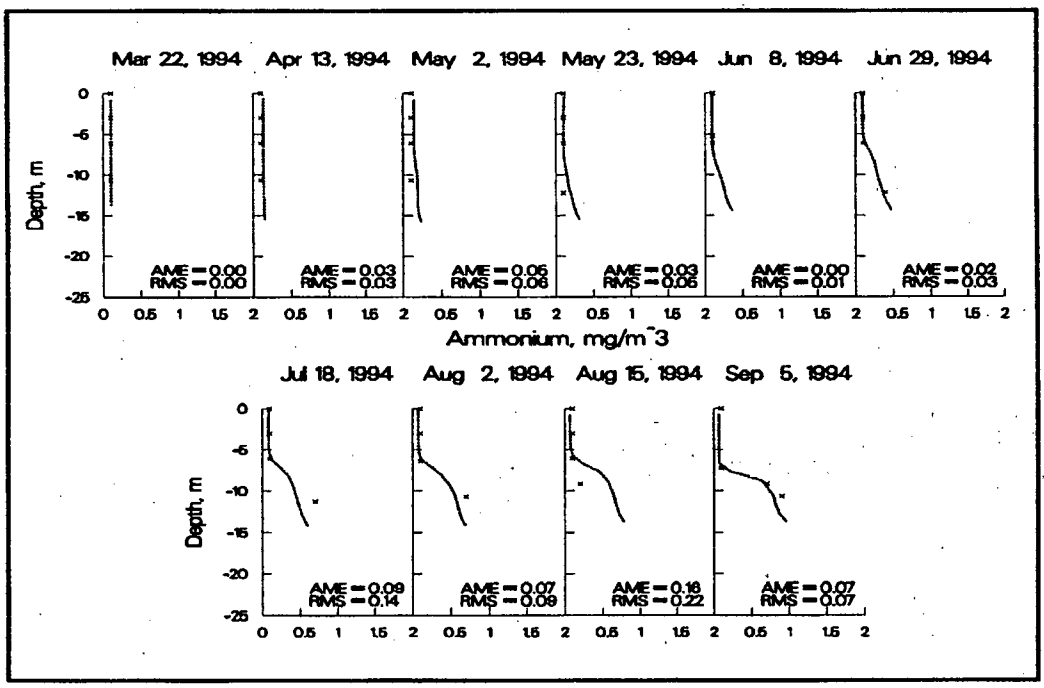

Figure 15. 1994 computed versus observed ammonium at station 35

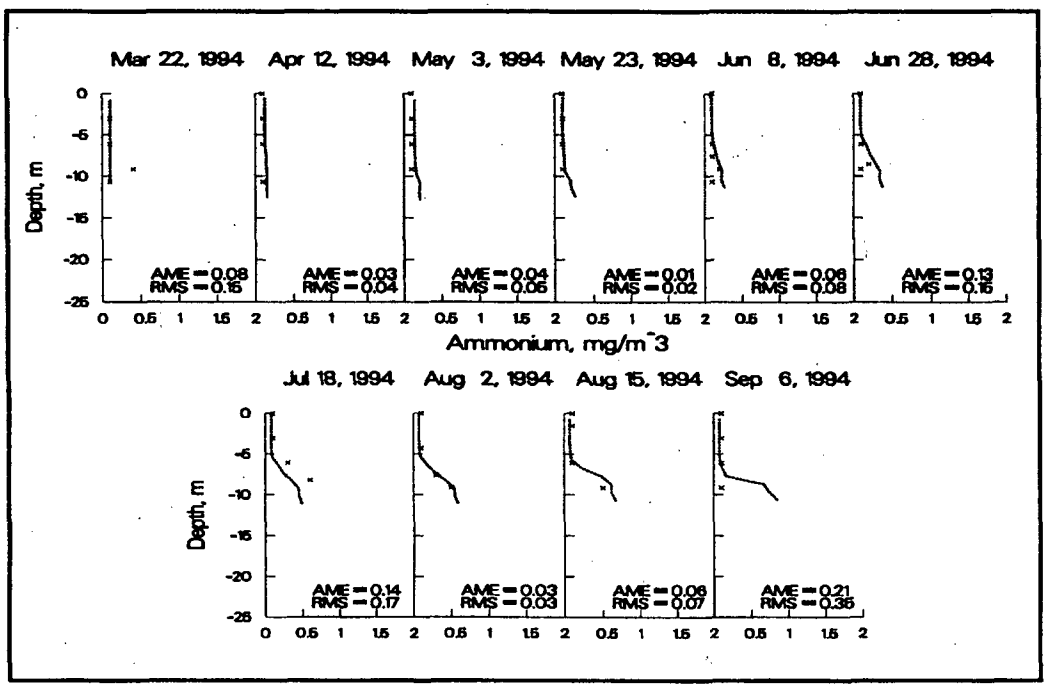

Figure 16. 1994 computed versus observed ammonium at station 3

Nitrate-nitrite. Results for nitrate-nitrite are given in figures 17-19. The model is capturing the trends of decreasing nitrate throughout the water column during the stratification season. The model is also capturing the additional decrease in hypolimnetic concentrations in May and June. Although the model underpredicts hypolimnetic concentrations in July through September, this is believed due to detection limits for the observed data.

The increase in hypolimnetic nitrate-nitrite concentrations from April to May at station 1 is illustrative of the care that must be taken when evaluating model performance. There is no mechanism in the model that can account for increased nitrate-nitrate concentrations other than through ammonia nitrification or inflow loadings. A near doubling of concentration over the period from April 11 to May 2 is unlikely due to ammonia nitrification. If the data are to be believed, then the only other mechanism in the model and in the prototype that could account for this increase is an increase in loadings. The sparsity of upstream data means that the model could not be expected to account for the increase in hypolimnetic nitrate-nitrite concentrations.

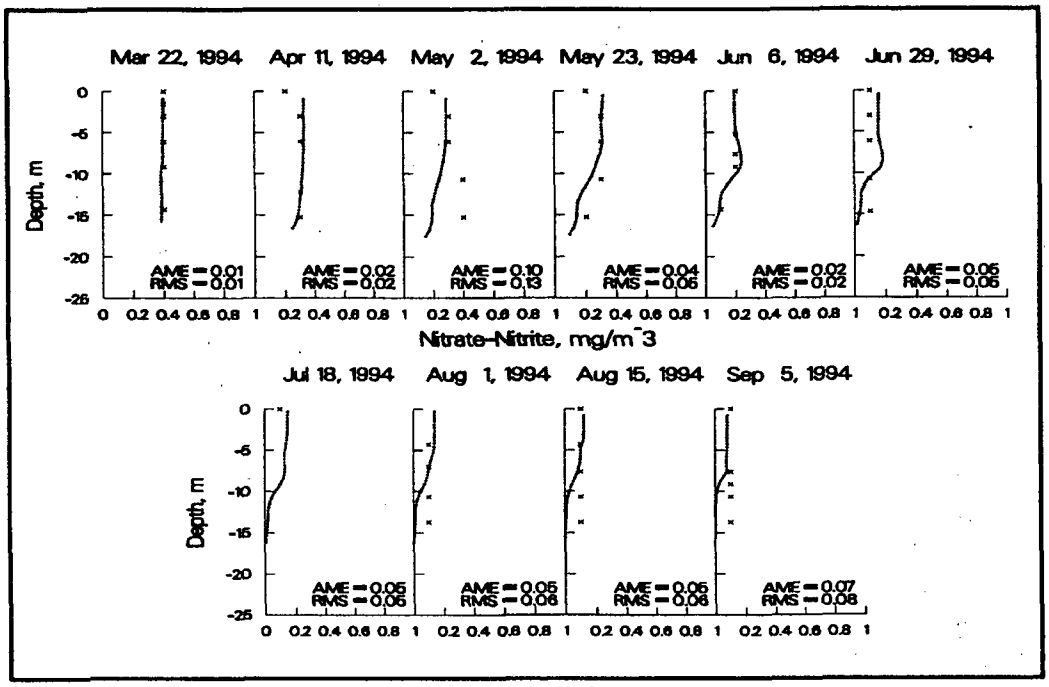

Figure 17. 1994 computed versus observed nitrate-nitrite at station 1

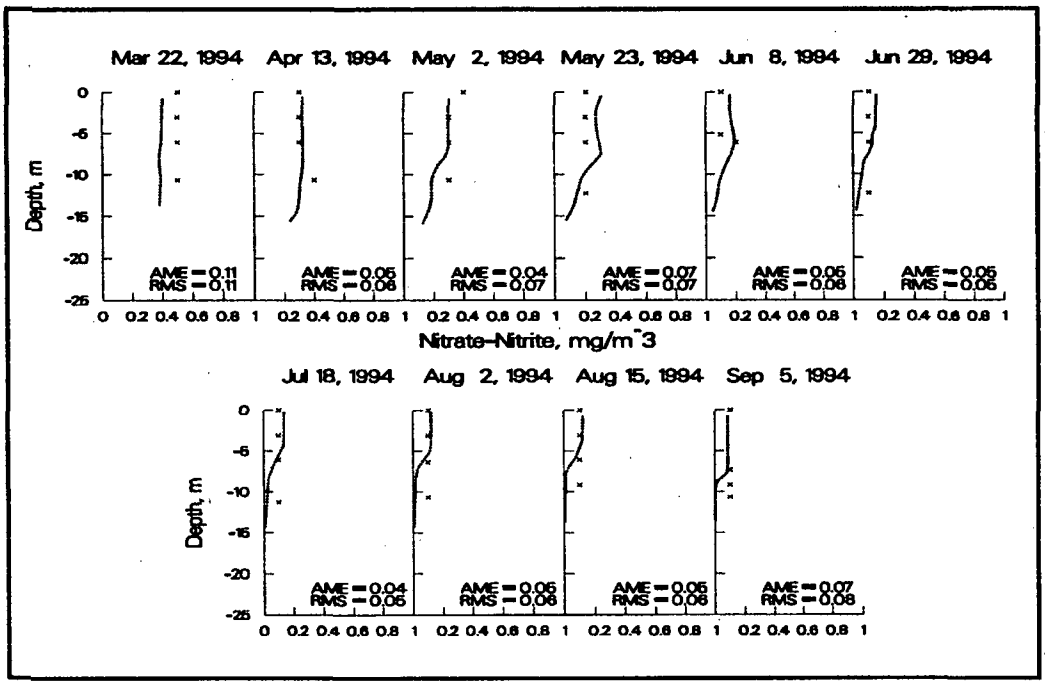

Figure 18. 1994 computed versus observed nitrate-nitrite at station 35

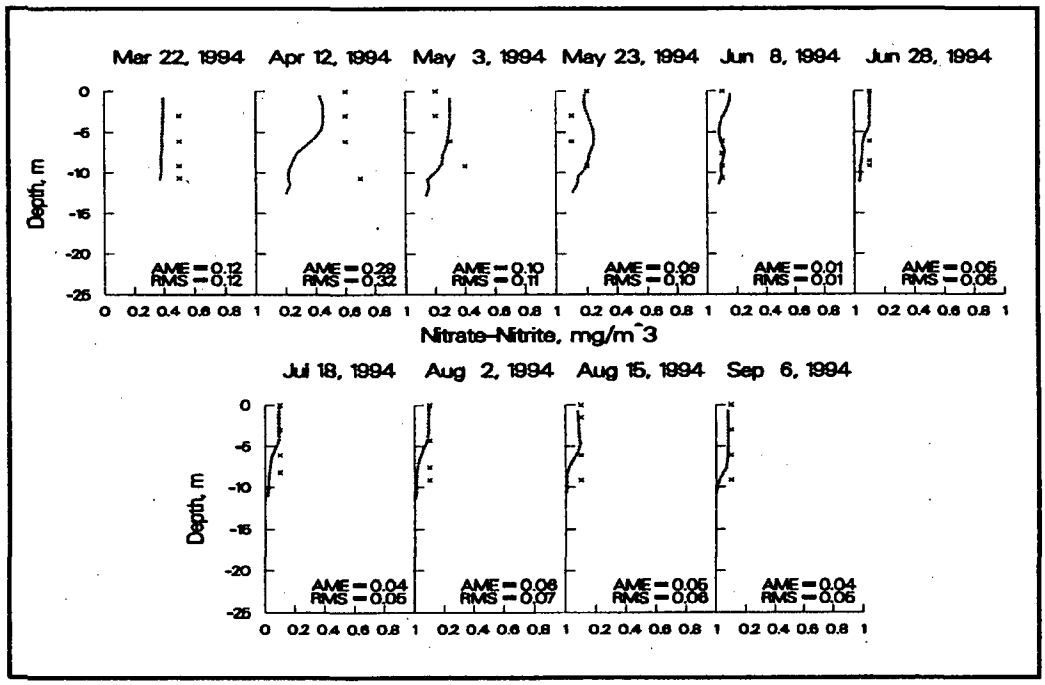

Figure 19. 1994 computed versus observed nitrate-nitrite at station 3

Algae. Figures 20-22 show computed and observed algal profiles for the three stations. Algae in the figures represents the sum of diatoms, greens, and cyanobacteria. For most dates there is close agreement between computed and observed profiles indicating that the algal/nutrient dynamics are being correctly simulated. The model was able to reproduce the large increase in algal biomass from May 24 to June 7. Given the problems associated with determining algal biomass from chlorophyll *a* measurements, the model is doing a good job of simulating algal dynamics.

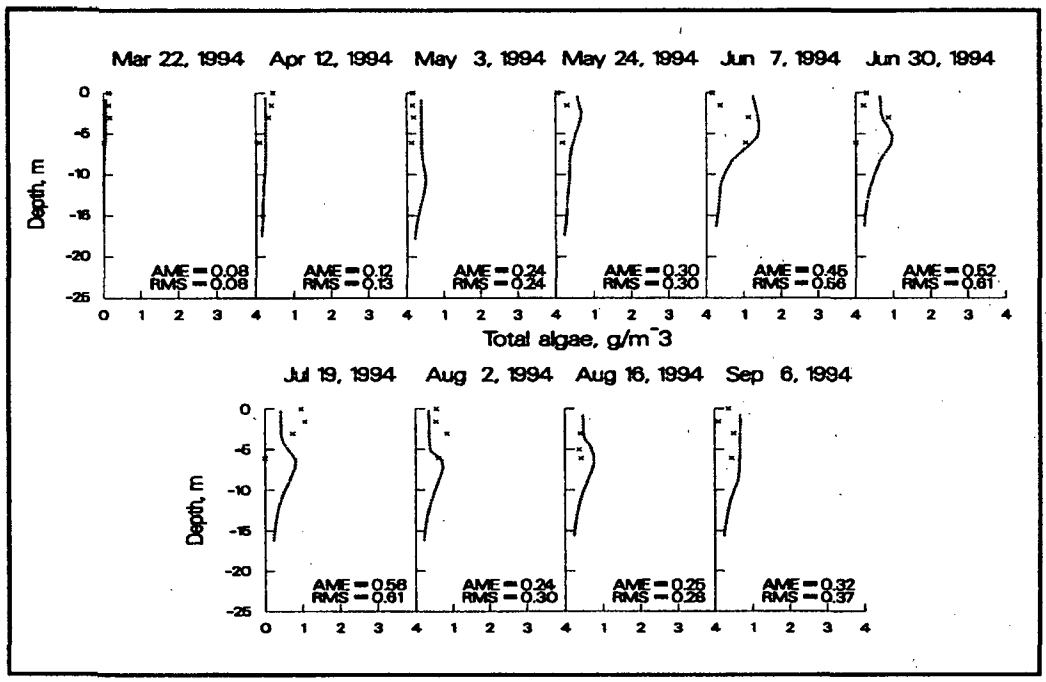

Figure 20. 1994 computed versus observed algae at station 1

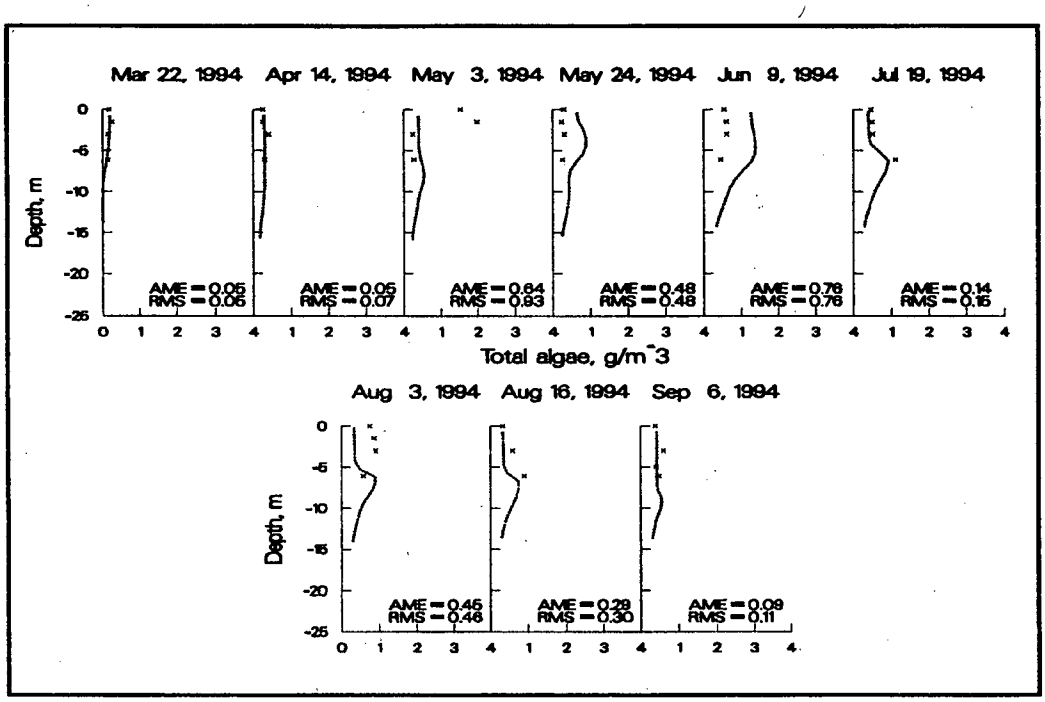

Figure 21. 1994 computed versus observed algae at station 35

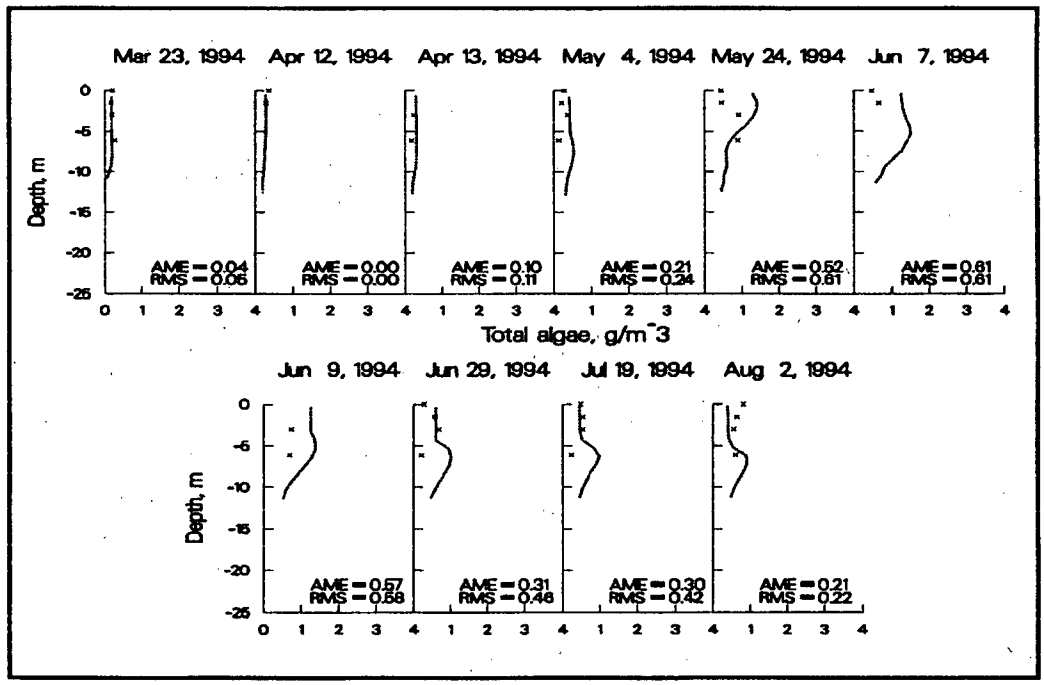

Figure 22. 1994 computed versus observed algae at station 3

1992

Water Surface Elevations. Compared to 1994, water surface elevations showed more variation throughout the summer. An increase of less than one meter occurred in spring followed by another increase at the beginning of August. Predicted elevations are almost an overlay of the observed values (Figure 23).

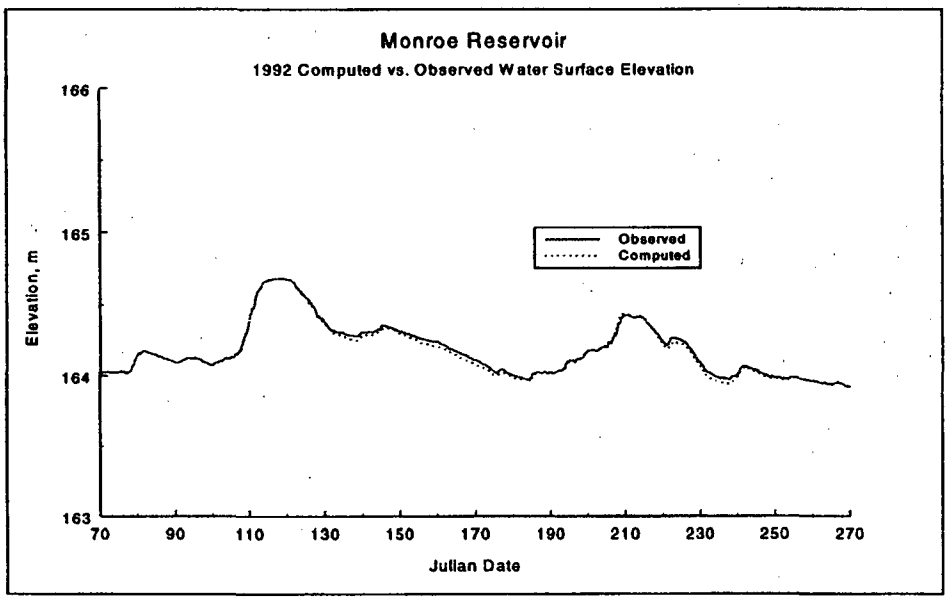

Figure 23. 1992 computed versus observed water surface elevations

Temperature. Figures 24-26 show the computed and observed temperature profiles at the three stations. Spatial and temporal trends at all stations were captured by the model. Computed and observed profiles at station 1 for all dates are generally in agreement, except for June 17. On this date, the temperatures in the epilimnion are colder compared to observed. However, model predictions are in much closer agreement than either June 16 or June 18. Computed results at station 35 had only two dates for comparison but both were in close agreement with observed. Computed results at station 3, which again had only two dates available for comparison, were also in close agreement.

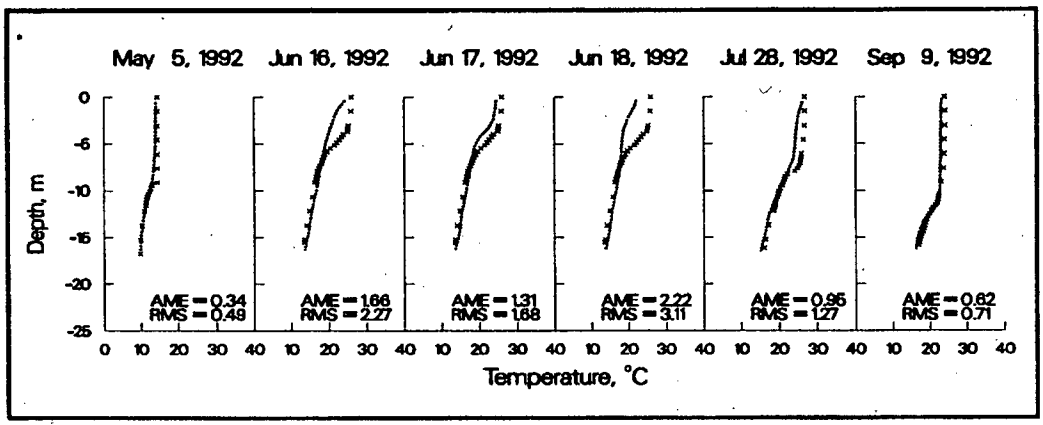

Figure 24. 1992 computed versus observed temperatures at station 1

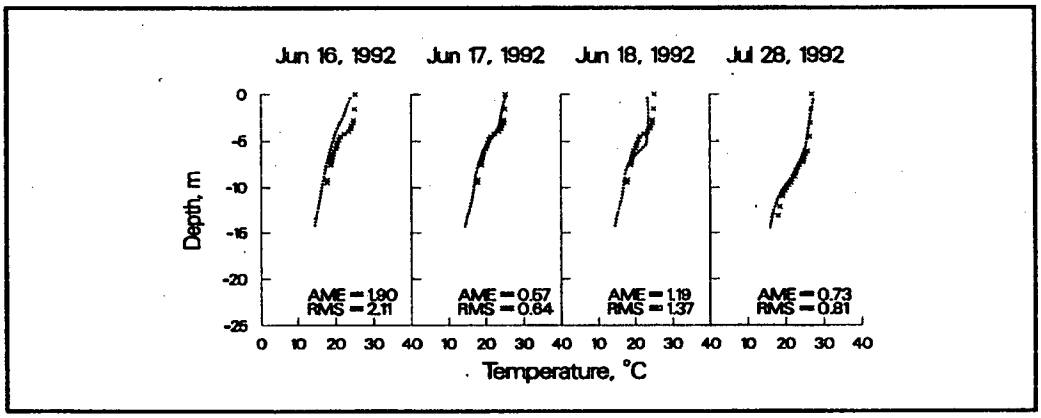

Figure 25. 1992 computed versus observed temperatures at station 35

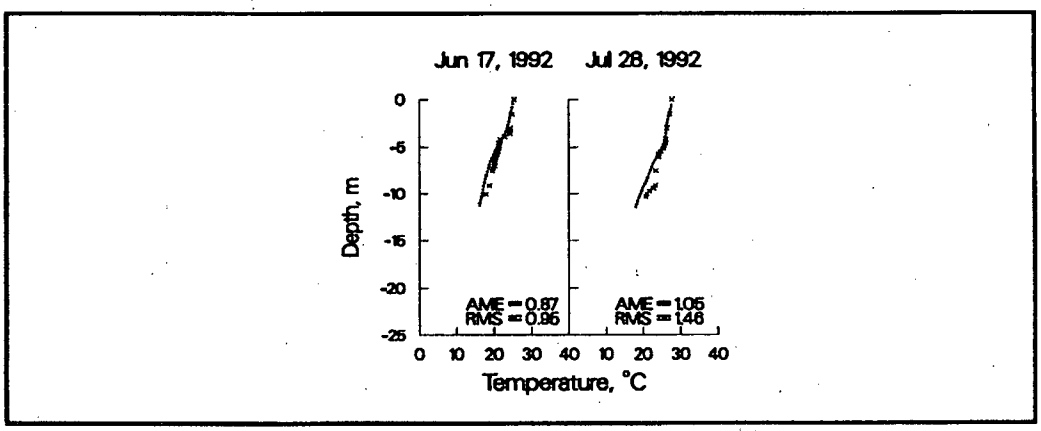

Figure 26. 1992 computed versus observed DO at station 1

Dissolved Oxygen. Computed and observed DO profiles are shown in Figures 27- 29 for the three stations. Although the model is capturing the increased DO demand in warmer months,

the chemocline at all stations is deeper than the observed for most dates. As in 1994, this is attributed to inaccuracies in upstream inflow temperatures.

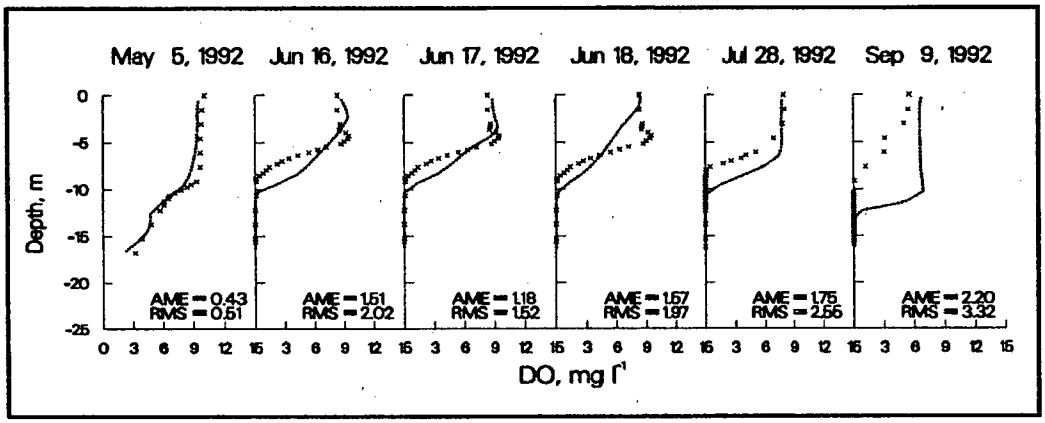

Figure 27. 1992 computed versus observed DO at station 3

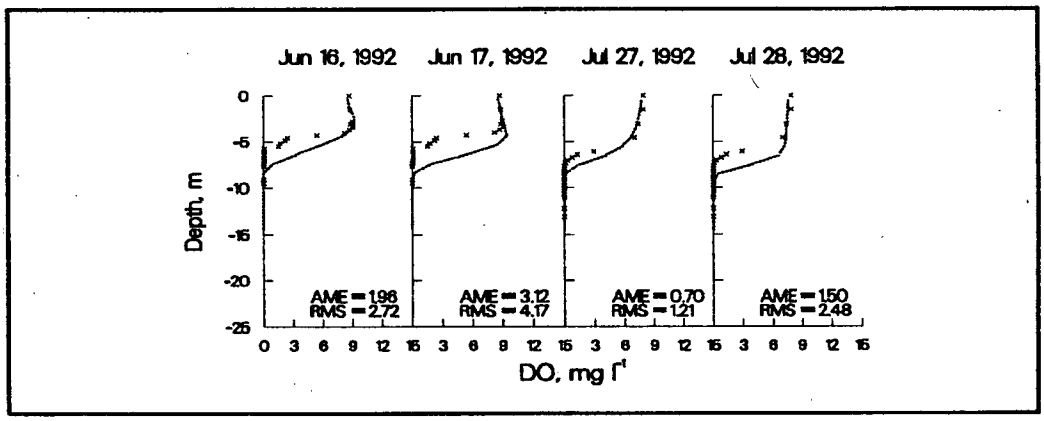

Figure 28. 1992 computed versus observed temperatures at station 3

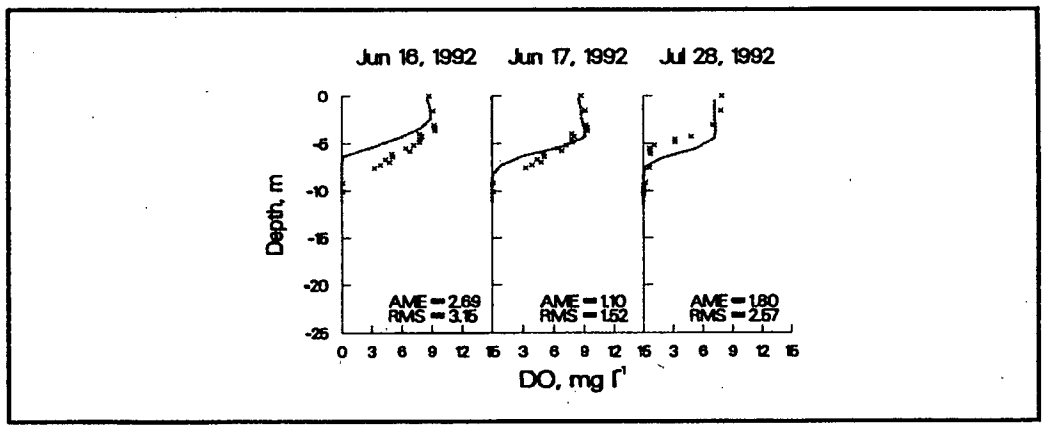

Figure 29. 1992 computed versus observed DO at station 35

Algae. Figures 30-32 present computed and observed algal profiles. For most dates, algal concentrations are overpredicted by approximately 1 gm m^{-3} at most. Overprediction of algae is attributed to not having actual inflow nutrient and algal data for this year. Inflow data from 1994 were used instead. Inaccuracies in algal predictions also affected DO predictions due to excessive oxygen production in the photic zone.

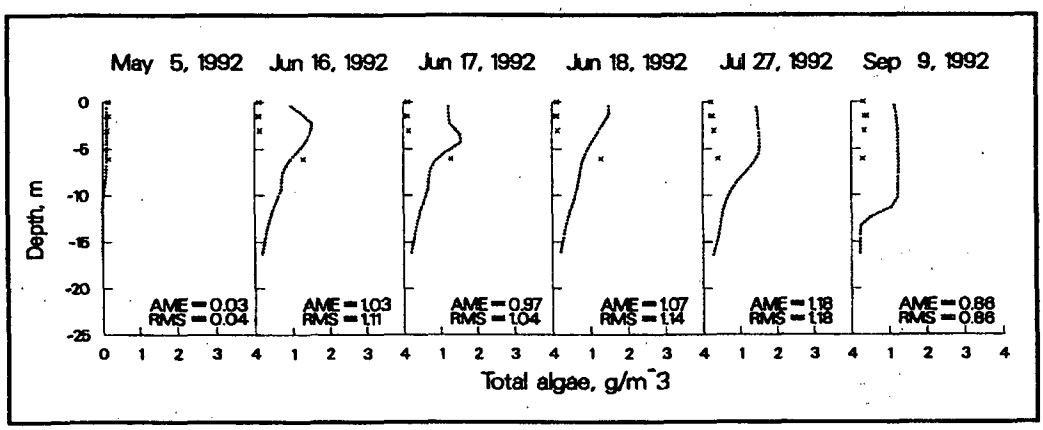

Figure 30. 1992 computed versus observed algae at station 1

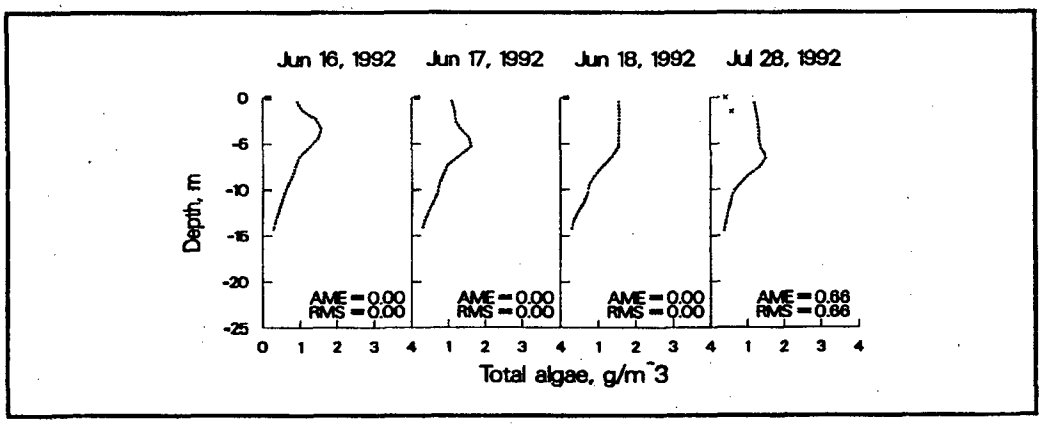

Figure 31. 1992 computed versus observed algae at station 35

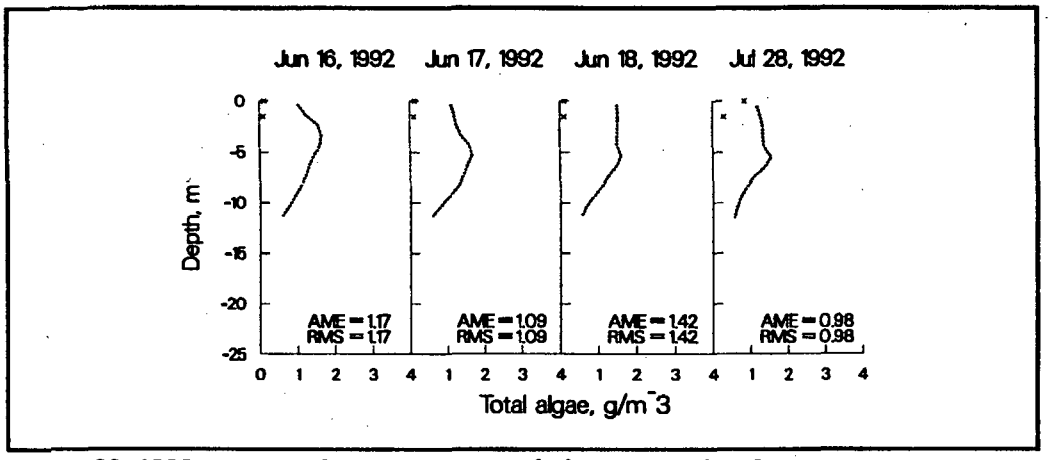

Figure 32. 1992 computed versus observed algae at station 3

1995

Water Surface Elevations. Water surface elevations showed a much larger increase (≈4 m) which extended later into the year than in either 1994 or 1992. Another slight increase occurred at the end of August. Predicted water surface elevations almost an overlay of the observed values (Figure 33).

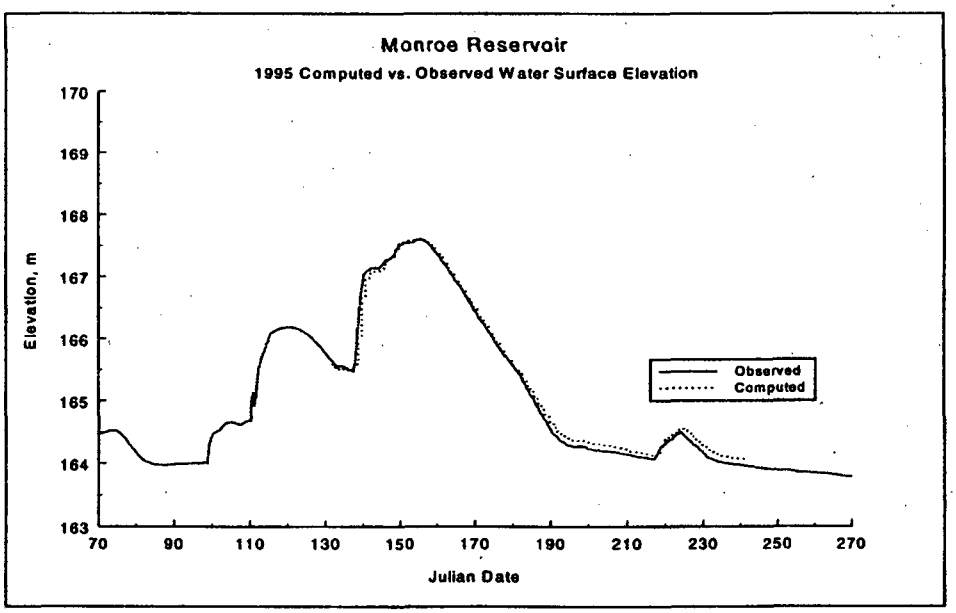

Figure 33. 1995 computed versus observed water surface elevation

Temperature. Figures 34-36 show the computed and observed temperature profiles at the three stations. As in 1994 and 1992, the spatial and temporal trends are being captured by the model. During 1995, most of the temperature profiles at all stations are slightly underpredicted. The additional plots for June 20 are due to additional profiles taken on this date.

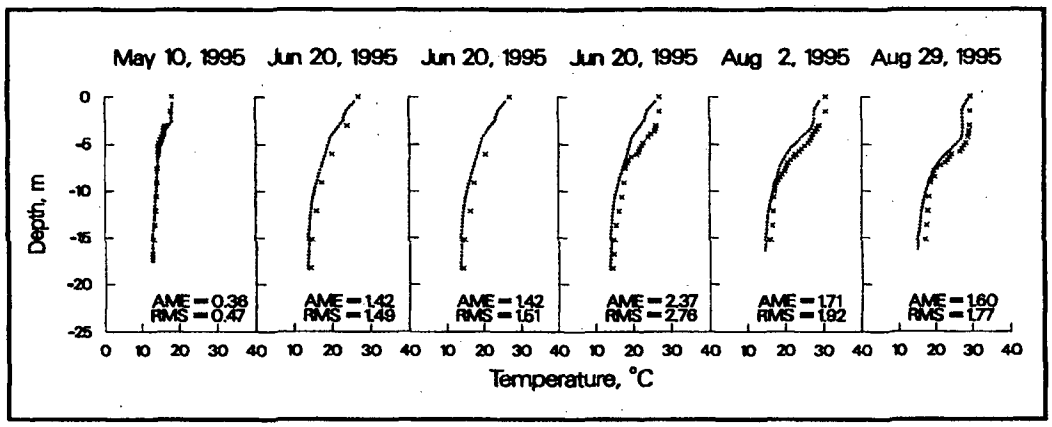

Figure 34. 1995 computed versus observed temperature at station 1

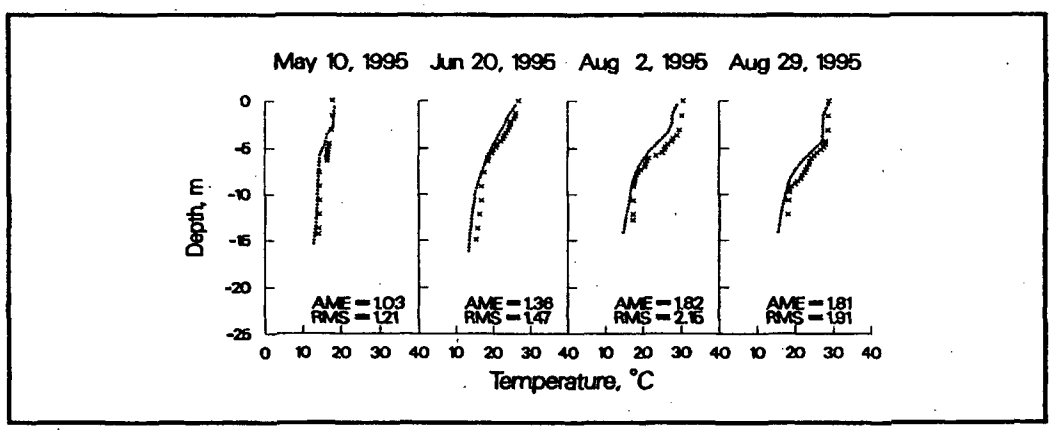

Figure 35. 1995 computed versus observed temperature at station 35

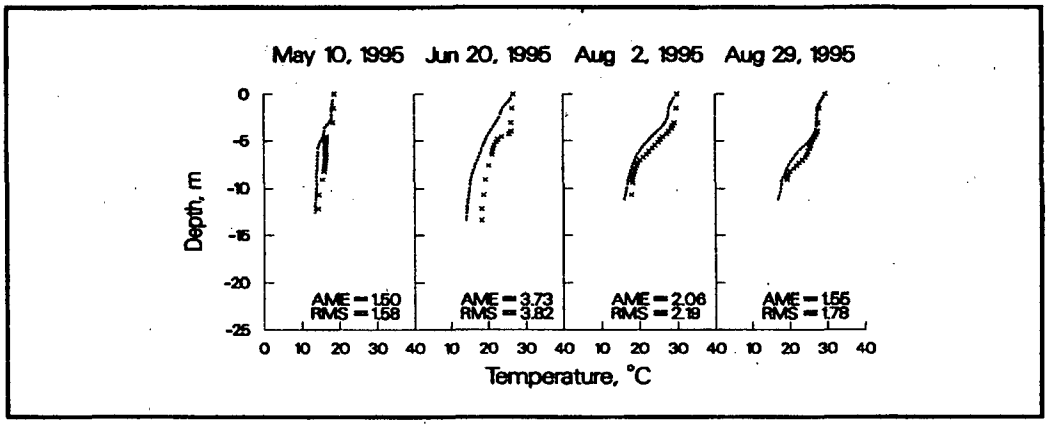

Figure 36. 1995 computed versus observed temperature at station 3

Dissolved Oxygen. Computed and observed DO profiles are shown in Figures 37-39 for the three stations. The model is capturing the trend in oxygen demand as summer progresses to fall. Computed and observed profiles at all stations were generally in close agreement except on June 20 where the chemocline depth at stations 1 and 35 is overpredicted.

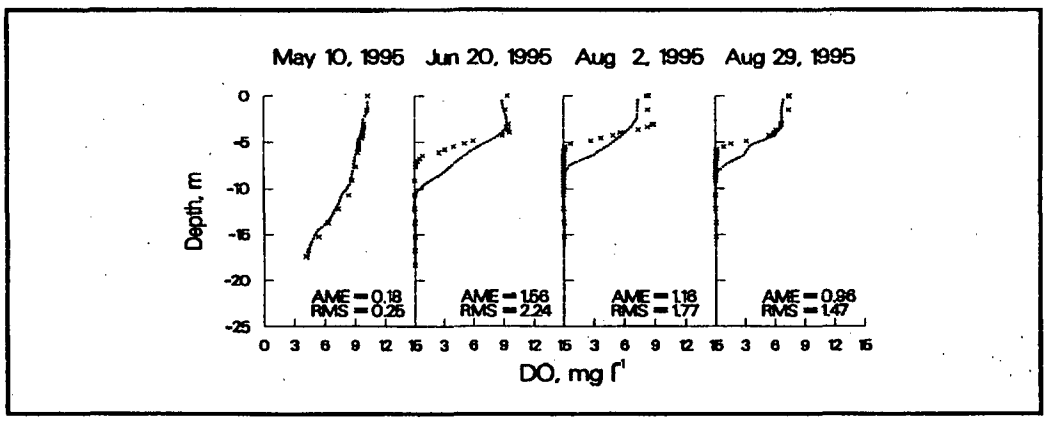

Figure 37. 1995 computed versus observed DO at station 1

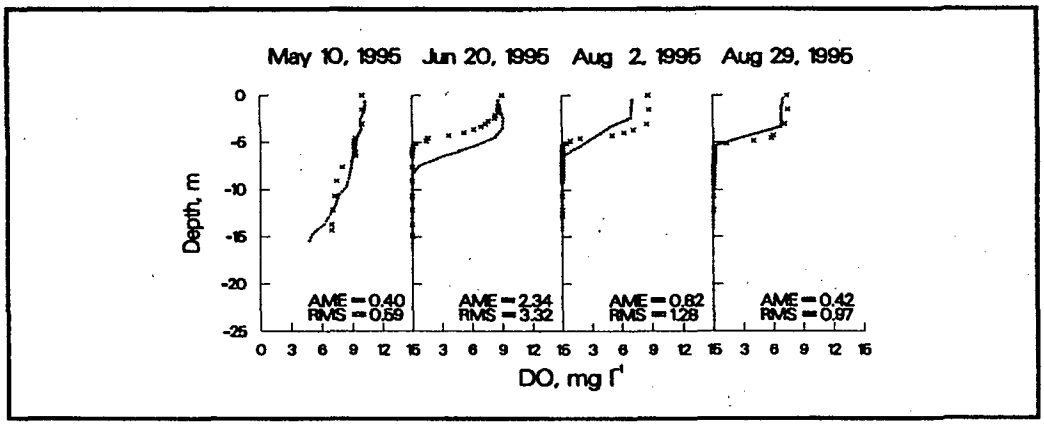

Figure 38. 1995 computed versus observed DO at station 35

Algae. Figures 40-42 show computed and observed algal profiles for the three stations. Inflow algal and nutrient data were unavailable and 1994 data were used. Comparison of observed and computed profiles again show overprediction of algae concentrations for most dates except August 2 where the model is capturing the increase in algal biomass with depth. The overprediction is attributed to inaccuracies in nutrient and algal loadings.

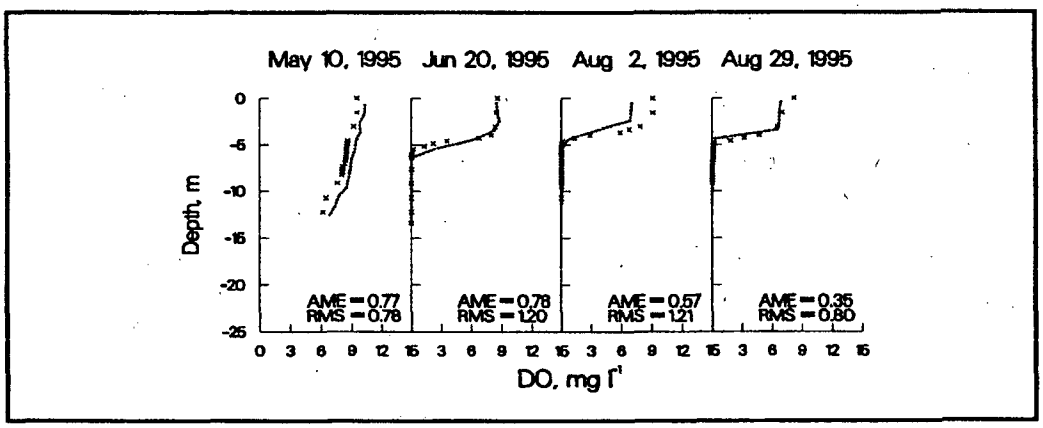

Figure 39. 1995 computed versus observed DO at station 3

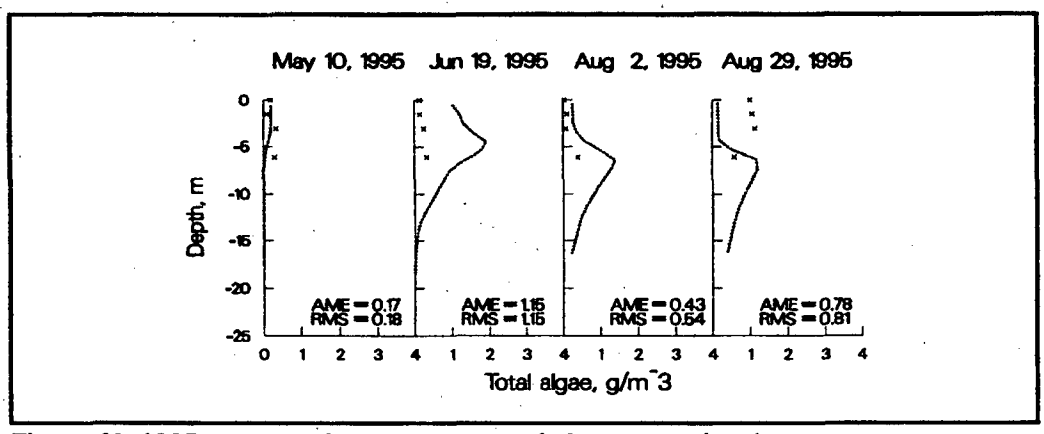

Figure 40. 1995 computed versus observed algae at station 1

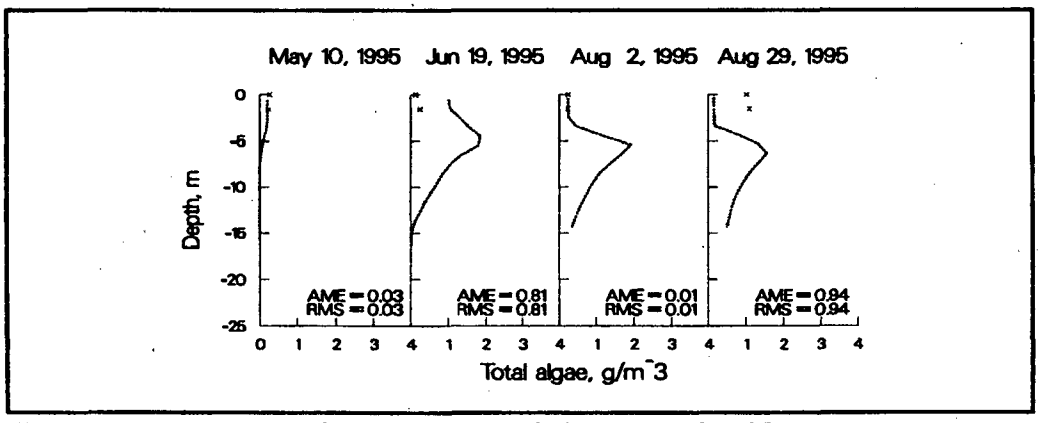

Figure 41. 1995 computed versus observed algae at station 35

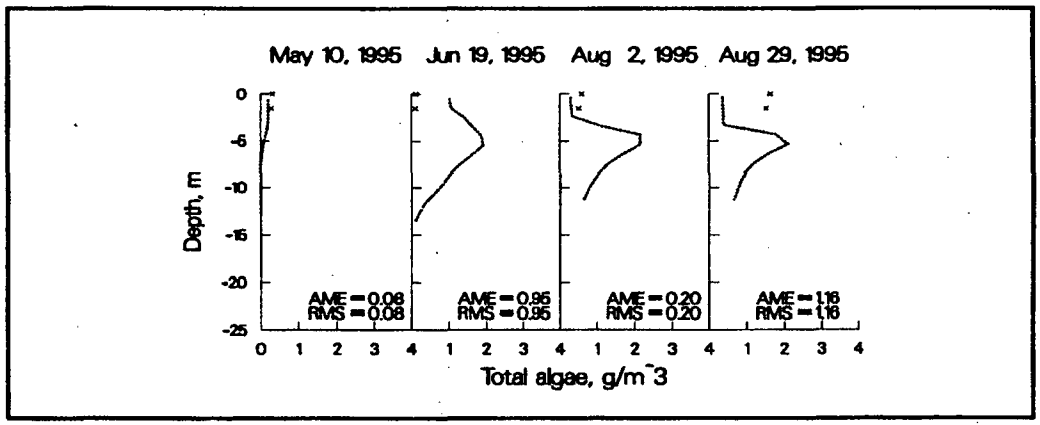

Figure 42. 1995 computed versus observed algae at station 3

1996

Water Surface Elevations. Water surface elevations increased the greatest (≈5 m) for this year compared to any of the other calibration years. The increased elevations continued on later into the year and the return to 164 m did not occur until August. Predicted elevations were an almost exact overlay of the observed (Figure 46).

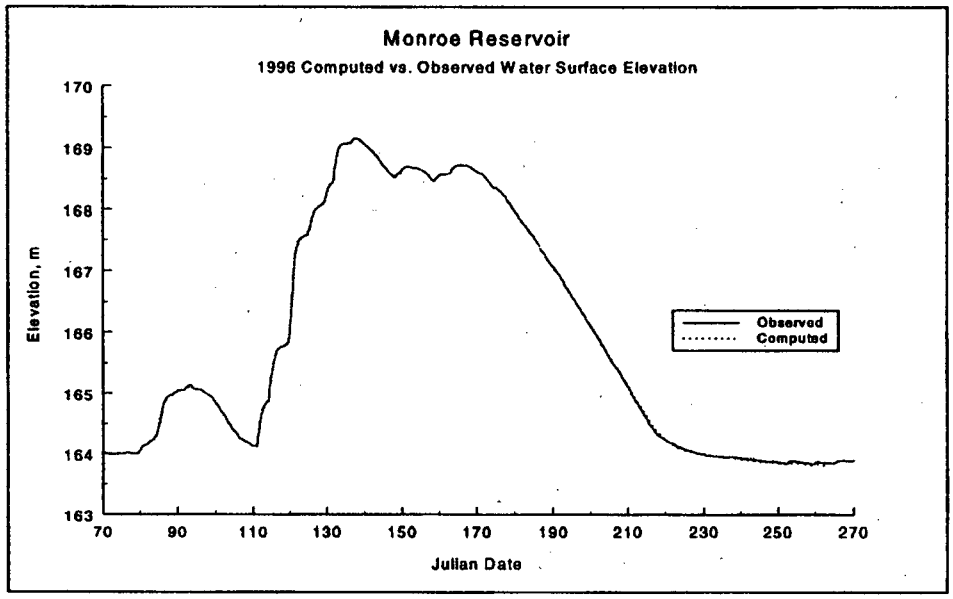

Figure 43. 1996 computed versus observed water surface elevations

Temperature. Figures 44-46 show the computed and observed temperature profiles for the three stations. The model is reproducing the observed thermal stratification at all stations. An additional plot at station 1 on August 14 is due to an additional profile taken on this date. It is interesting to note that the method of sampling can affect perceived results for model predictions. The first plot of August 14 has an AME of 0.61 and an RMS of 0.72 whereas comparison with the other profile resulted in worse statistics. The greatest differences between computed and observed temperatures occurred at stations 35 and 3 on July 16. The discrepancies are the result of using option 2 to set initial conditions for the reservoir. This option set initial conditions for each segment in the grid based on the vertical profile at station 1. By the next observed date, computed profiles at these stations were in good agreement.

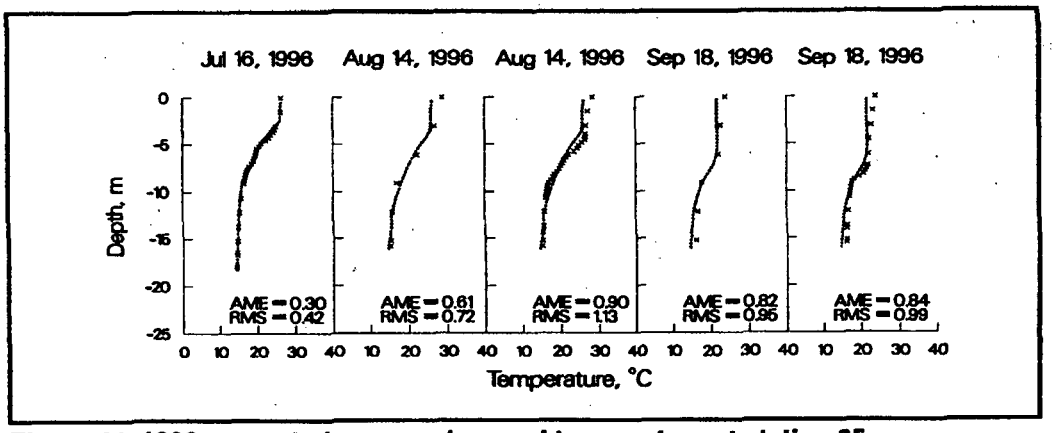

Figure 44. 1996 computed versus observed temperature at station 35

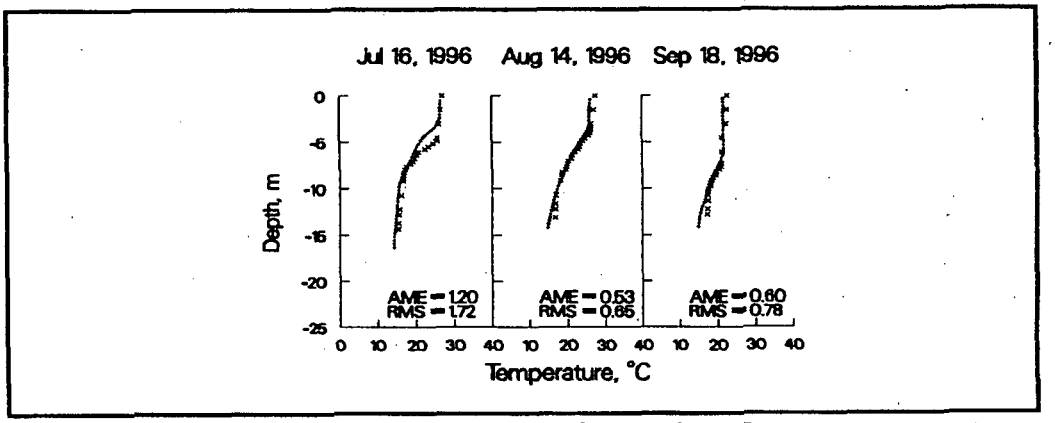

Figure 45. 1996 computed versus observed DO at station 35

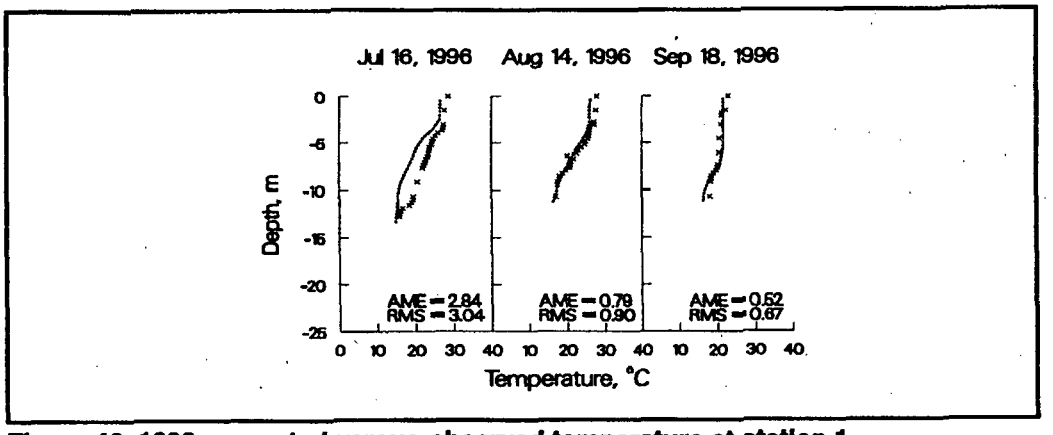

Figure 46. 1996 computed versus observed temperature at station 1

Dissolved Oxygen. Computed and observed DO profiles are shown in Figures 47-49 for the three stations. Computed and observed profiles for all stations were generally in close agreement. Note the change in chemocline depth on September 18 at Station 1. This is due to seiching in the model which can have a dramatic effect on the chemocline depth. This

to seiching in the model which can have a dramatic effect on the chemocline depth. This again illustrates the importance of comparing model output one day before, the day of, and one day after the observed date in order to determine how well the model is reproducing conditions in the prototype.

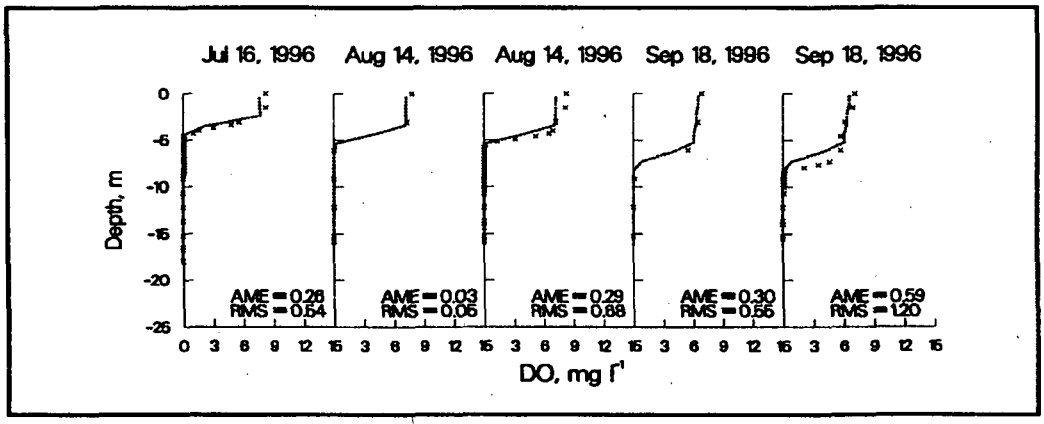

Figure 47. 1996 computed versus observed DO at station 1

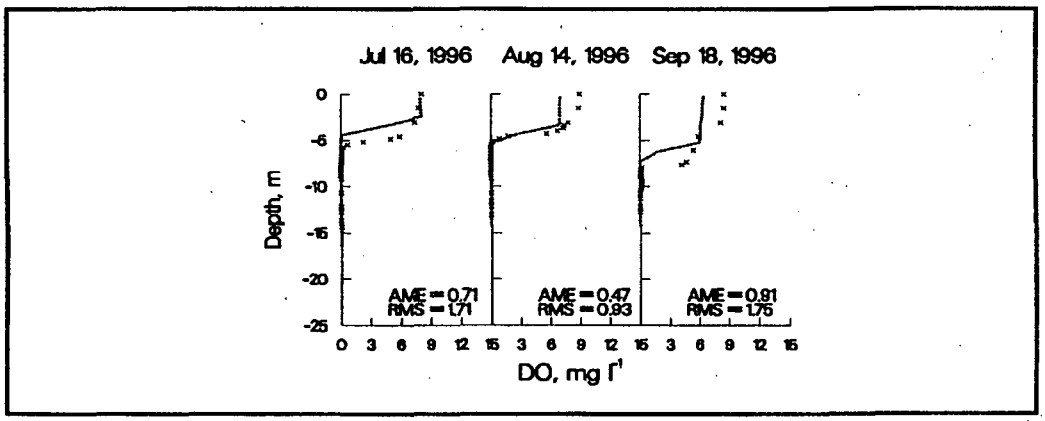

Figure 48. 1996 computed versus observed temperature at station 3

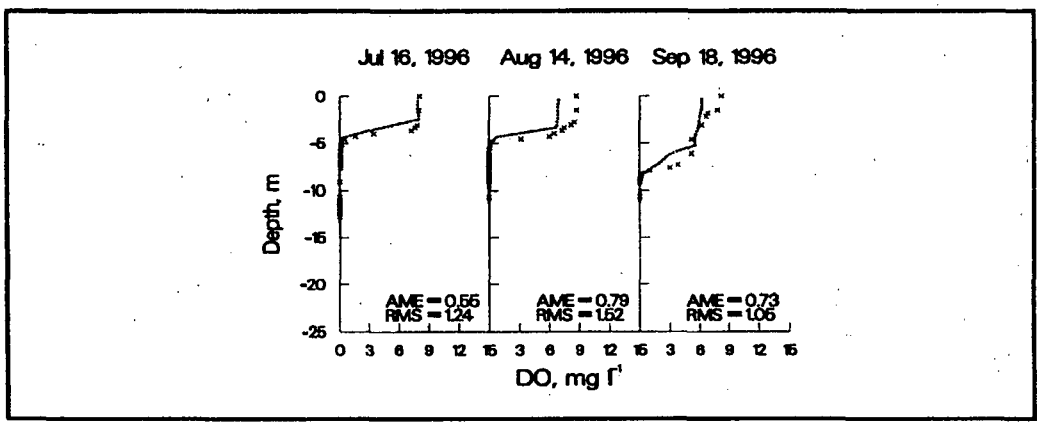

Figure 49. 1996 computed versus observed DO at station 3

Algae. Figures 50-52 show computed and observed algal profiles for the three stations. Inflow nutrient data were available for only one day during this simulation, thus 1994 data were used for the rest of the simulation. The overprediction of algae is attributed to inaccurate estimates of nutrient and algal loadings.

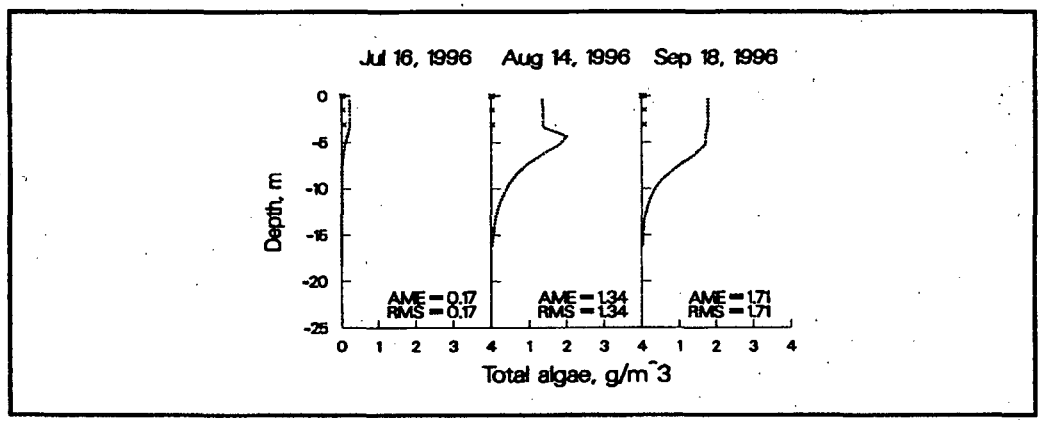

Figure 50. 1996 computed versus observed algae at station 1

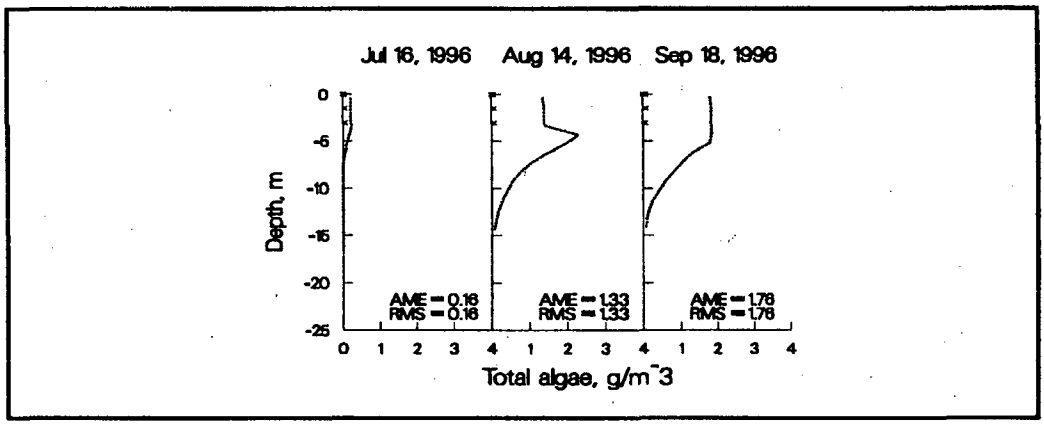

Figure 51. 1996 computed versus observed algae at station 35

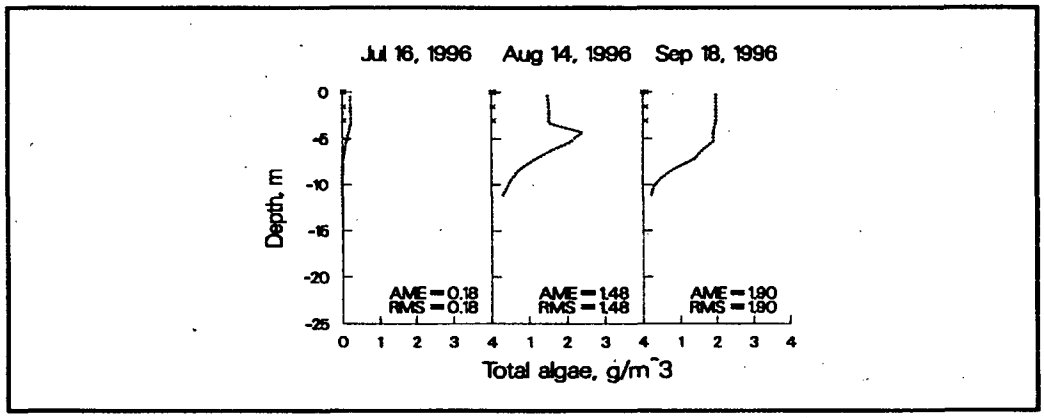

Figure 52. 1996 computed versus observed algae at station 3

Calibration Summary

Accurate simulation of temperature and algal/nutrient dynamics was necessary to correctly simulate DO. Normally, there is only one dominant forcing function affecting temperature predictions. However, thermal calibration for Lake Monroe was especially difficult because of the nearly equal sensitivity of thermal predictions to bathymetry, inflow temperature, wind sheltering, and outflow specification. A summary of the important calibration variables follows.

Water Surface Elevations. For the four calibration years, computed water surface elevations were an almost exact overlay of observed elevations. Differences in flow years and reservoir operations were reflected in the patterns of water surface elevation changes for each of the calibration years. The 1994 spring increase in elevation peaked in mid-May and then decreased about 2 m by the end of May. The maximum change in elevation was approximately 2 m in the spring and the water surface fluctuated little for the remainder of

the year. During 1992, Lake Monroe experienced less fluctuation in water surface elevation than in 1994. The maximum change was less than 1 m. In early August, the elevation increased by about 0.5 m. During the spring of 1995, the reservoir elevation increased more than 3 m and did not stop decreasing in the summer until the middle of July. In 1996, water surface elevations exhibited their greatest fluctuation of more than 5 m and the decrease in water surface elevation did not stop until the middle of August.

The model accurately captured the differences between the years. In order to capture the decline in water surface elevations during middle to late summer, negative inflows were required, which indicates that there may still be slight errors in the bathymetry or that groundwater seepage or seepage through the dam might be occurring. However, the negative flows were slight and should not impact the results.

Temperature. Computed temperatures for the four calibration years closely followed the trends in the observed data over the summer stratification period and also the differences in thermal structure during the same time period for different years. For example, in early May during 1994 and 1992 the epilimnion extended to a depth of about 8 m, but in 1995 the epilimnetic depth was only 3 m. The greatest discrepancies between computed and observed temperatures occurred mainly in the epilimnion and hypolimnion where the model tended to underpredict the observed temperatures by no more than 1 °C. Much of the epilimnetic variation is attributed to uncertainty in the meteorological data.

Dissolved Oxygen. The model is reproducing the trends in DO stratification throughout the summer depletion period. The greatest discrepancies between model predictions and observed data occur in the metalimnion where the model tended to overpredict the chemocline depth by about 2 m for station 1 (Figures 27 and 37). Since the model is accurately reproducing the thermocline depth during this time, the inaccuracies must be due to a source of oxygen in the metalimnion. The source can be either through inflow placement of higher oxygenated waters into the metalimnion, or DO production from algal photosynthesis. Sensitivity analyses showed that increasing inflow temperatures positively affected DO predictions by moving more oxygenated water higher into the metalimnion. For calibration years other than 1994, the model was also overpredicting algal concentrations in the metalimnion, which may also be affecting the chemocline location.

Judgement of how well the model is reproducing DO should be tempered with the realization that model predictions (and observed data) can change significantly over short time periods. Figure 28 illustrates how much DO can change over a 24 hour period. From June 16 to June 17, the AME changed from 2 to 3 mg l^{-1} and from July 27 to July 28, the AME doubled from 0.7 to 1.5 mg l^{-1}.

Phosphorus. Phosphorus concentrations were only available for 1994. Observed phosphorus concentrations showed no trends to reproduce as all observed concentrations were at or below the detection limit (Figures 11-13). The model could have been forced to reproduce the observed phosphorus data by eliminating phosphorus release from the sediments during anoxic conditions, but without clear evidence, there was no justification to override the current paradigm of sediment phosphorus release during anoxia.

Ammonium. The model accurately reproduced the increase in hypolimnetic ammonium throughout the summer during 1994 (Figures 14-16).

Nitrate-Nitrite. The model is capturing the trend of decreasing nitrate-nitrite concentrations throughout the water column during the summer growing season (Figures 17-19). The model underpredicts the hypolimnetic concentration in mid to late summer, but this is due to the reporting of detection limits in the hypolimnion.

Algae. For 1994, the model is capturing the trends in algal biomass concentrations during the growing season (Figures 20-22). For the other calibration years, the model is overpredicting algal biomass. This is attributed to using 1994 boundary concentrations for inflow nutrient and algal biomass. Since computed algal concentrations vary significantly for these years, the model is sensitive to changes in hydrodynamics, loadings, and meteorology. For example, using inflow phosphorus concentrations set to detection limits, the model predicts algal concentrations two times greater in 1992 and 1996 than in 1994. The model is also sensitive to changes over short time periods as evidenced in 1992 where algal biomass at the surface doubled over a two day period from June 16 to June 18 (Figures 30-32). Given the uncertainties in determining algal biomass from chlorophyll *a*, the model is doing a good job of reproducing the trends in algal biomass over time.

5 Scenarios

Scenarios were conducted to determine effects on water quality, especially algal biomass and DO concentrations. Six scenario runs were made based on the following conditions requested by the Louisville District:

1. low flow, high air temperatures, low inflow nutrient concentrations
2. low flow, high air temperature, high inflow nutrient concentrations
3. high flow, low air temperatures, low inflow nutrient concentrations
4. high flow, low air temperatures, high inflow nutrient concentrations
5. average flow, average air temperatures, low inflow nutrient concentrations
6. average flow, average air temperatures, high inflow nutrient concentrations

The base run for which all scenario runs were compared was the 1994 calibration results. During scenario runs, 1994 input files and initial conditions were used except for the various changes in flow, air temperature, and inflow nutrient concentrations. For example, the first set of scenario runs used 1992 inflows and outflows, 1973 meteorology, and reducing/increasing 1994 nutrient concentrations by 50%. All other boundary or initial conditions remained at the 1994 setting.

To determine a low, average, and high flow and air temperature year, meteorologic and hydrological conditions were ranked by mean annual values for each year the data were available. Air temperatures were available from 1948 to 1996 and calculated inflow data were available from 1984 to 1996. A frequency analysis was performed on these data to determine the 10%, 50%, and 90% probability of occurrence. The 10%, 50%, and 90% probability of occurrence occurred in 1976, 1992, and 1973, respectively, for air temperature and 1992, 1994, and 1996, respectively for flow.

Scenario boundary concentrations representing low/high nutrient loadings were estimated by decreasing or increasing the inflow nutrient concentrations by 50%. Initially, linear regression was conducted to develop equations for nutrient loads using available inflow nutrient data for each tributary along with calculated inflows of Lake Monroe. However, resulting r^2 values for the equations were not acceptable, in part due to the limited inflow concentration data and from not having gaged flow data for each major tributary (North, South, and Middle Salt Creek). The calculated inflows represented the sum of the flows for all tributaries discharging into Lake Monroe. Using these flows with measured concentrations on each tributary established a weak relationship since the independent and dependent variables were not truly represented.

Low Flow, High Air Temperature, Low/High Inflow Nutrient Concentrations

Scenario 1 used 1992 inflows (low flow year), 1973 meteorology (high air temperatures), and a 50% reduction in 1994 nutrient inflow concentrations. Scenario 2 used the same hydrology and meteorology with a 50% increase in inflow nutrient concentrations. Results for these scenarios are shown in Figures 53-59 for station 1.

The results show little difference between scenarios 1 and 2. However, there are differences when compared to the 1994 base line. A combination of low inflows and warmer air temperatures resulted in warmer water temperatures during late summer (Figure 53). As a result, reaction rates that drive DO/algal/nutrient dynamics caused changes in nutrient, DO, and algal concentrations (Figures 54-56, 57, and 58, respectively). Differences in nutrient concentrations were most evident in the hypolimnion where concentrations were reduced. Algal concentrations were also reduced and DO concentrations at the beginning of the simulation were reduced but increased toward the end.

Although 1994 inflow nutrient concentrations were increased and decreased, there was a minimal effect on inlake concentrations. Because inflow concentrations were so low, decreasing and increasing the values had little effect on water quality. Scenario 2 was rerun with inflow phosphorus concentrations increased from 0.007 to 0.03 to determine the effect on algal concentrations since phosphorus was the limiting nutrient. Results are shown in Figure 74 for algae at station 1. Although phosphorus inflow concentrations were increased by nearly an order of magnitude, in lake concentrations at station 1 are only slightly increased (Figure 74). As will be shown, increases in mass loadings drive algal production. Increased phosphorus concentrations translated into relatively small increases in mass loadings as a result of the low inflows.

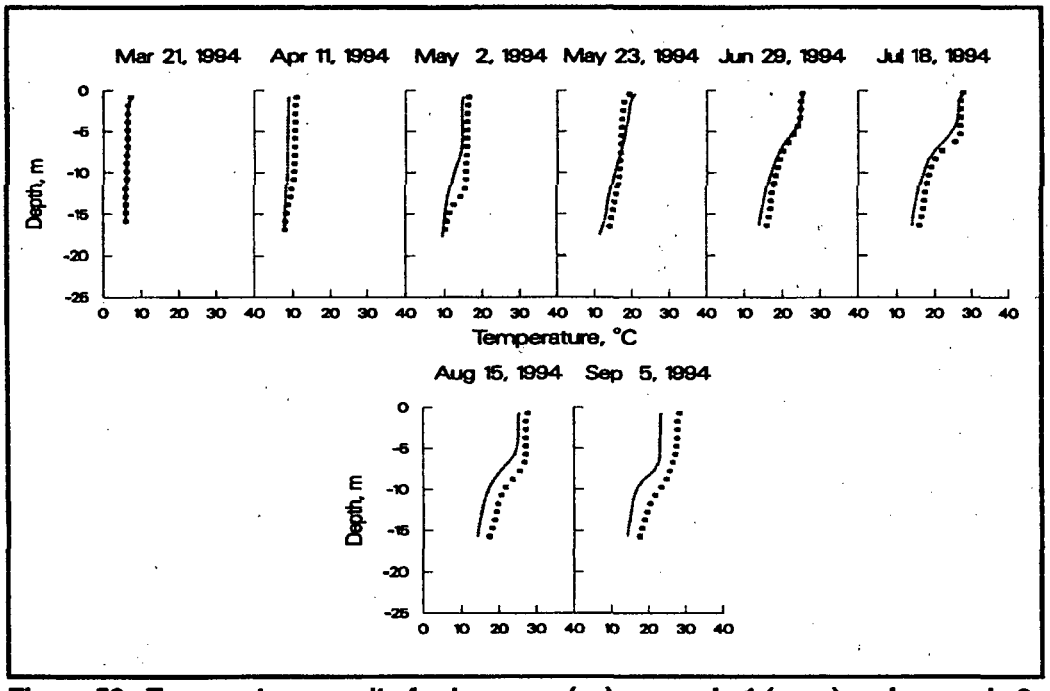

Figure 53. Temperature results for base run (....), scenario 1 (xxxx) and scenario 2 (oooo)

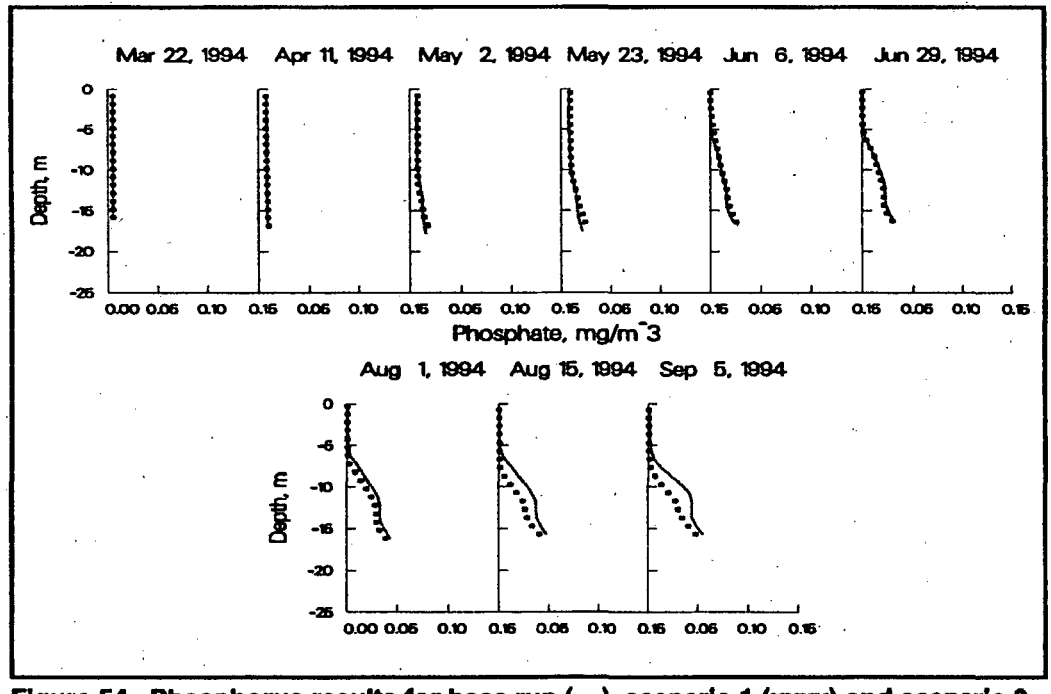

Figure 54. Phosphorus results for base run (....), scenario 1 (xxxx) and scenario 2 (oooo)

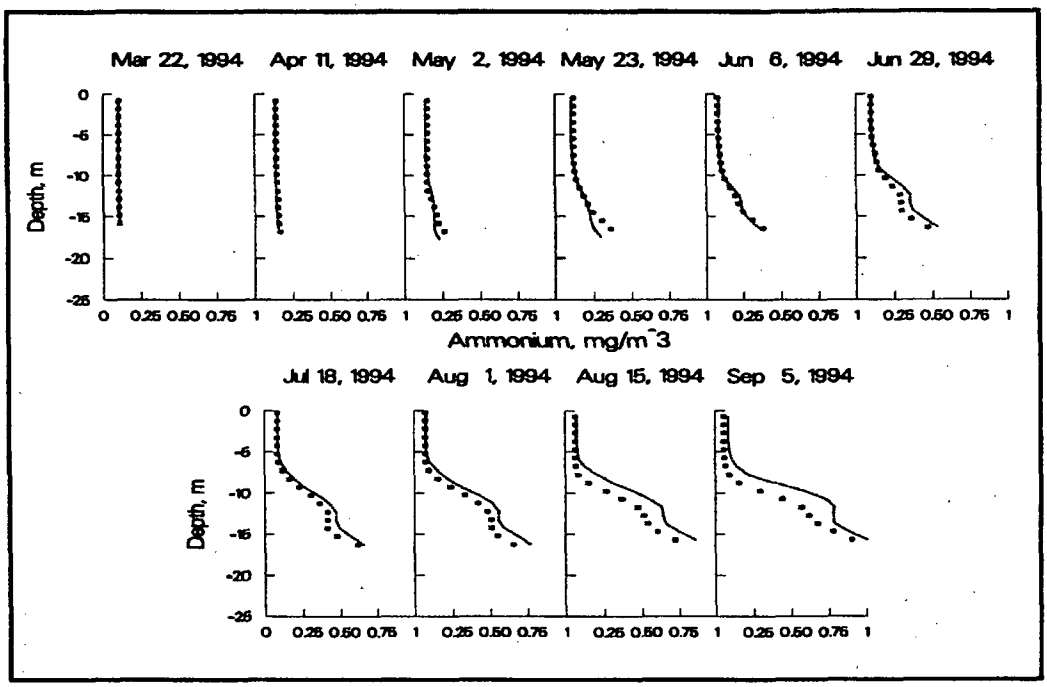

Figure 55. Ammonium results for base run (....), scenario 1 (xxxx) and scenario 2 (oooo)

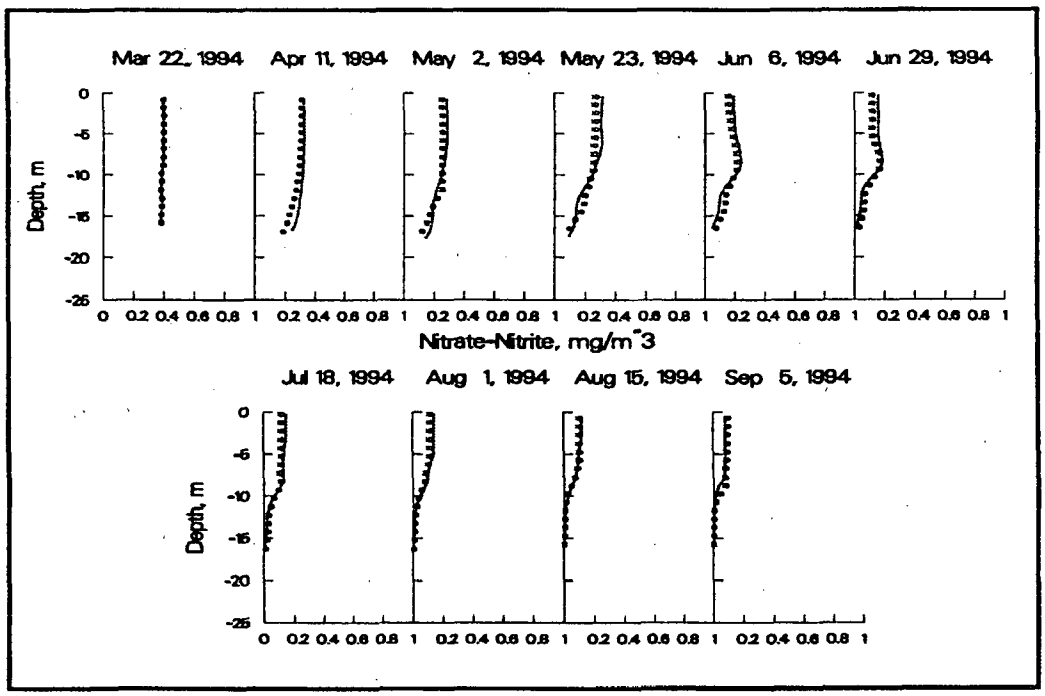

Figure 56. Nitrate-nitrite results for base run (....), scenario 1 (xxxx) and scenario 2 (oooo)

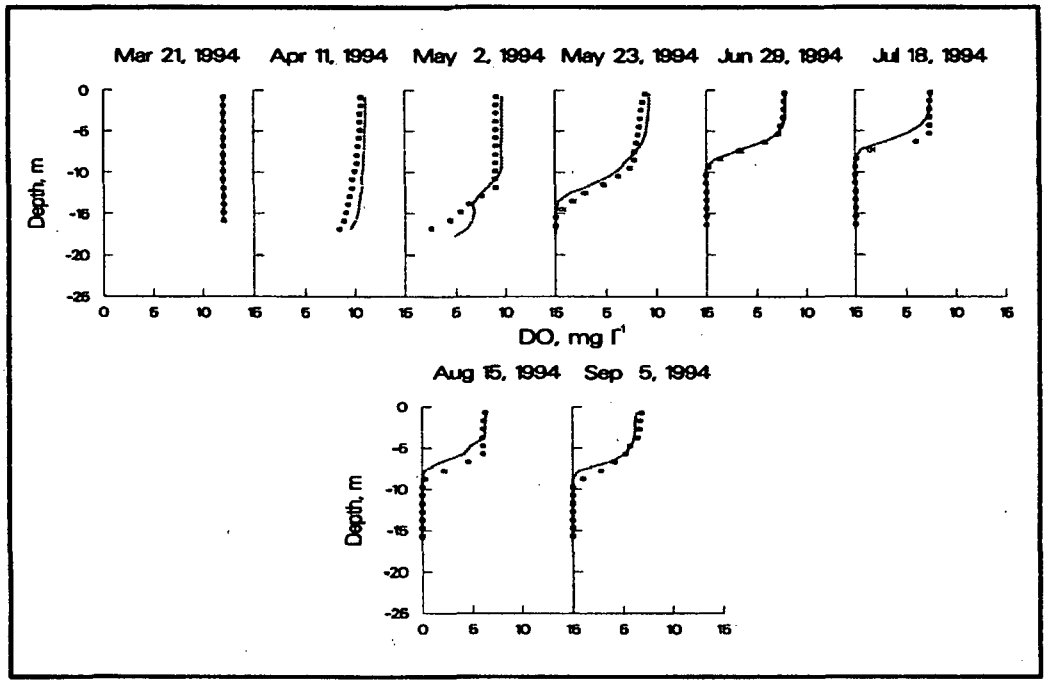

Figure 57. DO results for base run (....), scenario 1 (xxxx) and scenario 2 (oooo)

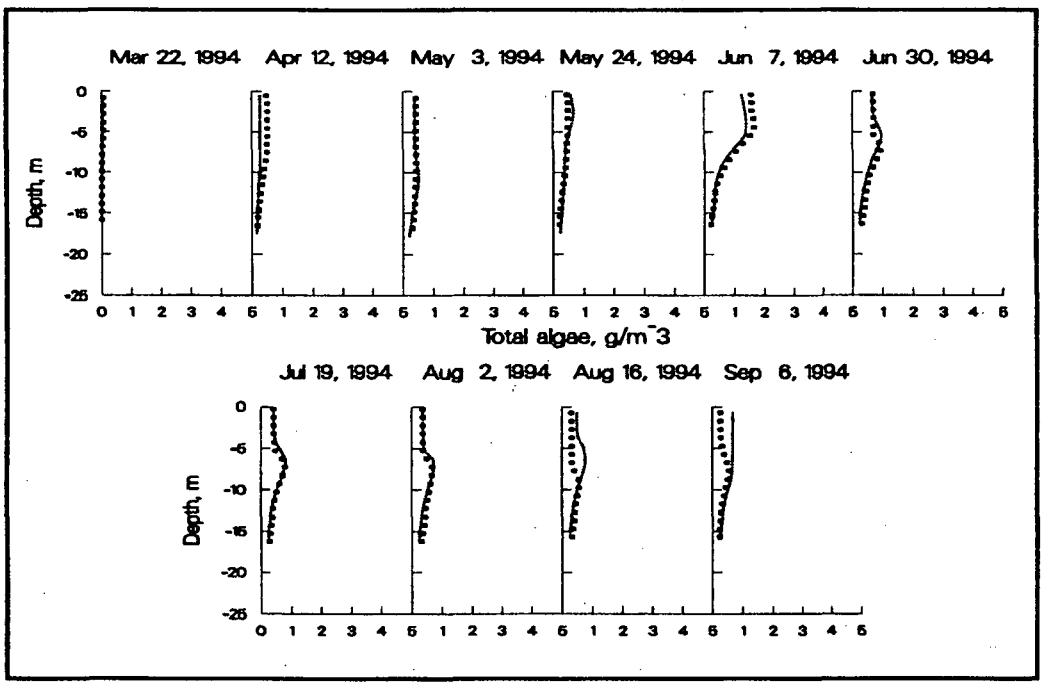

Figure 58. Algal results for base run (....), scenario 1 (xxxx) and scenario 2 (oooo)

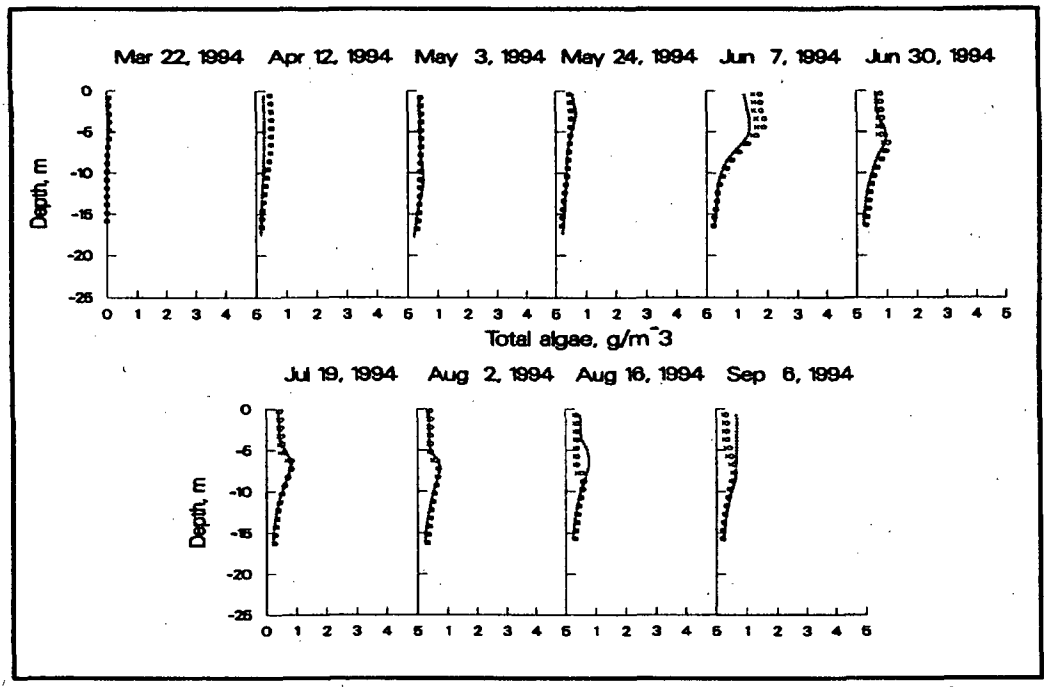

Figure 59. Algal results for base run (....), scenario 1 (xxxx) and scenario 2 (oooo) with inflow phosphorus concentrations increased from 0.007 to 0.03 mg l^{-1}

High Flow, Low Air Temperature, Low/High Inflow Nutrient Concentrations

Scenario 3 used 1996 flows (high flow year), 1976 meteorology (low air temperatures), and a 50% decrease in inflow nutrient concentrations. Scenario 4 used the same hydrology and meteorology with a 50% increase in inflow nutrient concentrations. Results for these scenarios are shown in Figures 60-65 for station 1.

The results show little difference between scenario 3 and 4 except for nitrate-nitrite. When both are compared to 1994 calibration results, there are some differences. Using meteorological data from 1976 and flows from 1996 resulted in less thermal stratification (Figure 60) for both scenario runs when compared to the base run. This was attributed to a decrease in residence time due to the higher inflows. Similar to scenario 1 and 2 results, phosphorus and ammonium concentrations were reduced in the hypolimnion (Figures 61-62). Nitrate-nitrite results show more differences between the two scenario runs than the previous scenario runs discussed (Figure 63). Scenario 3 nitrate-nitrite concentrations are lower than scenario 4 concentrations. However, neither are much greater than the base run results. The reason for this is probably due to the higher flows being used in both scenario runs. Algal concentrations (Figure 65) for the most part were less stratified than the base results, and DO concentrations (Figure 64) showed the most differences in May and June when the mixed layer was deeper.

Scenario 4 was also rerun increasing inflow phosphorus concentrations from 0.007 to 0.03 to see what effects that would have on algae since phosphorus was the limiting nutrient. Results are shown in Figure 66 for algae at station 1. The increased phosphorus loadings

resulting from the increased concentrations and inflows resulted in a twofold increase in algal biomass compared to the base case.

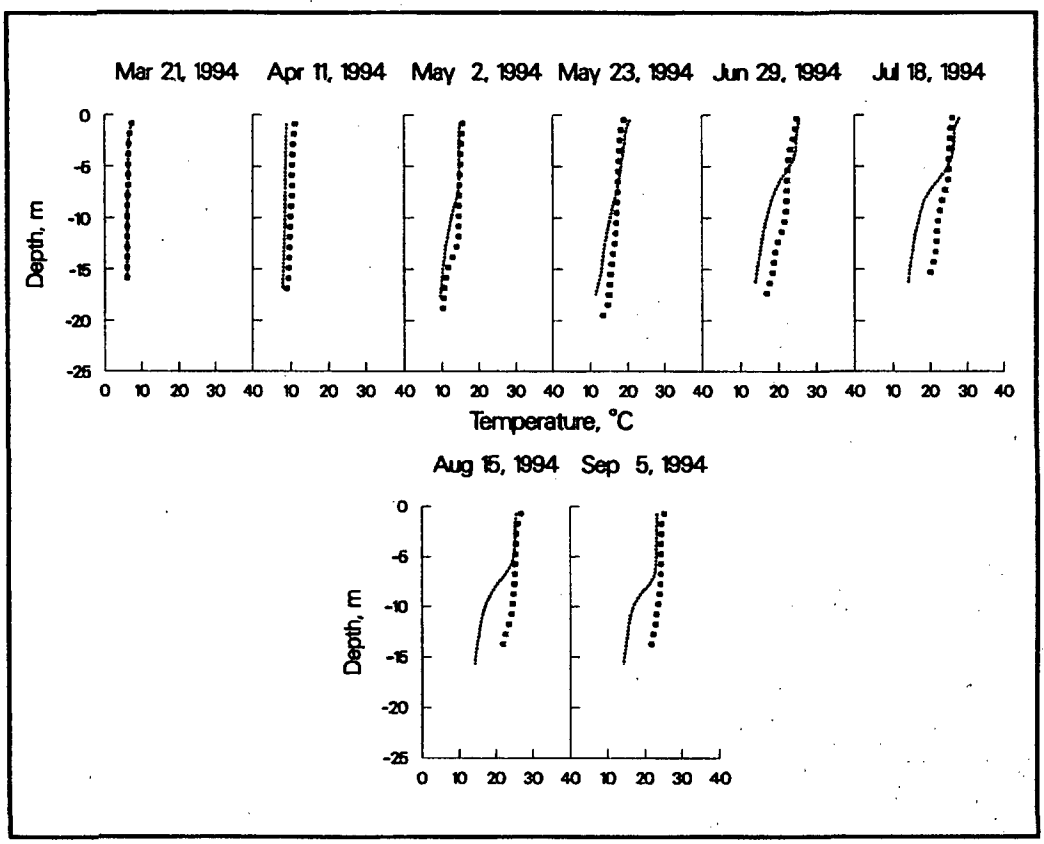

Figure 60. Temperature results for base run (....), scenario 3 (xxxx) and scenario 4 (oooo)

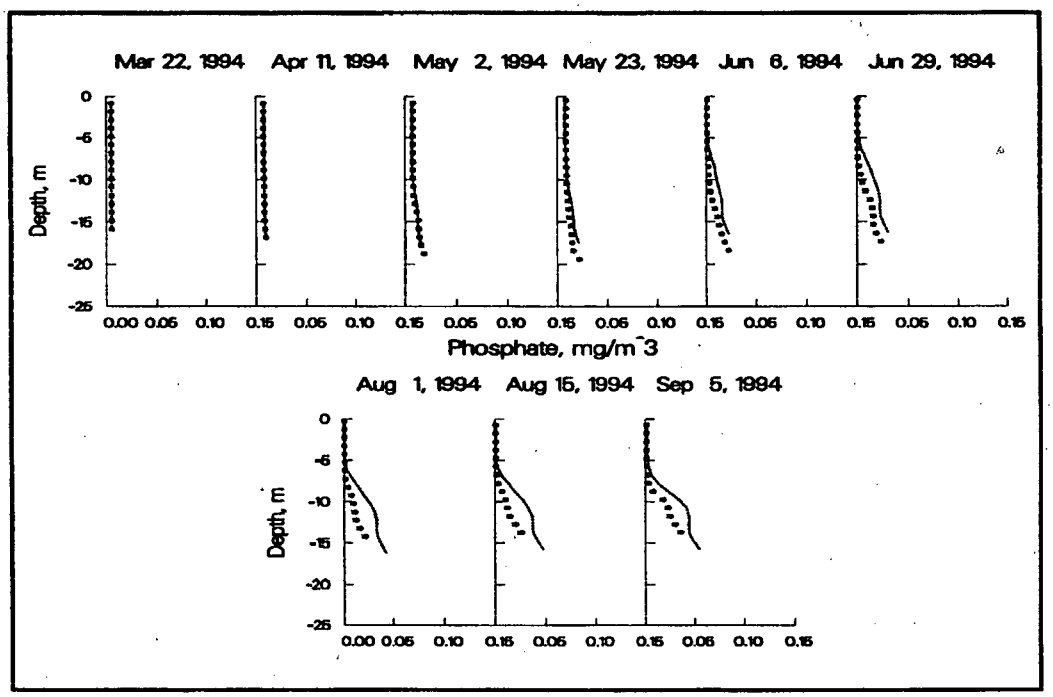

Figure 61. Phosphorus results for base run (....), scenario 3 (xxxx) and scenario 4 (oooo)

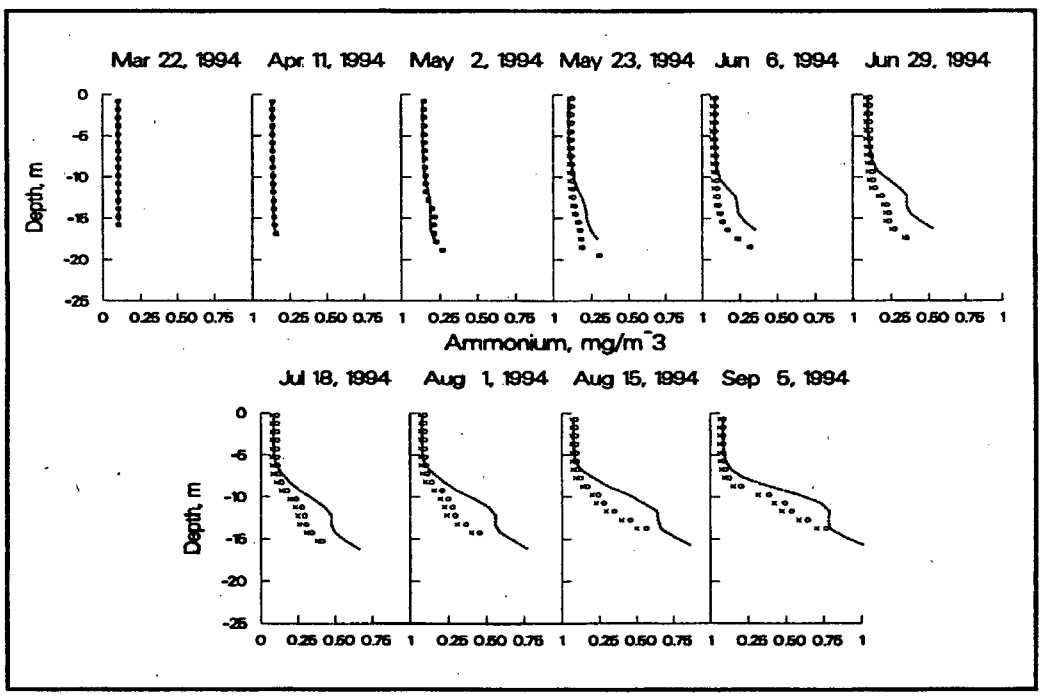

Figure 62. Ammonium results for base run (....), scenario 3 (xxxx) and scenario 4 (oooo)

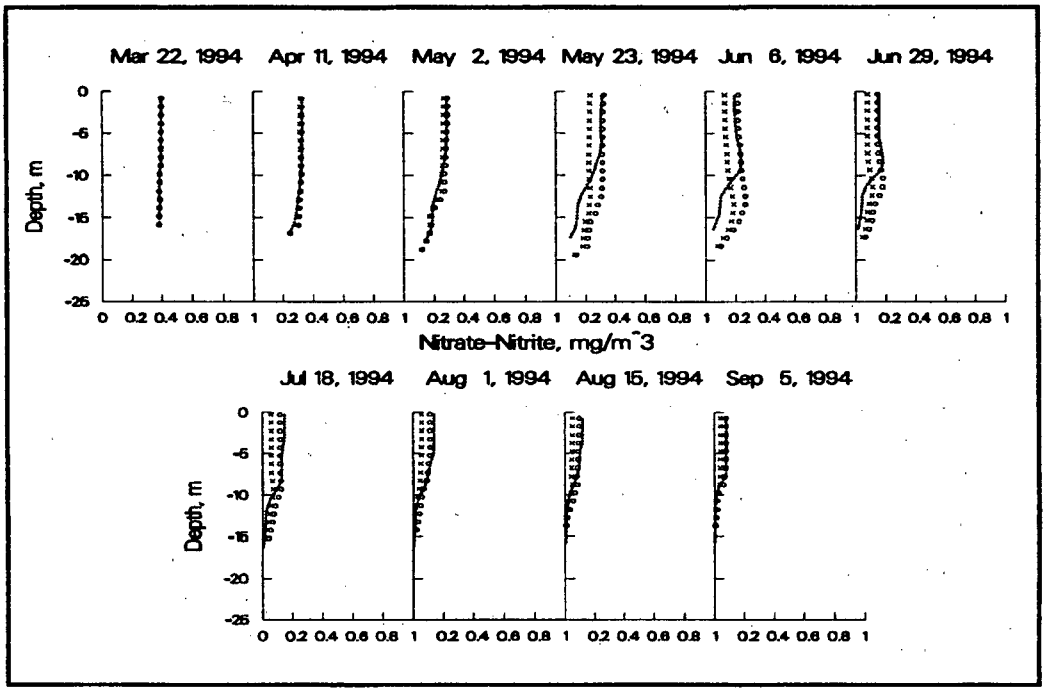

Figure 63. Nitrate-nitrite results for base run (....), scenario 3 (xxxx) and scenario 4 (oooo)

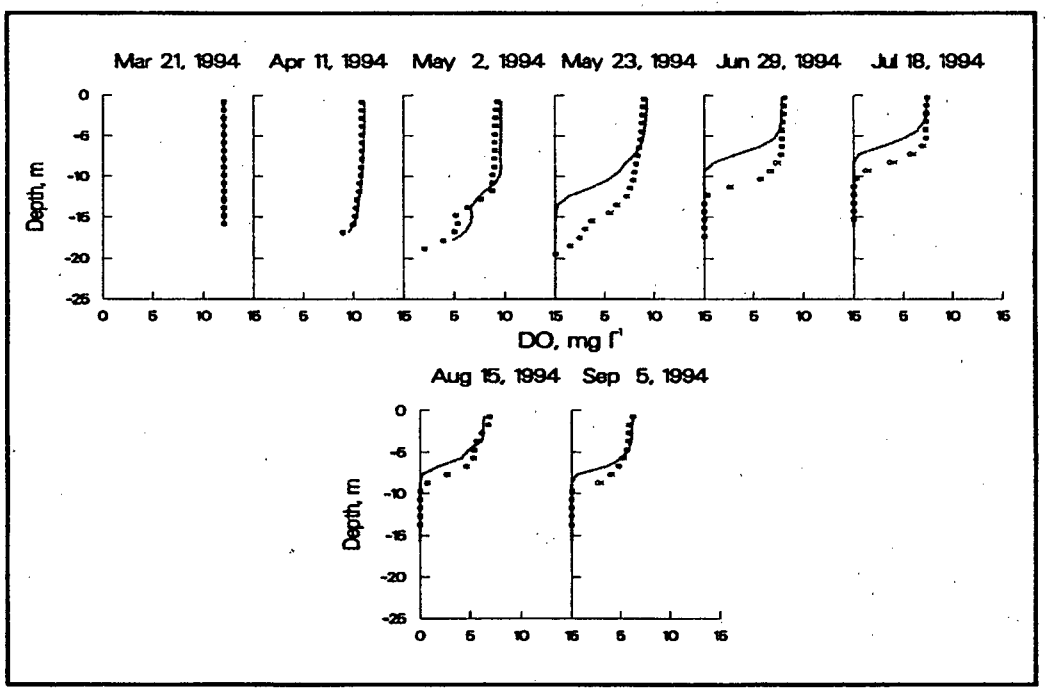

Figure 64. DO results for base run (....), scenario 3 (xxxx) and scenario 4 (oooo)

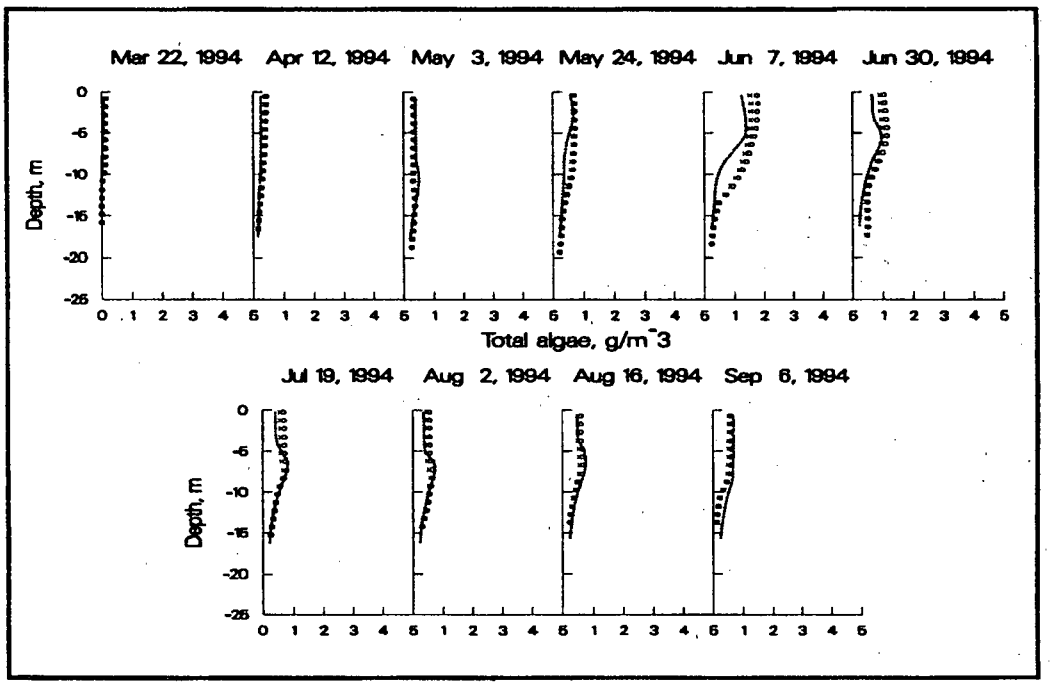

Figure 65. Algal results for base run (....), scenario 3 (xxxx) and scenario 4 (oooo)

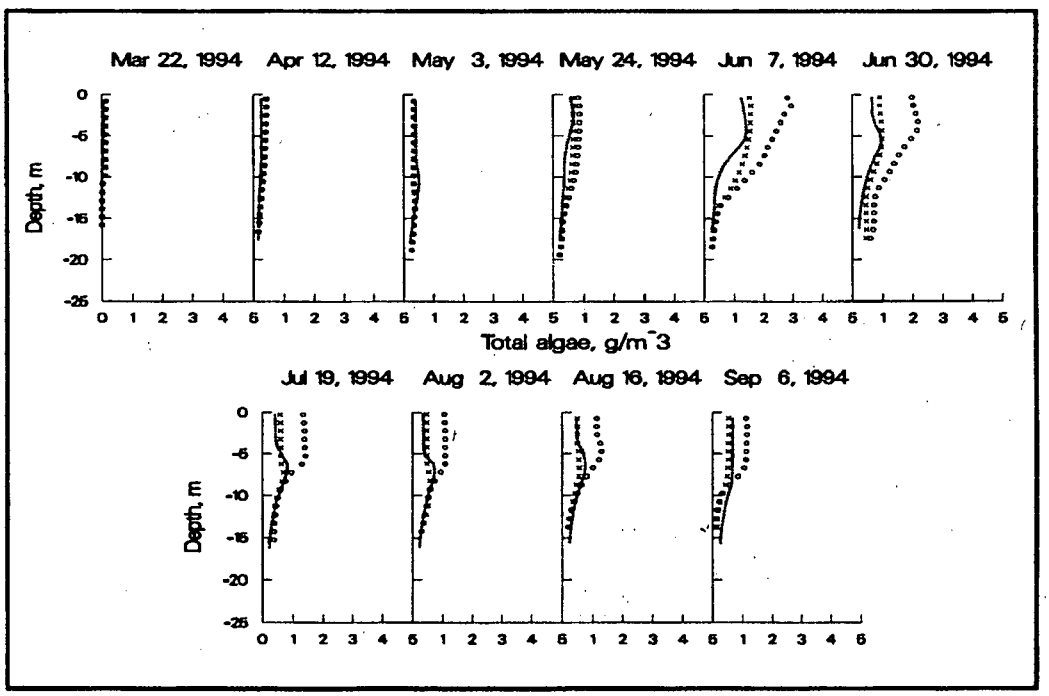

Figure 66. Algal results for base run (....), scenario 3 (xxxx) and scenario 4 (oooo) with inflow phosphorus concentrations increased from 0.007 to 0.03 mg l^{-1}

Average Flows, Average Air Temperature, Low/High Inflow Nutrient Concentrations

Scenario 5 used 1994 flows (average flow year), 1992 meteorology (average air temperature), and a 50% reduction in inflow nutrient concentrations. Scenario 6 used the same hydrology and meteorology with a 50% increase in inflow nutrient concentrations. Results for both scenario runs are shown in Figures 67-72 for station 1.

Like scenarios 3 and 4, the figures show that there are very little differences between scenarios 5 and 6 except for nitrate-nitrite. As previously discussed, when both are compared to 1994 calibration results there are some minor differences. Since the inflows and outflows for the base run and these scenarios are the same, water temperature differences are the result of using 1992 meteorological data. As seen in Figure 67, epilimnetic water temperatures are cooler until August when they become closer to the base run results. In August the hypolimnetic temperatures become warmer than the base run for both scenarios. This behavior can be attributed to the different meteorological data being used. Phosphorus and ammonium concentrations (Figures 68 and 69) were only slightly different from the base run.

Like scenarios 3 and 4, nitrate-nitrite results show more differences than what occurs between scenario 1 and 2 runs. Scenario 5 nitrate-nitrite concentrations are noticeably lower than scenario 6 concentrations until August when they become very similar (Figure 70). However, neither scenarios' concentrations are ever much greater than the base run results. When DO concentrations show differences, their concentrations are usually higher than the base run for both scenarios (Figure 71). Algal concentrations for both scenario runs (Figure 72) were greater in the epilimnion beginning in June than the base run results with scenario 6 algal concentrations being slightly greater than scenario 5.

Scenario 6 was rerun with inflow phosphorus concentrations increased from 0.007 to 0.03 to see what effects that would have on algae since phosphorus was the limiting nutrient. Results are shown in Figure 73 for algae at station 1. By increasing phosphorus inflow concentrations by almost an order of magnitude, inlake algal concentrations at station 1 are increased almost threefold in the epilimnion. Like the second run of scenario 4, increased mass loadings result in increased algal populations.

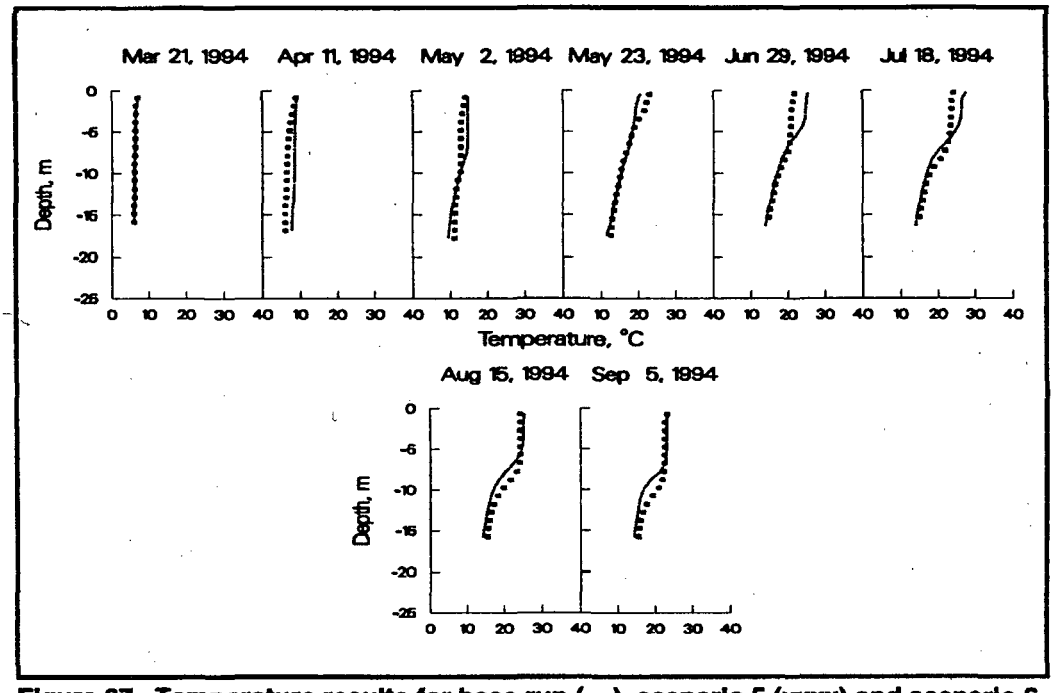

Figure 67. Temperature results for base run (....), scenario 5 (xxxx) and scenario 6 (oooo)

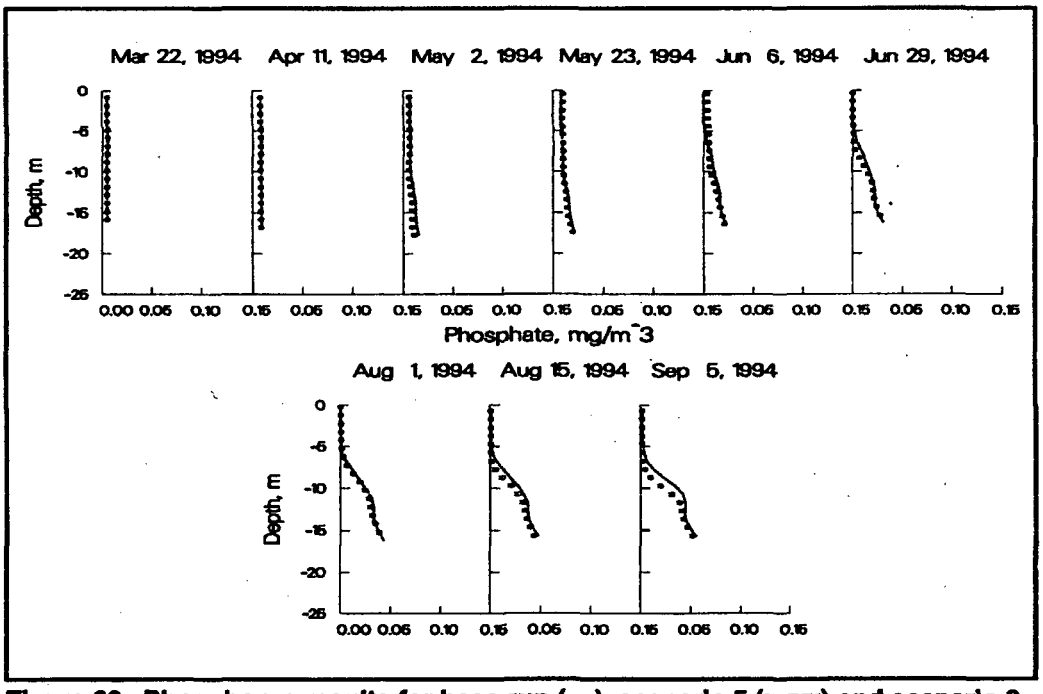

Figure 68. Phosphorus results for base run (....), scenario 5 (xxxx) and scenario 6 (oooo)

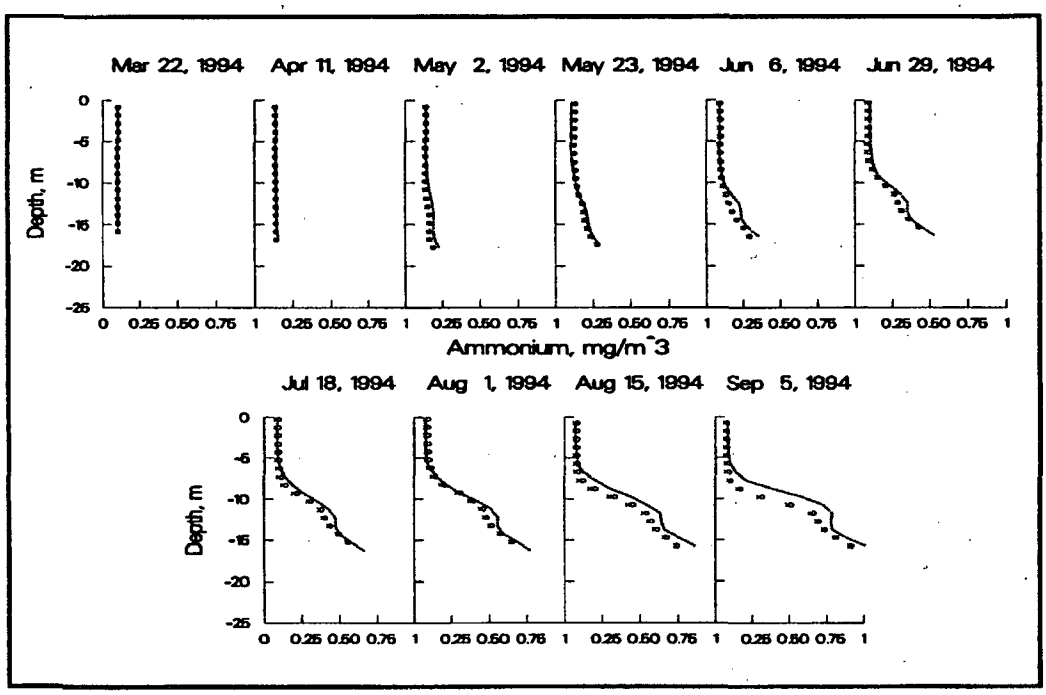

Figure 69. Ammonium results for base run (....), scenario 5 (xxxx) and scenario 6 (oooo)

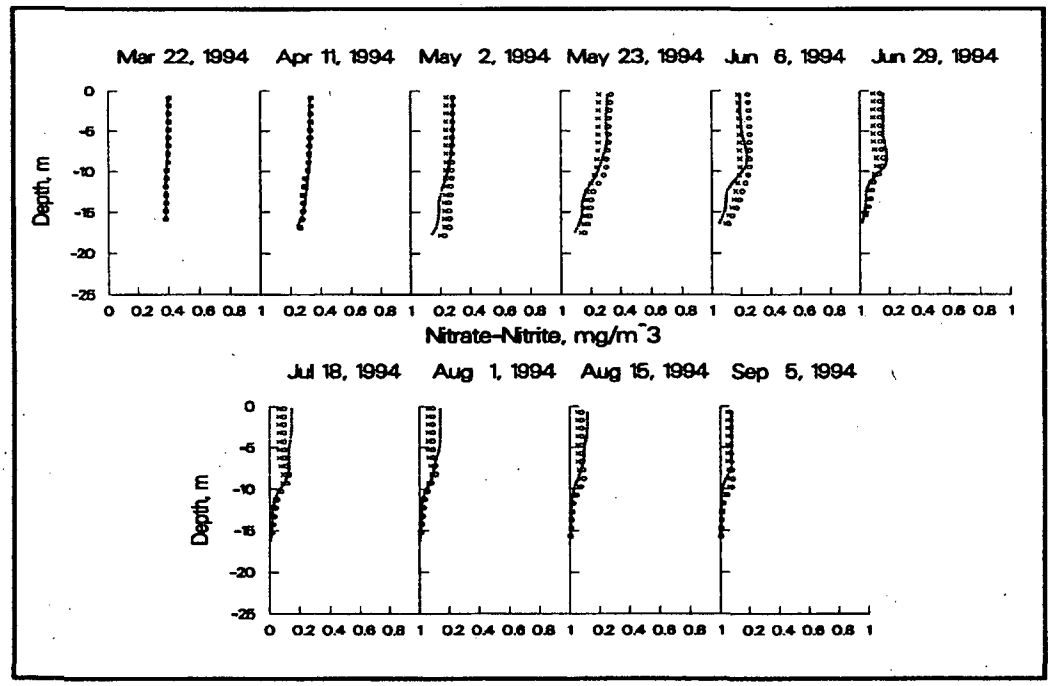

Figure 70. Nitrate-nitrite results for base run (....), scenario 5 (xxxx) and scenario 6 (oooo)

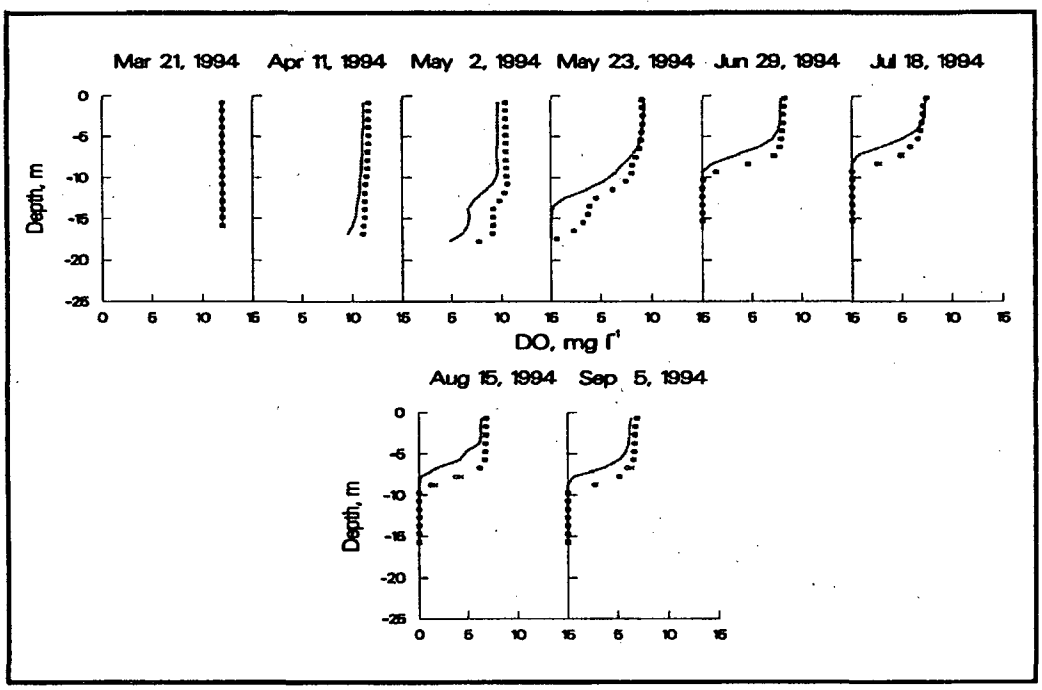

Figure 71. DO results for base run (....), scenario 5 (xxxx) and scenario 6 (oooo)

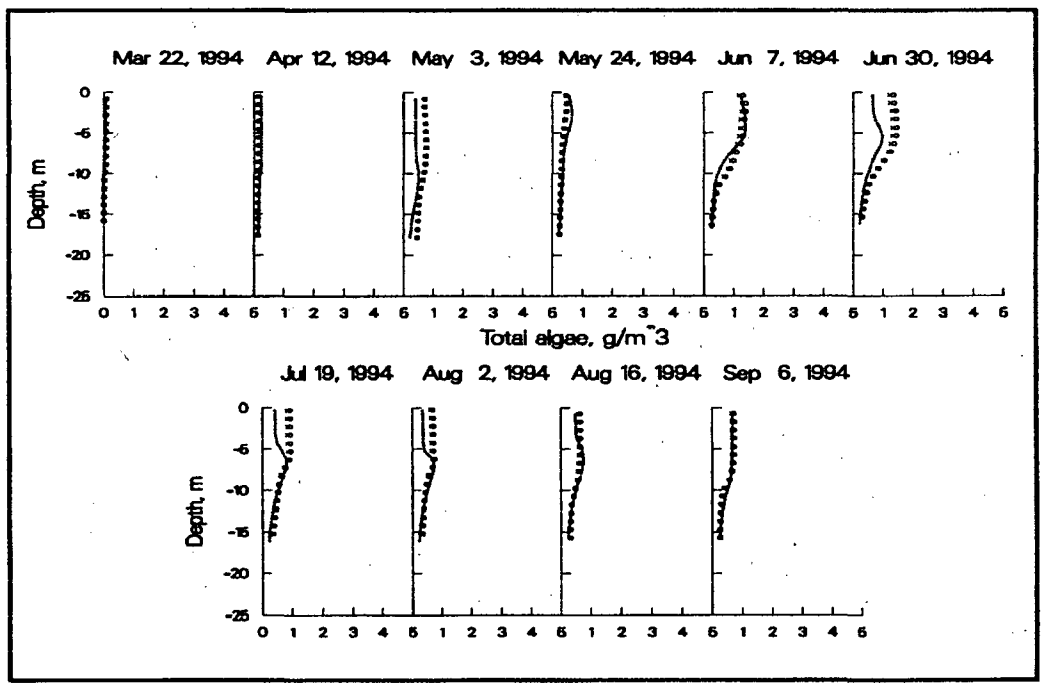

Figure 72. Algal results for base run (....), scenario 5 (xxxx) and scenario 6 (oooo)

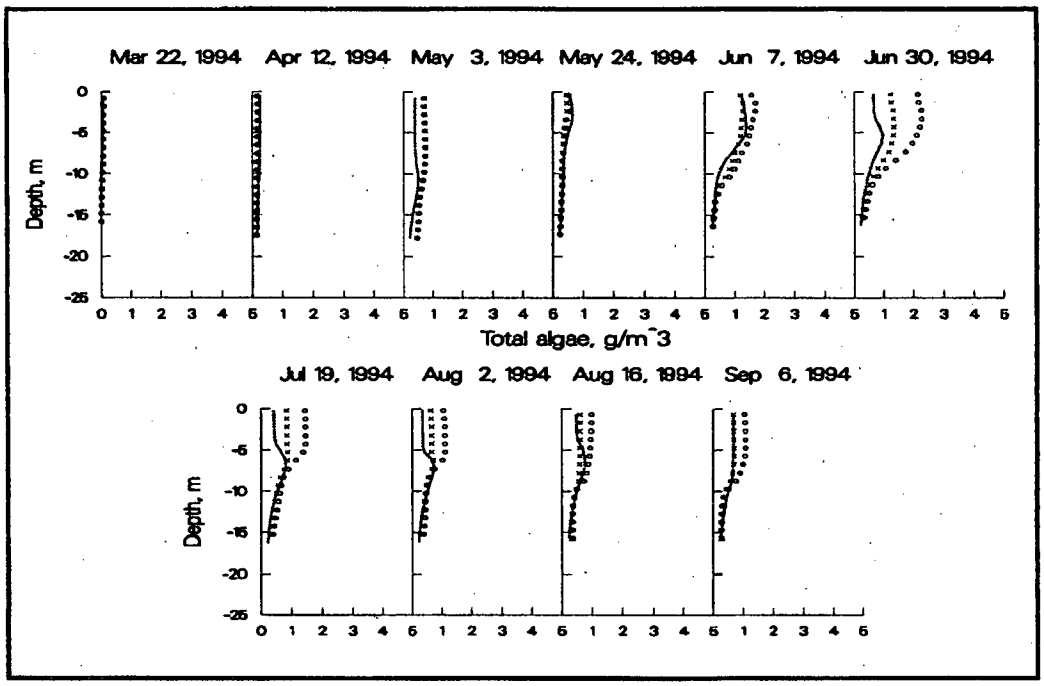

Figure 73. Algal results for base run (....), scenario 5 (xxxx) and scenario 6 (oooo) with inflow phosphorus concentrations increased from 0.007 to 0.03 mg l^{-1}

6 Summary and Conclusions

CE-QUAL-W2 was calibrated for four years on Lake Monroe. The initial calibration year chosen was 1994 since this year had the most complete collection of water quality data. The other calibration years were 1992 (low flow year), 1995 (slight above average flow year), and 1996 (high flow year).

Calibration results for all years except 1994 were affected by having limited inflow and inlake profile data. Most years had temperature, DO, and algal profiles, but limited or no nutrient and TOC inflow or profile data. When no data were available, 1994 values were used. Given the limitations in the boundary condition data used to drive the model, the results are quite acceptable.

Six scenario runs were conducted to determine the effects of low/high inflows, air temperatures, and nutrient loadings on water quality, especially algal biomass production and DO concentrations. The 1994 calibration results were used as the base run for scenario comparisons.

Dissolved oxygen generally showed an increase in the different scenarios. As far as changes to algal biomass, scenarios 1 and 2 demonstrated that the low flows controlled mass loadings to the system resulting in little change in algal populations compared to the base run results when phosphorus concentrations were increased. Scenarios 3 and 4 demonstrated that with increased mass loadings of phosphorus, algal concentrations could increase more than twofold. Scenarios 5 and 6 were similar to 3 and 4 resulting in increased algal production due to increased phosphorus loadings. The increased algal production resulted in increased DO near the thermocline as algal populations produced more oxygen than was consumed by respiration processes. High flow years also had a positive impact on DO due to reduced residence times and thermal stratification.

According to these scenarios, increasing nutrient loadings to the system results in better DO conditions in the reservoir. However, care must be taken when making conclusions about the long-term health of the system with regards to DO. Scenarios with increased nutrient loadings should be run for a minimum of 10 years before making conclusions. Increased loadings might result in a short-term DO increase, but should result in a long-term decrease in DO.

If the model is to be used to forecast water quality conditions under different loading conditions, additional phosphorus data, both boundary and in-pool, should be collected in order to more accurately characterize sediment-water column recycling dynamics and phosphorus loadings to the system. Unfortunately, there is no accepted method for accurately measuring bioavailable phosphorus. However, SRP is the closest available measurement that

can be used to represent bioavailable phosphorus and is the recommended measurement. Because there is some question involving the accuracy of the existing SRP data, other phosphorus forms should also be measured to ensure consistency among the measured phosphorus forms.

7 References

Buchak, E. M. and J. E. Edinger. (1982). "User Guide for LARM2: A Longitudinal-Vertical, Time-Varying Hydrodynamic Reservoir Model," Instructional Report E-82-3, US Army Engineer Waterways Experiment Station, Vicksburg, MS.

Buchak, E. M. and J. E. Edinger. (1984). "Generalized Longitudinal-Vertical Hydrodynamics and Transport: Development, Programming and Applications", Contract No. DACW39-84-M-1636, prepared for US Army Engineer Waterways Experiment Station, Vicksburg, MS.

Cole, Thomas M. and Herbert H. Hannan. (1990). "Dissolved Oxygen Dynamics", *Reservoir Limnology: Ecological Perspectives*. Kent W. Thornton, Bruce L. Kimmel, and Forrest E. Payne, eds., John Wiley & Sons, Inc., New York, NY.

Cole, Thomas M. and Edward M. Buchak. (1995). "CE-QUAL-W2: A Numerical Two-Dimensional, Laterally Averaged, Hydrodynamic and Water Quality Model: Version 2 User Manual", Instructional Report EL-95-1, US Army Engineer Waterways Experiment Station, Vicksburg, MS.

Wetzel, Robert G. (1975). *Limnology*. W. B. Saunders Company, Philadelphia, PA.

Appendix A

This appendix contains plots of all inflow/outflow, inflow temperatures, and meteorology used for the four calibration years.

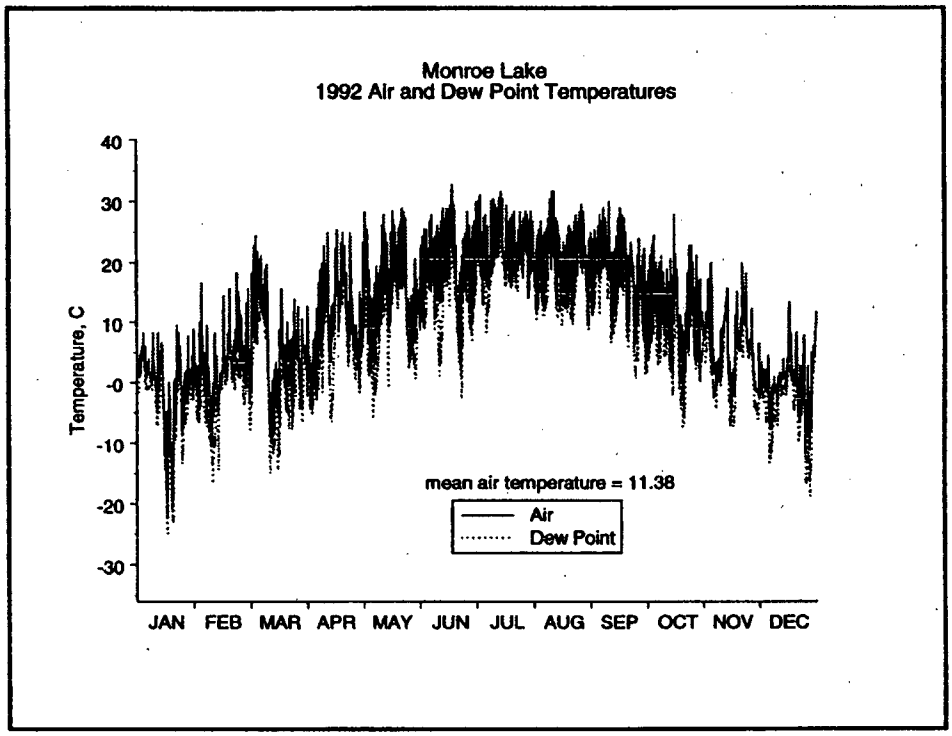

Figure A1. 1992 air and dew point temperatures

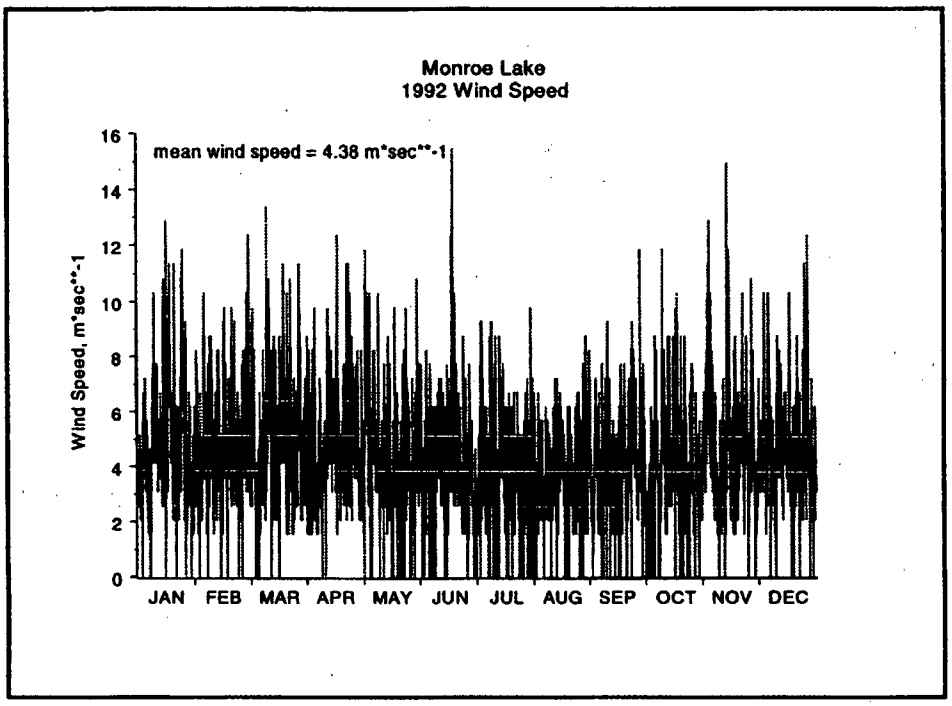

Figure A2. 1992 wind speed

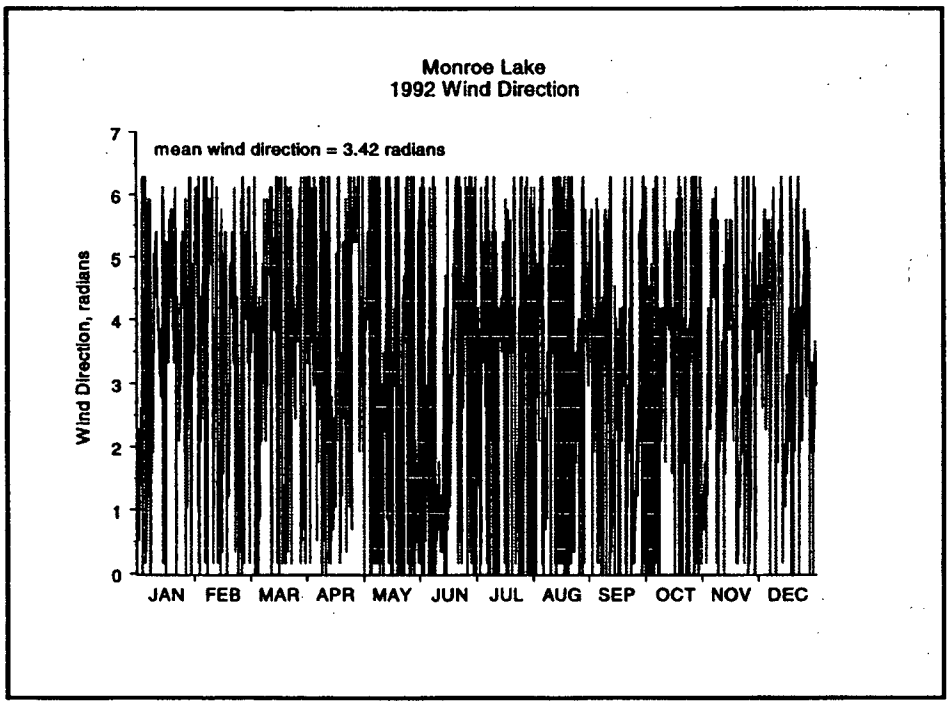

Figure A3. 1992 wind direction

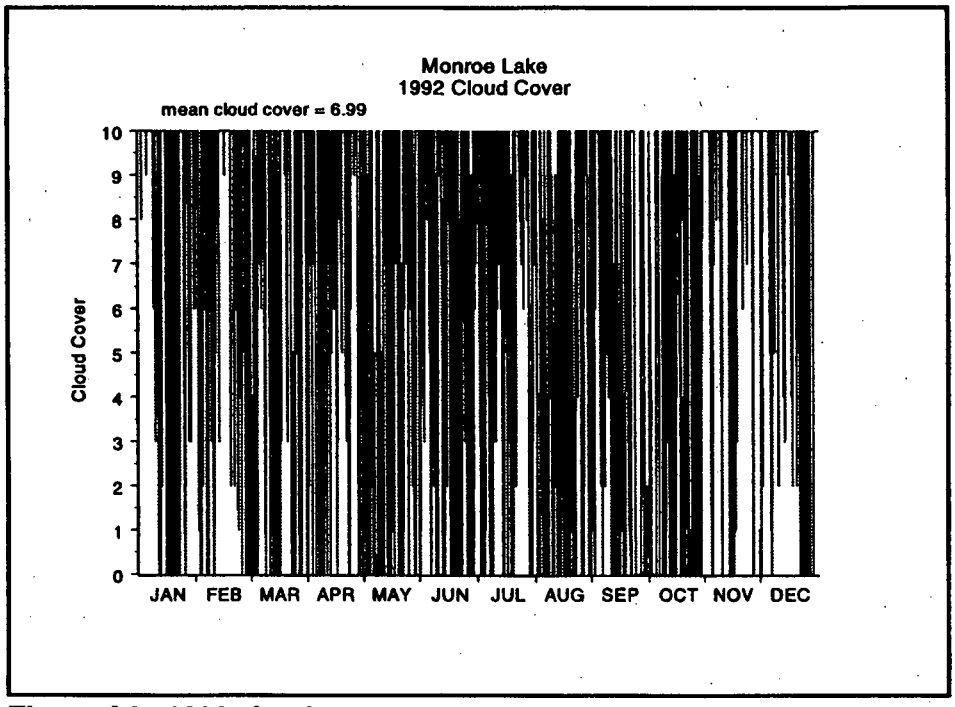

Figure A4. 1992 cloud cover

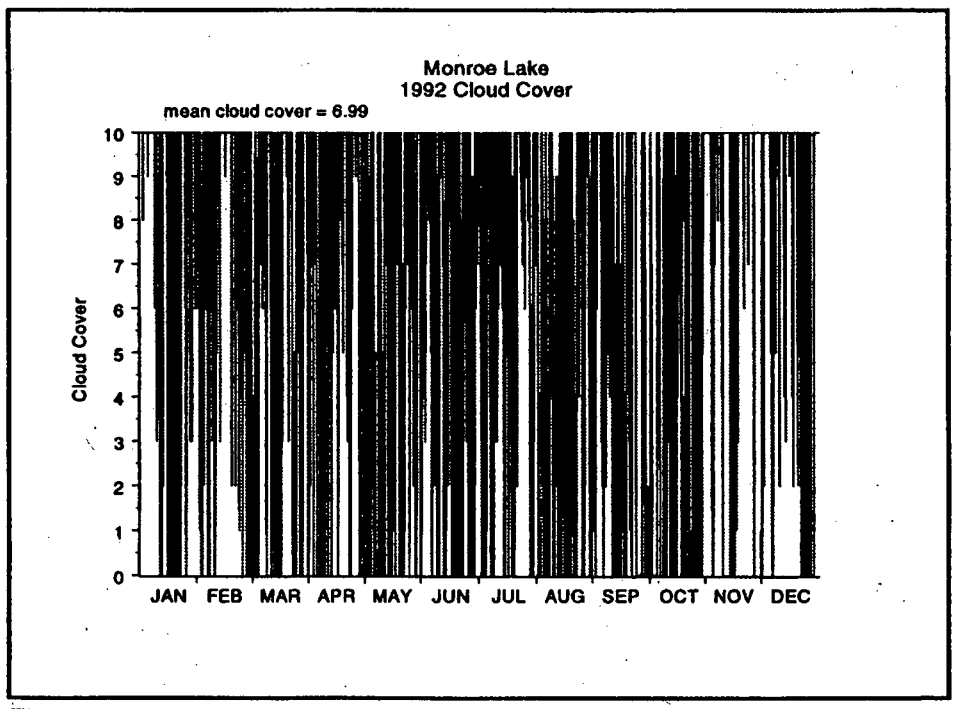

Figure A4. 1992 air and dew point temperatures

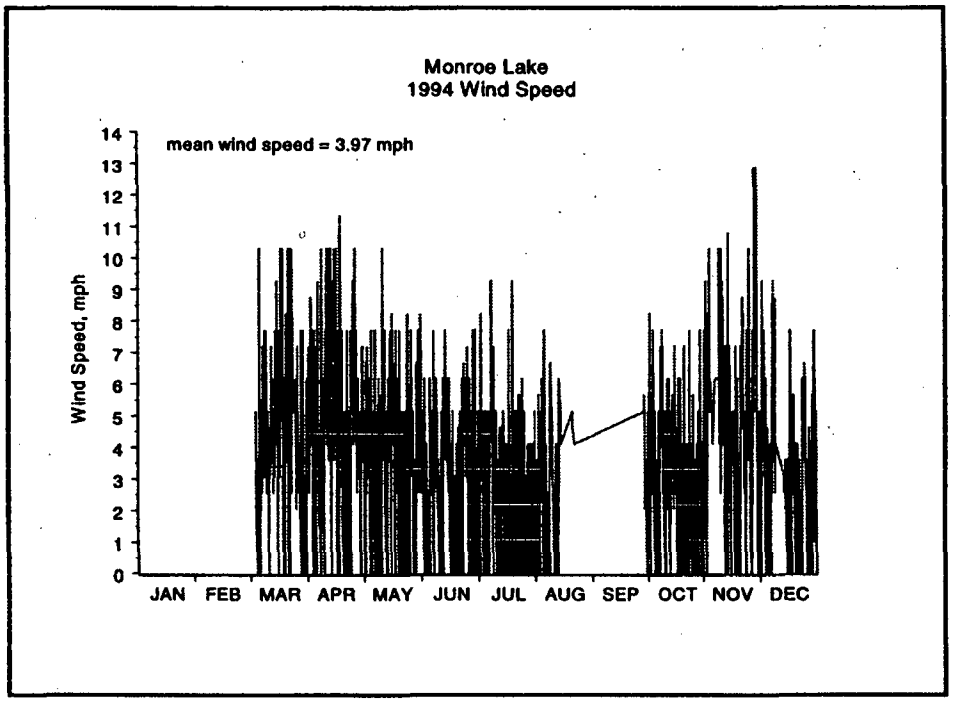

Figure A6. 1994 wind speed

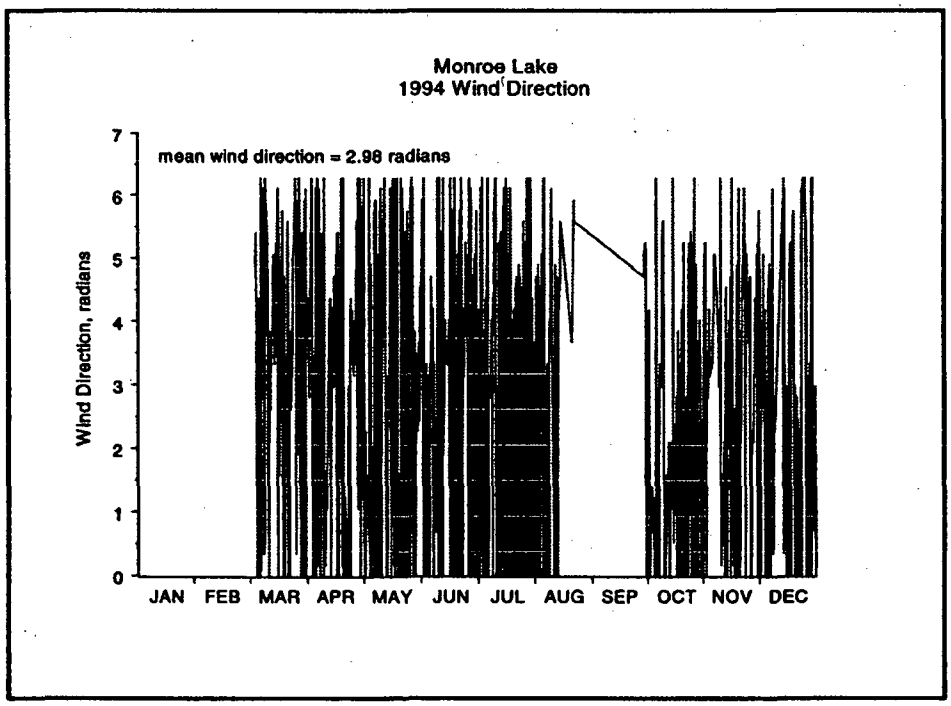

Figure A7. 1994 wind direction

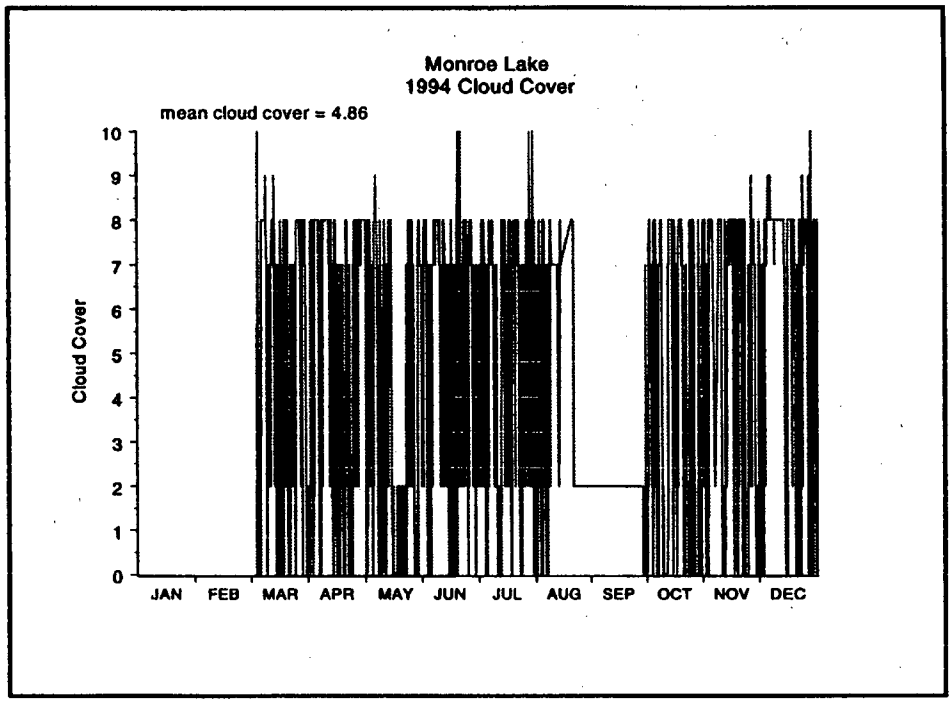

Figure A8. 1994 cloud cover

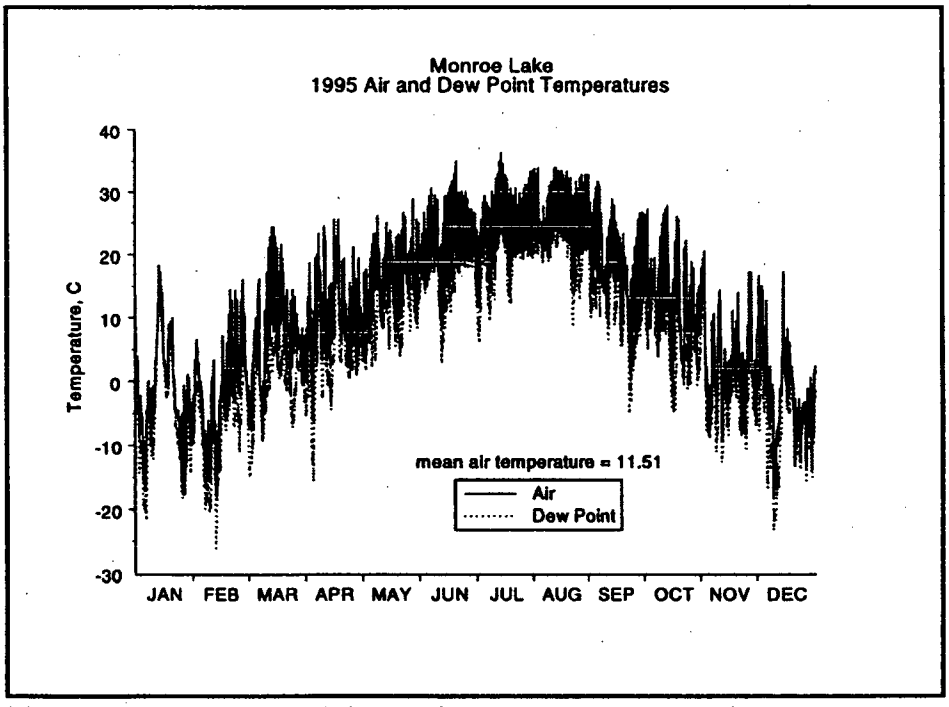

Figure A9. 1995 air and dew point temperatures

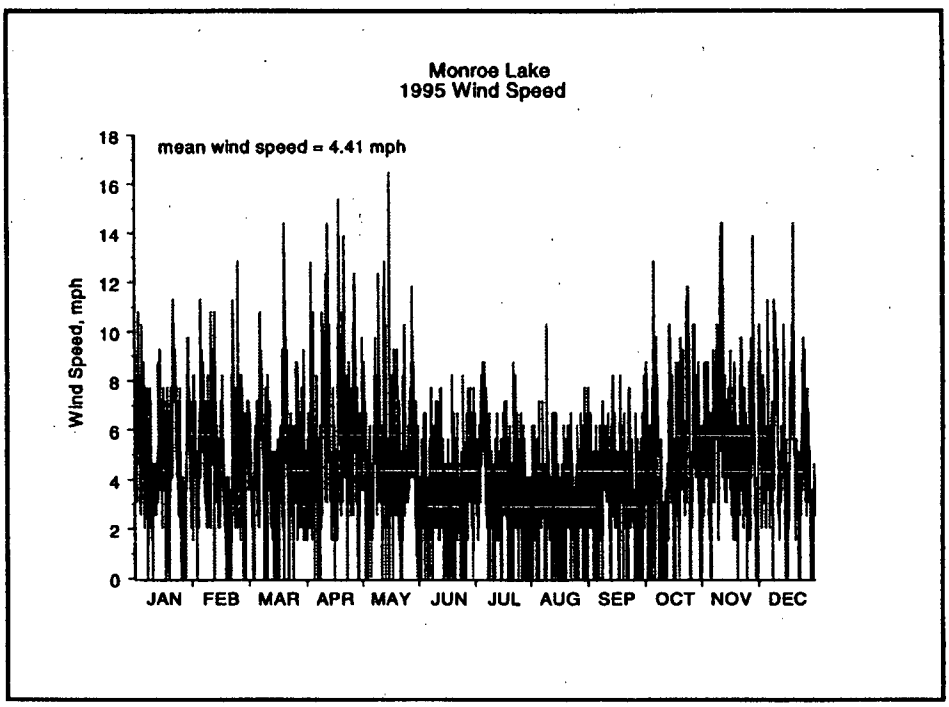

Figure A10. 1995 wind speed

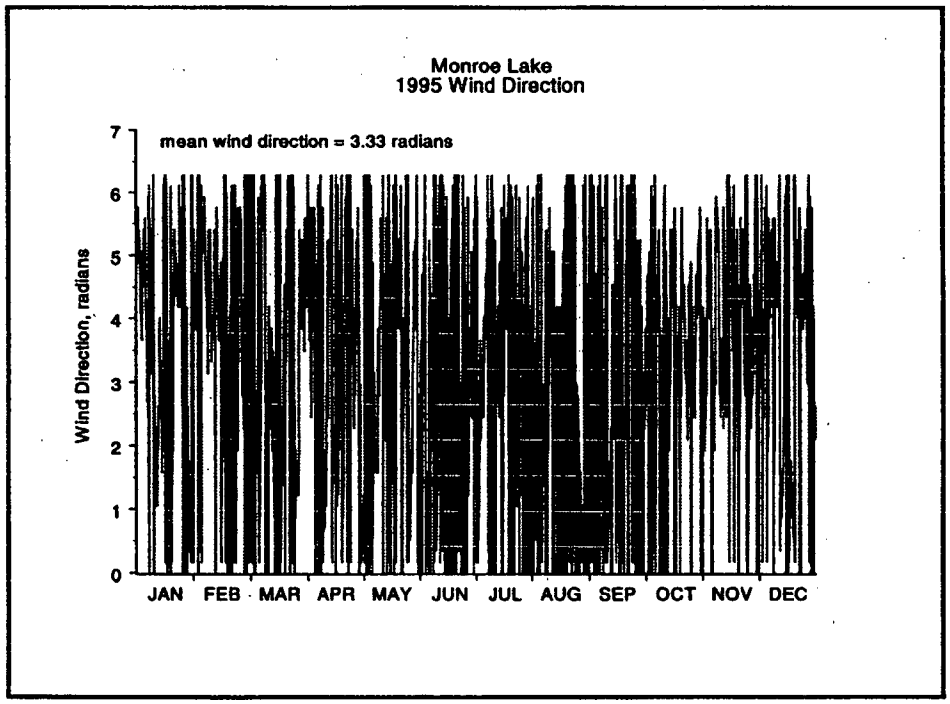

Figure A11. 1995 wind direction

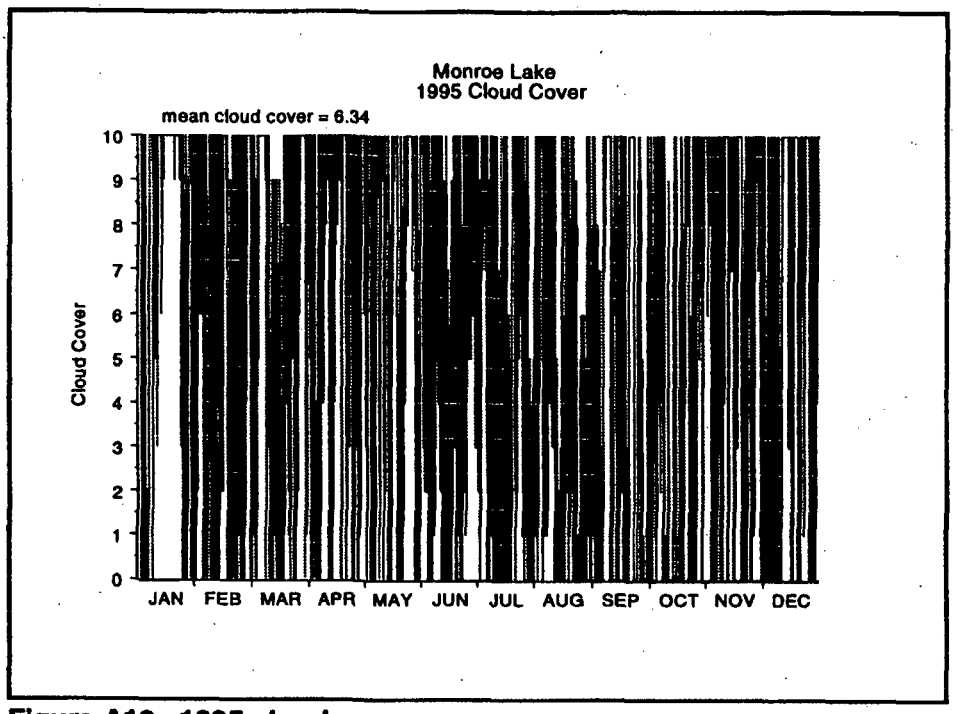

Figure A12. 1995 cloud cover

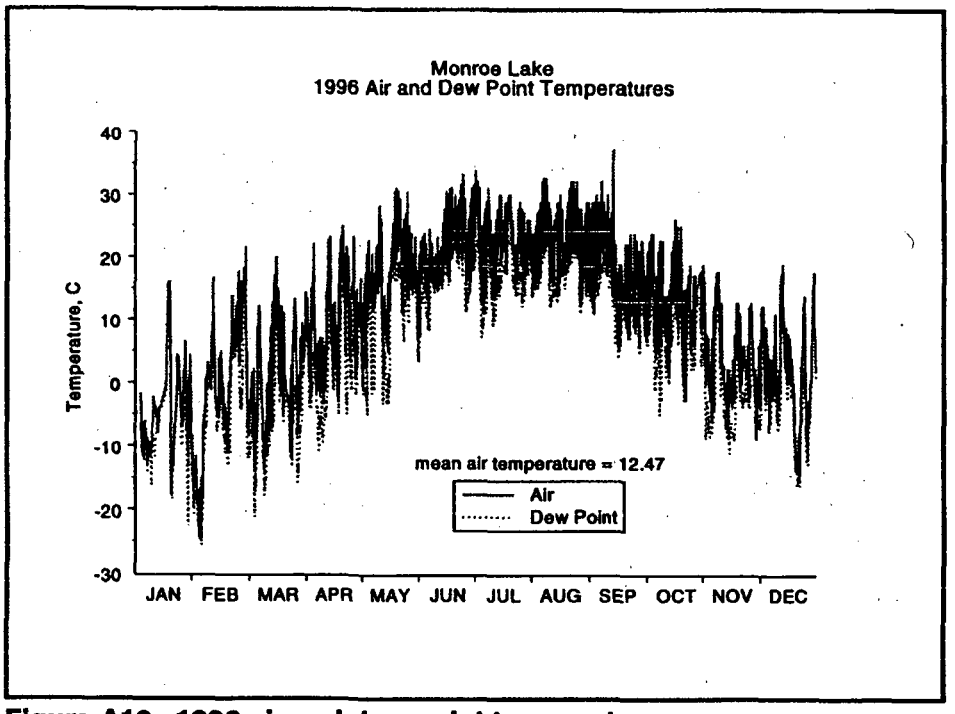

Figure A13. 1996 air and dew point temperatures

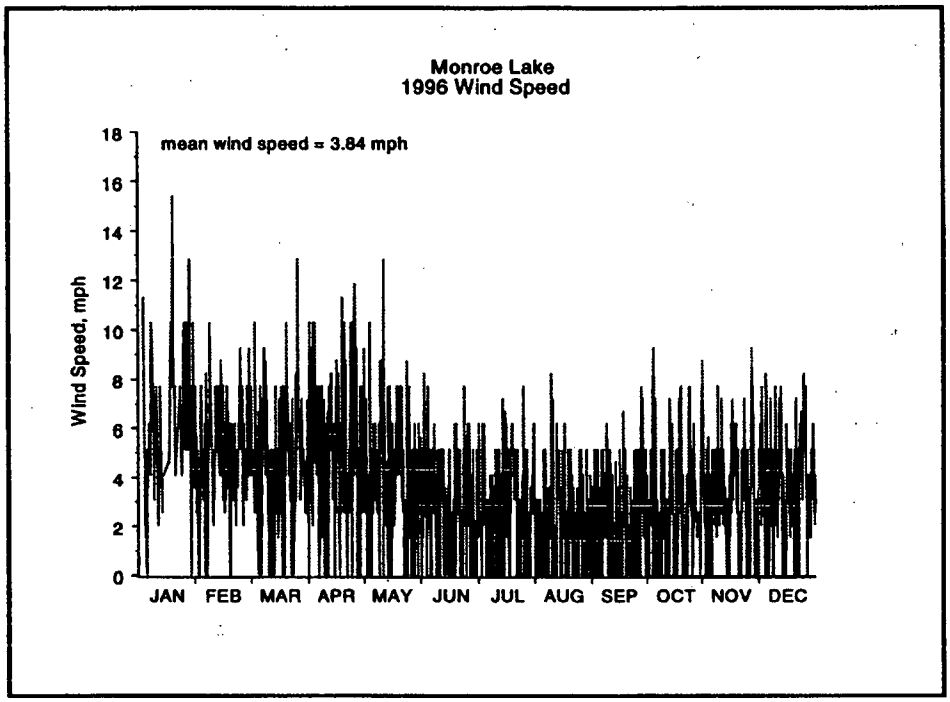

Figure A14. 1996 wind speed

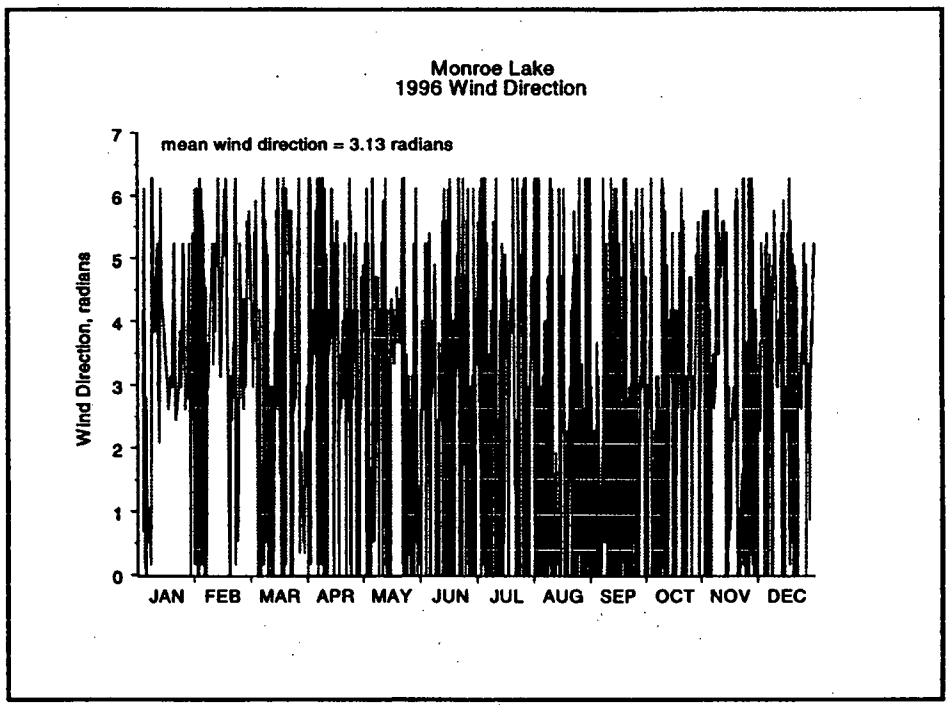

Figure A15. 1996 wind direction

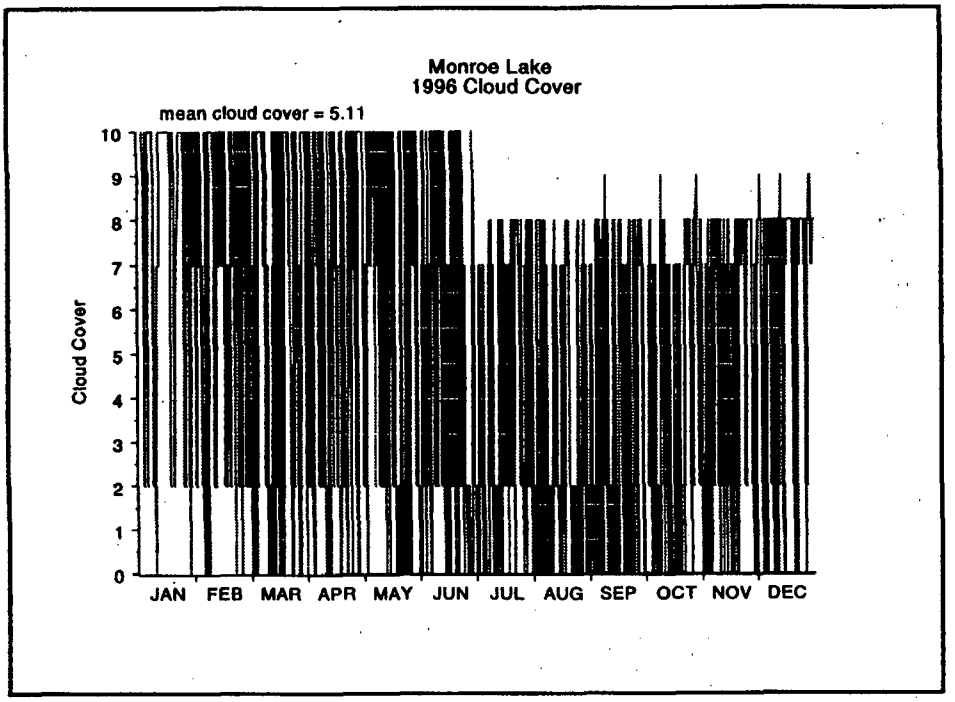

Figure A16. 1996 cloud cover

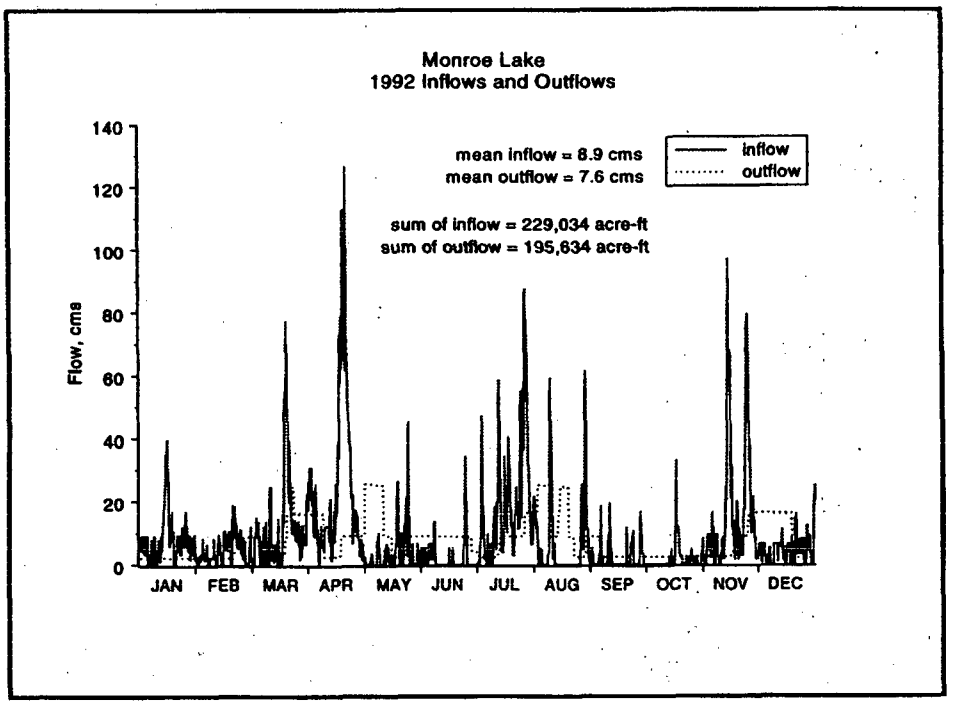

Figure A17. 1992 inflows and outflows

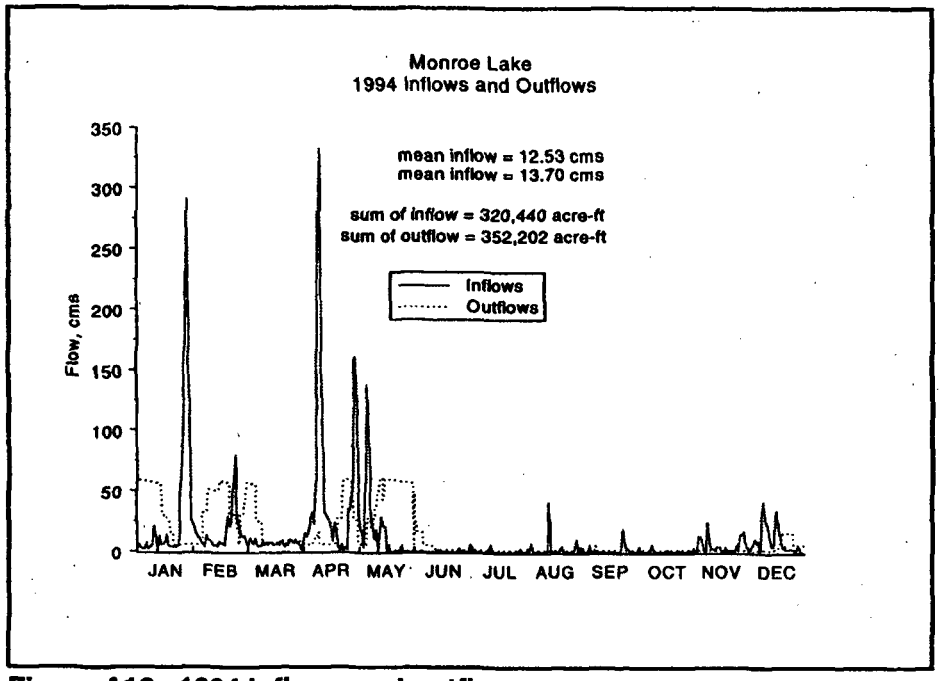

Figure A18. 1994 inflows and outflows

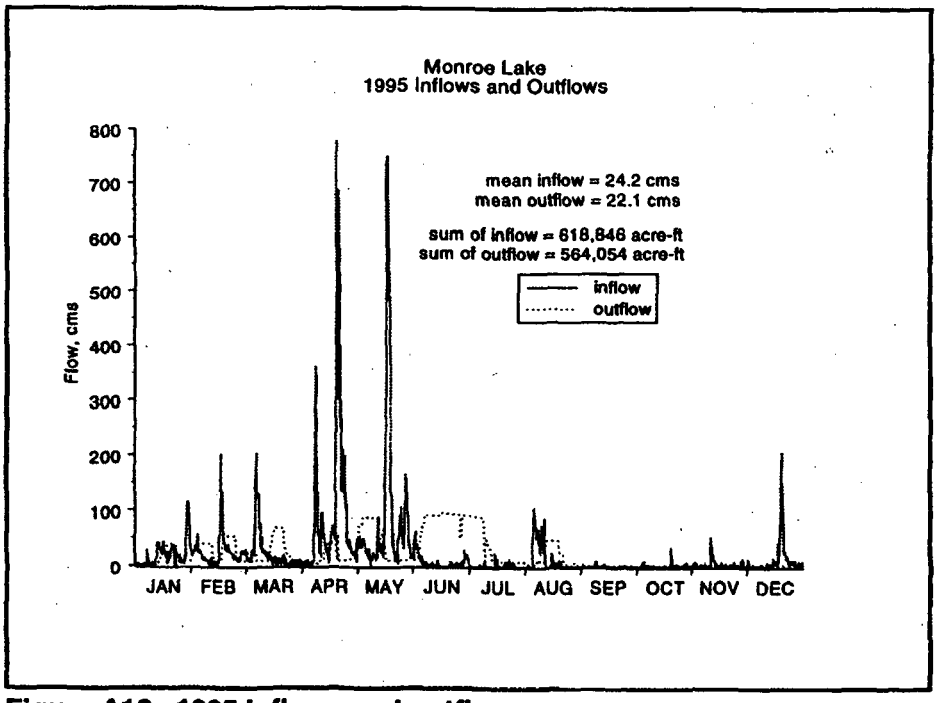

Figure A19. 1995 inflows and outflows

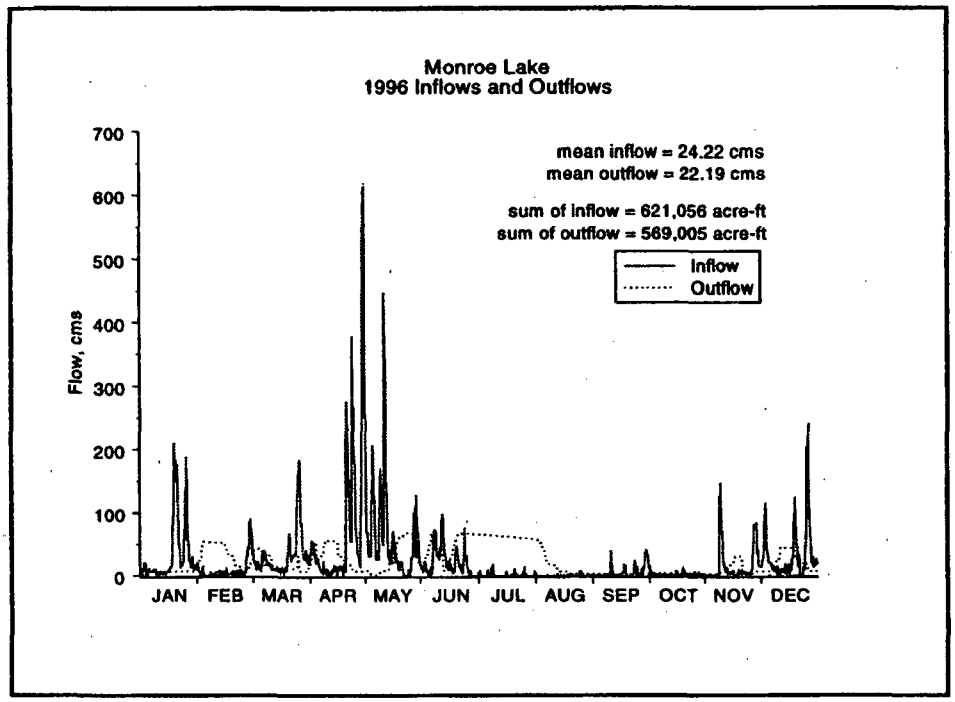

Figure A20. 1996 inflows and outflows

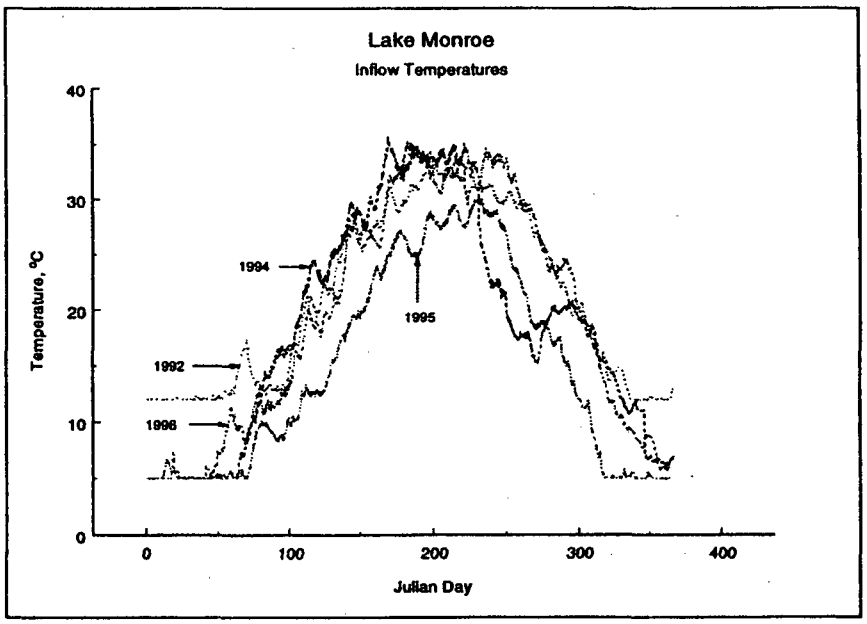

Figure A21. 1992, 1994, 1995, and 1996 inflow temperatures

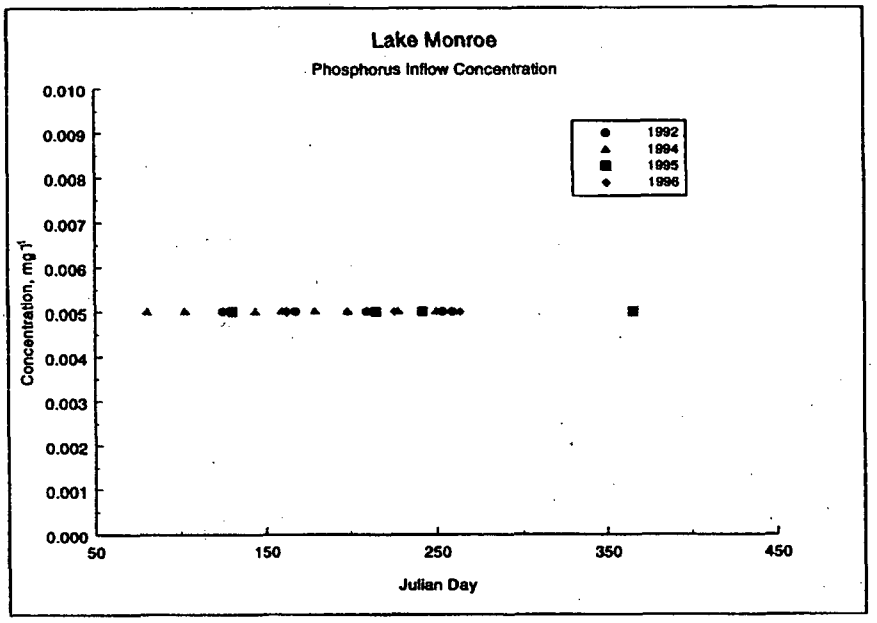

Figure A22. 1992, 1994, 1995, and 1996 inflow phosphorus concentrations

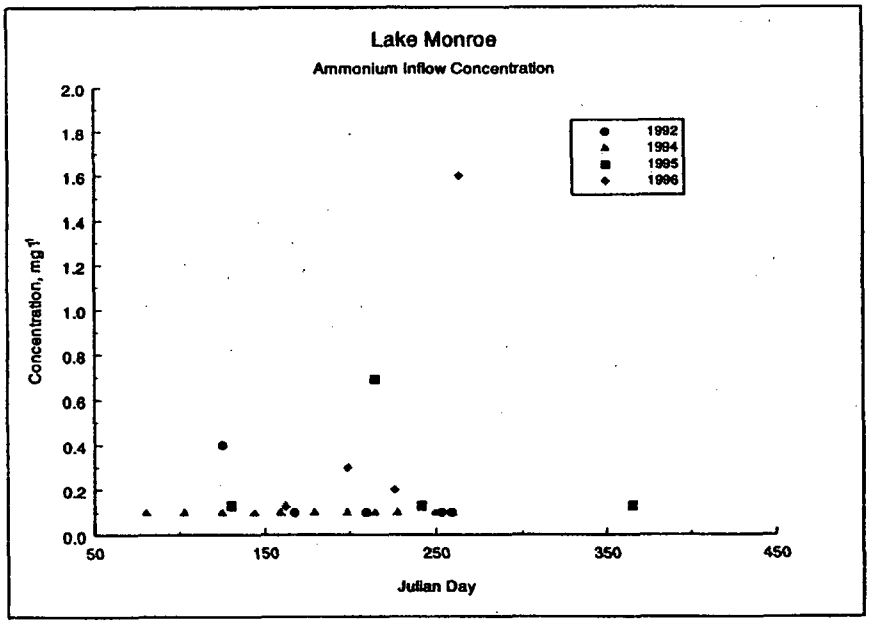

Figure A23. 1992, 1994, 1995, and 1996 inflow ammonium concentrations

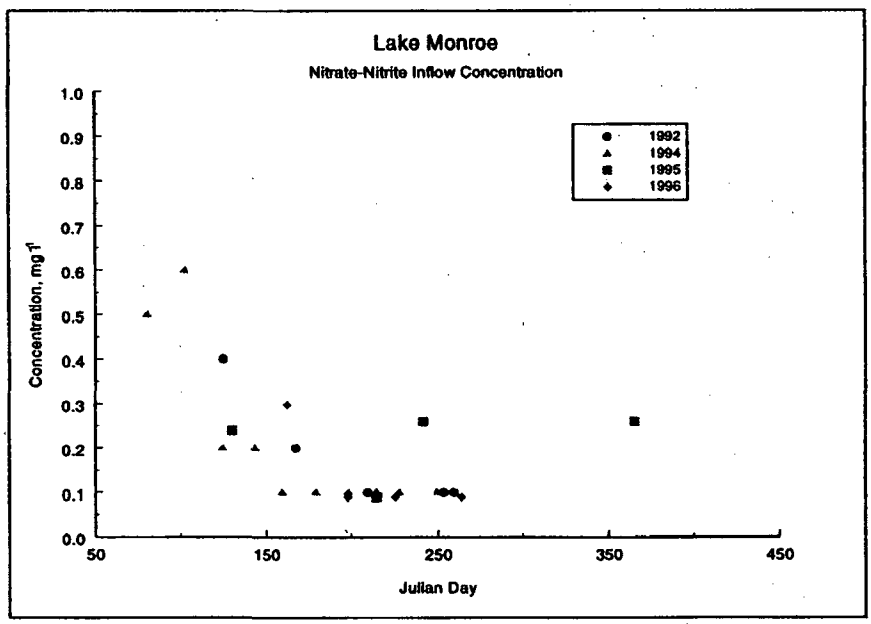

Figure A24. 1992, 1994, 1995, and 1996 inflow nitrate-nitrite concentrations

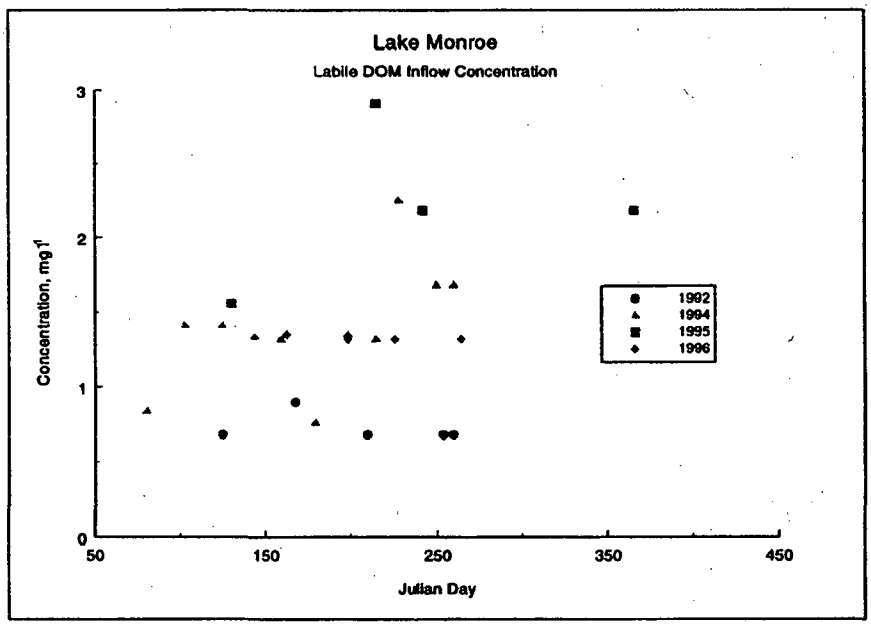

Figure A25. 1992, 1994, 1995, and 1996 inflow labile DOM concentrations

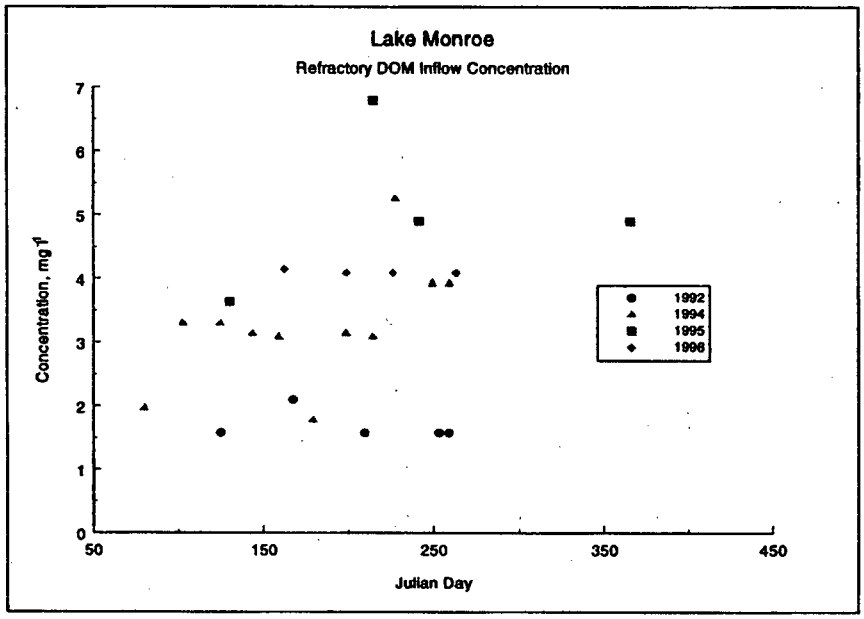

Figure A26. 1992, 1994, 1995, and 1996 inflow refractory DOM concentrations

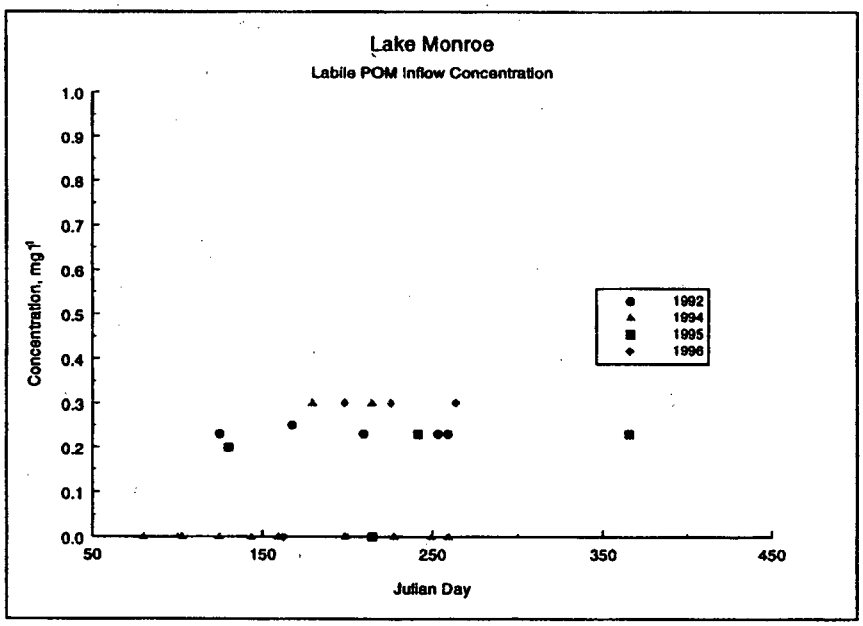

Figure A27. 1992, 1994, 1995, and 1996 inflow labile POM concentrations

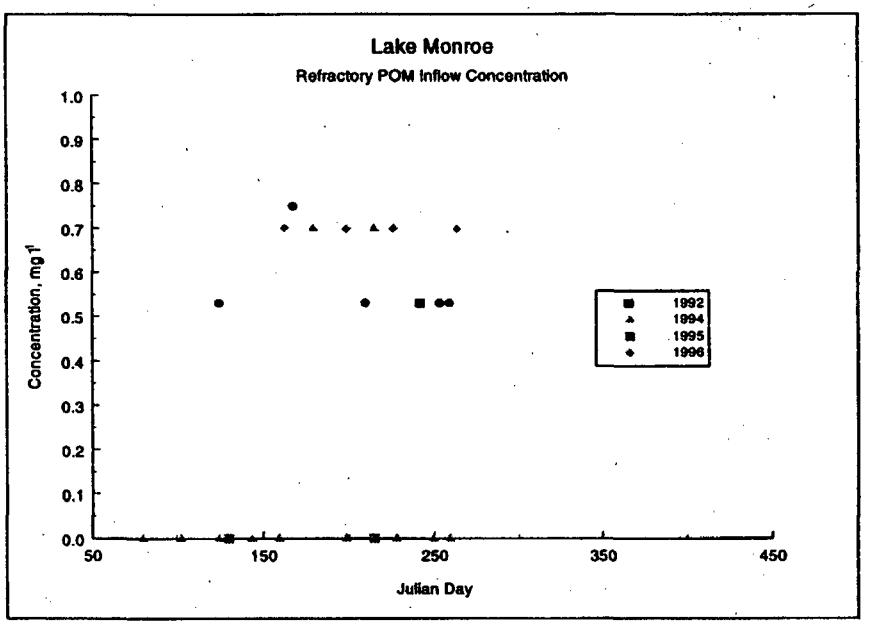

Figure A28. 1992, 1994, 1995, and 1996 inflow refractory POM concentrations

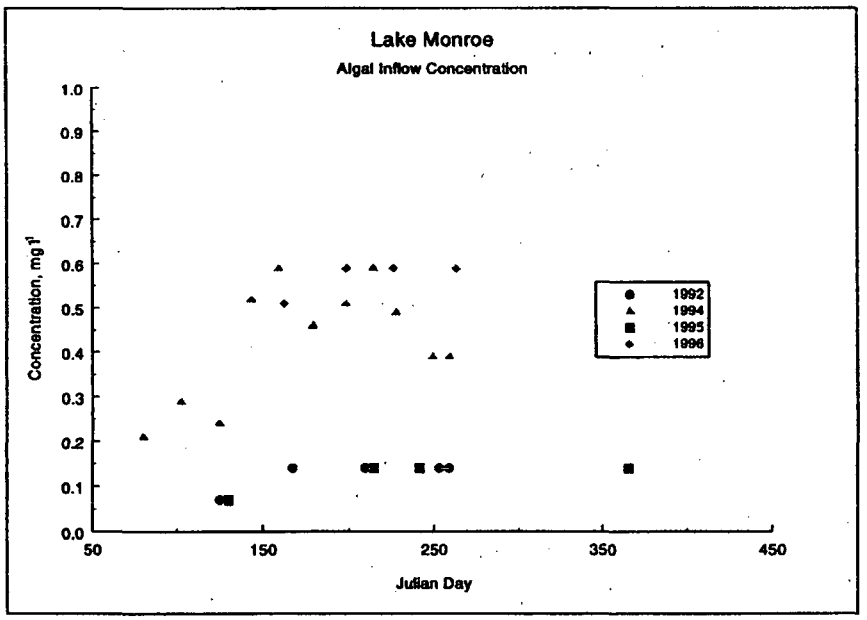

Figure A29. 1992, 1994, 1995, and 1996 inflow algal concentrations

REPORT DOCUMENTATION PAGE

Form Approved
OMB No. 0704-0188

1. AGENCY USE ONLY *(Leave blank)*	2. REPORT DATE	3. REPORT TYPE AND DATES COVERED
	January 1999	Final report

4. TITLE AND SUBTITLE
Water Quality Modeling of Lake Monroe Using CE-QUAL-W2

5. FUNDING NUMBERS

6. AUTHOR(S)
Thomas M. Cole, Dorothy H. Tillman

7. PERFORMING ORGANIZATION NAME(S) AND ADDRESS(ES)
U.S. Army Engineer Waterways Experiment Station
3909 Halls Ferry Road
Vicksburg, MS 39180-6199

8. PERFORMING ORGANIZATION REPORT NUMBER
Miscellaneous Paper EL-99-1

9. SPONSORING/MONITORING AGENCY NAME(S) AND ADDRESS(ES)
U.S. Army Engineer District, Louisville
Louisville, KY 40201-0059

10. SPONSORING/MONITORING AGENCY REPORT NUMBER

11. SUPPLEMENTARY NOTES
Available from National Technical Information Service, 5285 Port Royal Road, Springfield, VA 22161.

12a. DISTRIBUTION/AVAILABILITY STATEMENT
Approved for public release; distribution is unlimited.

12b. DISTRIBUTION CODE

13. ABSTRACT ***(Maximum 200 words)***

CE-QUAL-W2 was applied to Lake Monroe to enable the Louisville District (CEORL-ED-H) to have the capabilities of evaluating changes in water quality from changes in environmental conditions. Calibration was conducted for 4 years of observed data provided by the CEORL-ED-H for six water quality constituents of interest. Calibration results for all years except 1994 were affected by having limited inflow and inlake profile data. Given the limitations to the boundary conditions to drive the model, favorable results were obtained for all years. After calibration was achieved, six scenario runs were conducted to determine effects of low/high inflows, air temperatures, and nutrient loadings on water quality using the 1994 calibration results as the base run for scenario comparisons. In general, the scenario results showed that increased nutrient loadings to the system resulted in improved dissolved oxygen concentrations in the reservoir. However, conclusions of this significance should be based on a run with increased nutrient loadings for a minimum of 10 years before final conclusions can be ascertained as to the long-term health of the system.

14. SUBJECT TERMS
Modeling
Two-dimensional
Water quality

15. NUMBER OF PAGES
94

16. PRICE CODE

17. SECURITY CLASSIFICATION OF REPORT	18. SECURITY CLASSIFICATION OF THIS PAGE	19. SECURITY CLASSIFICATION OF ABSTRACT	20. LIMITATION OF ABSTRACT
UNCLASSIFIED	UNCLASSIFIED		